MASARYK UNIVERSITY
Faculty of Medicine

HABILITATION THESIS

A quest to find out how human brain cells form and brain-related diseases develop

Yuh-Man Sun, PhD., MSc.

Table of contents

1. Abstract

It is magical how we develop from a single fertilised cell. During the phenomenal embryonic development, our brains form and render us abilities to think and behave. I am very fortunate that I am in control of my thinking and behaviour. Image how many people are suffering from neural-related diseases (e.g., Alzheimer's disease, schizophrenia, autism, Parkinson's disease, ..etc.), who have lost control of their thinking and behaviour. The plight of the sufferers (especially psychiatric patients) triggers my intention to employ my scientific expertise to develop something to ameliorate patients' suffing. My research interests are to gain insights into the fundamental molecular mechanisms governing how human brain cells form and how to generate every type of neural cells (e.g., glutamatergic, GABAergic, dopaminergic neurons, and astrocytes, oligodendrocytes). Moreover, I will employ the derived paradigms to generate each type of neural cells from psychiatric patients (schizophrenia and autism) and investigate what has happened in the individual neural cell types in relation to the disorders. I strongly believe that psychiatric disorders share a common causal mechanism (a defective neurodevelopmental process and synatopathies). To pursue my research interests, I have established human pluripotent stem cell (hPSC)-based brain developmental and disease modelling systems, which combine human embryonic stem cell (hESC)-based and human induced pluripotent stem cell (iPSC)-based systems. Using these modelling systems, my team explores two domains of research, **basic science** and **translational research**, which have an inseparable relationship, like Yin-Yang in Chinese philosophy. The knowledge derived from biology (basic science) can shed light on disease progress, whereas the disease systems (translational research) can give insight into biology development. The goals of my research are to identify the molecular mechanisms underlying neural fate decisions, to define cellular pathophenotypes of psychiatric disorders, and to develop tailored treatments for the psychiatric patients.

2. Background

2.1 Introduction

Embryogenesis is the process by which the embryo forms and develops. During embryogenesis in mammals, a fertilised egg undergoes divisions and becomes the blastocyst, which consists of the inner cell mass (ICM) and trophectoderm. Only the ICM will develop into the embryo and it is also the source for the derivation of ESCs (Gilbert, 2010). In the process, the ICM will give rise to epiblasts, which will undergo gastrulation to form three primary germ layers that then proceed organogenesis to generate all the organs, tissues, and then to an embryo (Gilbert, 2010). The intrinsic regulatory networks governing embryogenesis in the human remain elusive.

The difficulties encountered by the scientists in the developmental biology field are as follows: 1) mammalian eggs are amongst the smallest in the animal kingdom, making them hard to manipulate experimentally; 2) the human zygote (a fertilised egg) is only 100μm in diameter, which is barely visible to the eye and less than 1/1000 the volume of a Xenopus Laevis egg, 3) mammalian zygotes are not produced in numbers comparable to sea urchin or frog zygotes so it is difficult to obtain enough material for biochemical studies, 4) the development of mammalian embryos is accomplished inside another organism (i.e. in the mother's womb) rather than in the external environment, and 5) there are ethical issues involved in using human embryos as experimental subjects. Before the development of hESC technology, developmental biologists investigate embryogenesis primarily using model organisms (non-human species), which include yeast, *Caenorhabditis elegans (worms),*

Drosophila melanogaster (flies), zebrafish, *Xenopus laevis*, and mouse, due to ethical issues and technical difficulties (e.g., impossible to assess and manipulate embryos in human embryos). Knowing how human embryos form is primarily based on the knowledge extrapolated from system organism-based studies, in which may cause erroneous translations due to the species differences derived from the evolutionary gap. However, the advent of hESC technology is changing the landscape in this field of science.

My research lies in the frontier of the adaptation of ESC technology to decipher the molecular mechanisms underlying early fate decision during neural development in mammals using ESC-based developmental modelling system. ESCs possess of the pluripotent property of the ICM so that ESCs can generate any type of cells in the body. Others and we have demonstrated that the process of ESC-derived differentiation recapitulates the developmental stages *in vivo* (Sun et al. 2008; Sakurai et al. 2009; Slawny and O'Shea 2013; Cimadamore et al., 2011). In this thesis, I described how I get to know the potential of ESCs, to establish ESC-based neural developmental system, to employ this modelling system to explore how brain cells form, and how to pursue my future career in translational research.

2.2 Development of my research direction

I have divided the development of my research direction into the following phases: 1) the recognition of potential of ESCs, 2) the usage of ESC as a research tool to explore the neural lineage, 3) the establishment of mouse ESC-based neural developmental modelling, and 4) the establishment of human ESC-based neural developmental modelling.

2.2.1 Phase 1: the recognition of ESC potential

After 3-year postDoc training, I secured my first research Fellowship from a highly competitive grant sponsored by the Journal of Reproduction and Fertility (Cambridge, U.K.). The project was to employ state-of-the-art gene targeting techniques to generate conditional knockout HP1β mice to investigate the role of heterochromatin protein 1β (HP1β) in different stages of spermatogenesis. To this end, I first designed and constructed a *HP1β* conditional knockout vector using the Cre-Lox system. I further generated a mouse ESC line in which one of the endogenous *HP1β* loci is replaced with the *HP1β* conditional knockout vector. The mouse ESC line was then injected into mouse blastocysts to produce conditional knockout HP1β mice. Within 2 years, I had also generated several heterchromatin-related gene knockout mouse ESC lines, including *HP1β*, *PH1γ*, *Su(var)h1* and *Su(var)h2*. Some of the work has been published in Biochem. Biophys. Res. Commun. 2005; 337(3):901-907. During this period of training, I was able to design and construct gene targeting vectors including conditional and straight knockout vectors, culturing ESCs and modifying genes in ESCs. The work about *HP1β* did not catch my attention much, rather, ESCs per se. From my debut in engaging with ESCs. I was intrigued by the power possessed by small and ordinary ESCs. It dawned on me that ESCs will be a powerful tool in studying development and inspired to pursue my research career in the ESC field in 2001. Moreover, gene targeting molecular biology techniques, which I have learnt in this period, laid a foundation for me to explore biological questions at the molecular level.

2.2.2 Phase 2: the usage of ESC as a research tool to explore neural development

ESCs are derived from the ICM of blastocysts, which are pluripotent and can form every cell in the embryo (Gilbert, 2010) (Fig. 1). Thus ESCs possess the capacity of the ICM and can give rise to any type of cells in the body. For this notion, I was very keen to adopt ESC system for my research interests in finding out how the neural lineage proceeds.

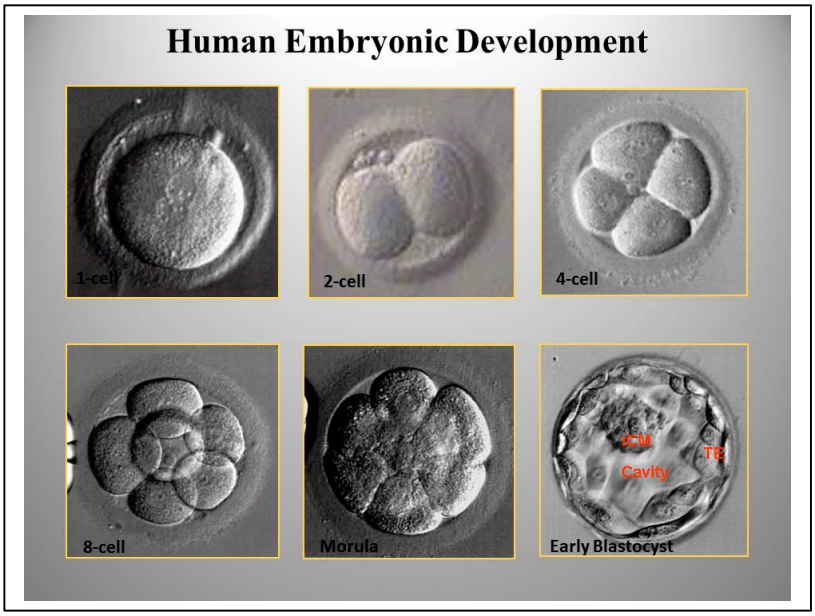

Fig. 1. The development of human embryos.

The fertilised egg undergoes cell division and develops into the early blastocyst at around embryonic day 4.5, which consists of inner cell mass (ICM) and trophoblast (TE). The embryonic stem cells are derived from the ICM.

At that time (2003), I was interested in *Rest* gene. Rest is a RE1 Silencing Transcription Factor/ Neuron Restrictive Silencer Factor (Rest/Nrsf) and is a zinc finger transcription repressor that has been postulated to act as a master regulator of neuronal gene expression in both the developing and mature nervous systems (Schoenherr et al., 1996; Chen et al., 1998). Rest interacts with RE1 sites and recruits corepressors including mSin3A (Huang *et al.,* 1999, Roopra *et al.,* 2000) and CoREST (Andre´s *et al.,* 1999, Ballas *et al.,* 2001), which in turn, recruit multiple cofactors and transcriptional regulators including histone deacetylases 1 and 2, G9a histone methyltransferase (Roopra *et al.,* 2004), H3 lysine 4 demethylase LSD1 (Shi *et al.,* 2004), and chromatin remodeling machinery, including BRG1, BAF57, and BAF 170 (Battaglioli *et al.,* 2002) and BRAF35 (Hakimi *et al.,* 2002). There are over 1300 RE1 sites in the human and murine genomes (Bruce *et al.,* 2004; www. bioinformatics.leeds.ac.uk/ group/online/RE1db/re1db_home.htm) and the majority encode ion channels, neurotrans-mitters, growth factors and hormones, and factors involved in axonal guidance and vesicle trafficking, and molecules involved in maintenance of the cytoskeleton and extracellular matrix (Schoenherr *et al.,* 1996; Bruce *et al.,* 2004). Because many of these target genes are expressed by postmitotic neurons, the role of Rest was originally perceived as that of silencer of neuron-specific genes in nonneuronal cells (Chong *et al.,* 1995; Schoenherr and Anderson, 1995). To prove this hypothesis, I was interested in establishing the role of Rest in neural lineage using the ESC system. First, I looked into the Rest expression in ESCs and investigated what the Rest target genes are in the ESC stage. As Rest acts as a master silencer of neuronal gene expression, I proposed that profiling Rest immediate target genes in ESCs should provide a clue as to what genes are involved in suppressing neural differentiation in ESCs. To this end, the first task was to establish an approach or methodology to identify the Rest target genes in ESCs.

Prof. N. Buckley's lab (in the U.K.), where I used to work, had developed a CHIP-on-CHIP method to identify potential RE1 sites. However, this methodology had proven to be laborious, not cost effective, not sensitive and generating high-false positive data. Based on my training background, I created a novel chromatin immunoprecipitation (ChIP) cloning strategy based on selective amplification of ChIP (called SACHI). I employed SACHI to identify Rest target genes in ES cells, hippocampal NS cell line,

MHP36 (Kershaw *et al.,* 1994) and mature hippocampus, all of which represent distinct stages of neuronal development. Using this technique, I identified 81 novel Rest targets and further, I showed that Rest occupies a unique subset of target genes in each cell type. The work has been published in Molecular Biology of the Cell (2005) 16:5630–5638 (the impact factor was 7.8 at the time of publication) (see Appendix 1). My contributions to this paper were generating ideas, designing experiments, conducting experiments, and writing the manuscript for publication (as a corresponding author). **It is worth noting that many scientists around the world applied this technique to their work due to the methodology being user friendly and economical. The paper has been cited over 83 times.**

2.2.3 Phase 3: the establishment of mouse ESC-based neural developmental modelling

2.2.3.1 Setting up ESC-based developmental modelling system

I was continuously investigating the role of Rest in neural development using ESC system. In 2005, ESC-derived neural differentiation was not well documented. However I knew the potential of ESC system. First, I endeavoured to set up ESC-based developmental modelling, which recapitulates the process of the neural lineage *in-vivo* from ESCs to neural stem cells (or neural rosettes), neural progenitors, and then to neurons (Fig.2). I adopted this modelling system to explore my scientific interests.

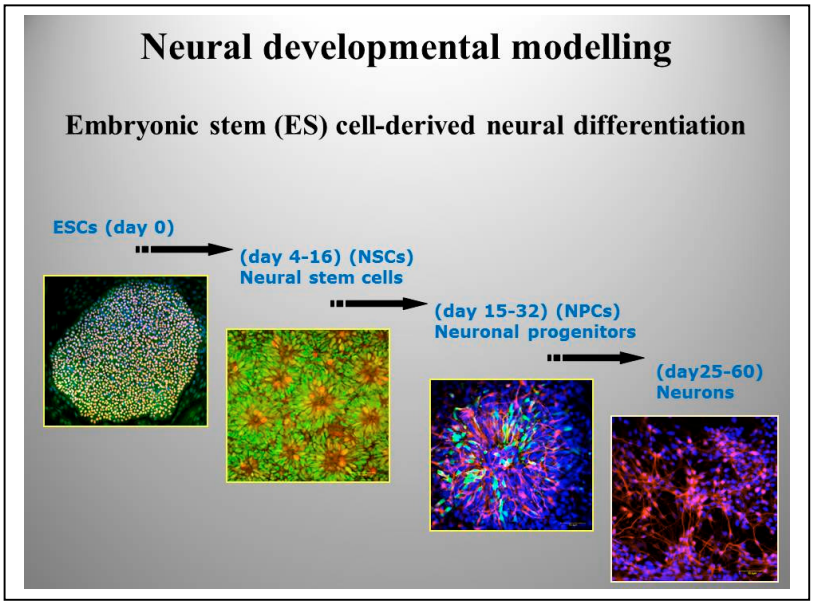

Fig. 2. The ESC-based neural developmental modelling. ESCs were plated out and driven toward neural differentiation in N2B27 neural differentiation medium. The different stages of development are indicated by the time when the specific cell type appears.

2.2.3.2 Identifying the genes that positively regulate neural induction

During mouse embryo development, the blastocyst differentiates into pluripotent primitive ectoderm and gives rise to a structure known as the epiblast (Coucouvanis and Martin, 1995). The epiblast responds to extrinsic signals and generates three primary germ layers (ectoderm, mesoderm and endoderm) (Gardner and Rossant, 1979). During neural induction, the ectoderm gives rise to the neuroectoderm in the form of a neural plate, which subsequently folds to generate the neural tube, composed of a single layer of neuroepithelial cells or neural stem cells (NSCs), where a series of ring-like constrictions mark the boundaries between the primordia of the major brain regions (Lawson and Pedersen, 1992; Rubenstein and Shimamura,1998). Thus neural induction is the first step of our central nervous formation. This process of neural development is orchestrated and accompanied by wholesale changes in transcriptional programmes and patterns of gene expression. However, due to

the difficulties in accessing and manipulating early embryos, the transcriptional network that regulates neural development is poorly understood, especially in mammals. ESCs derived from blastocysts retain the ability to recapitulate neural development in vitro, and offer an invaluable model to study early events in the neural lineage (Fig. 2).

First I established the course of neural development and found that neural induction occurs at around 4 days of differentiation from mouse ESCs, which period is called neural induction and is characterised by an increase in the gene expression of neural stem cell markers (Sox1 and Pax6) (Fig.3). Second, to investigate how neural induction occurs, I consider the up-regulated genes during neural induction will hold the key to this question. To this end, I divided the period that leads to neural induction into three time periods (i.e. day0 to day1, day1 to day3, and day3 to day6) and employed the selective subtractive hybridisation (SSH) approach to identify up-regulated genes during the three periods (Fig. 3). The goal of this project was to profile the potential genes that positively regulate neural induction, which laid a foundation for my research interest in unravelling molecular mechanisms underling neural induction.

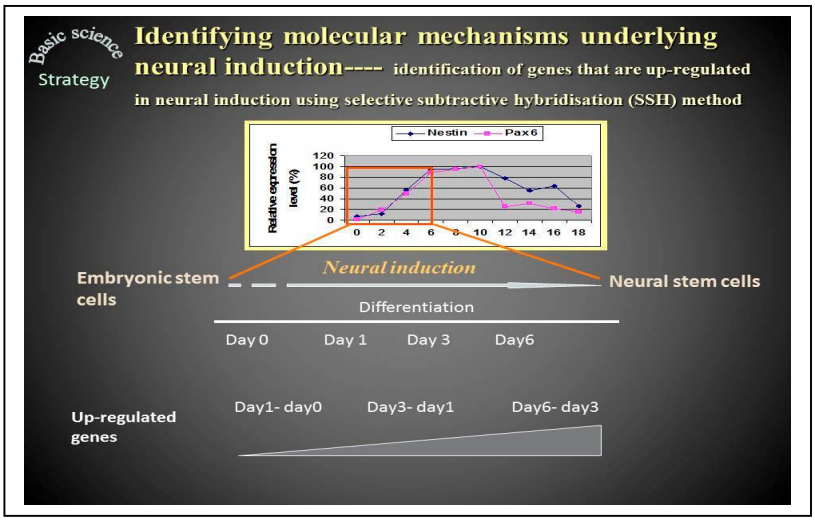

Fig. 3. A summary of the strategy employed to uncover the up-regulated genes during neural induction. Embryonic stem cells were driven to differentiate toward neural lineage. The cells were collected at different stages of differentiation: ESC, 1 day, 3 days, and 6 days of differentiation, respectively. The total RNAs isolated from the collected cells were used to make selective subtractive cDNA libraries.

The top 100 up-regulated genes were analysed and summarised in Fig. 4.

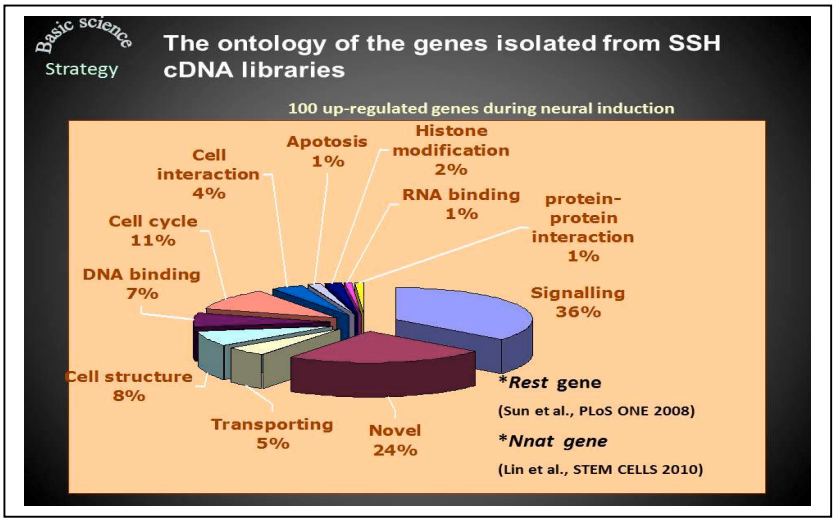

Fig. 4. The analysis of top 100 up-regulated genes obtained by the SSH methodology, which show that the majority of the up-regulated genes are involved in signalling at 36%, followed by novel genes at 24%

The derived data from this project are not published. However, I selected one of the genes, *Nnat*, for further investigation. The reason for selecting this gene is because I found the increase of *Nnat*

expression coincided perfectly with the course of neural induction. The *Nnat* project was described in section 2.2.3.4.

In parallel with this project, I was engaging with the Rest project, which was to define the role of Rest in different stages of neural development. The outcomes of the Rest project were described below.

2.2.3.3 Investigating the role of Rest in different stages of neural development

Rest has been postulated to act as a master regulator of neuronal gene expression in both the developing and mature nervous systems. Others and we have shown that Rest is highly expressed in blastocysts and ES cells, but that expression decreases as neural development proceeds (Sun, 2005; Ballas, 2005). In fact, downregulation of Rest has been proposed to be obligate for differentiation of neural progenitors (Ballas, 2005) and more recently, it has been proposed that Rest haplodeficiency results in loss of pluripotency markers and a reciprocal gain in differentiation markers (Singh et al., 2008). Taken together, these observations suggest that Rest may play a crucial role at several stages of neural development. I determined the function of Rest during neural development from ES cells through NSCs and neural progenitor cells (NPCs) to mature neurons using an in vitro ES cell-based developmental modelling system.

I have sought to address this issue by using a combination of gene targeting and RNAi to create ES lines expressing a range of Rest concentrations, which I have used to investigate the effect of Rest deficiency during ES cell-derived neural development. The study has been published in PLoS ONE (2008) 3 (11):e3656-e3668 (the impact factor was 4.7 at the time of publication) (see Appendix 2). We found that deletion of a single Rest allele does not result in any change in neural differentiation. Instead, we found that Rest levels have to be decreased by more than 92% to precipitate any phenotype. Rest ablation impairs the extracellular matrix (ECM) components and impedes the production of Nestin^{+} NSCs, NPCs and neurons. Furthermore, neurons derived from REST-null ES cells are devoid of elaborate processes, have defects in migration and undergo increased cell death. Importantly, all of these phenotypic effects of Rest ablation were rescued by treatment with laminins, a key component of the ECM that has been implicated in neuronal migration and more latterly in development of the neural plate. The major contribution of this paper is defining a novel mechanism by which Rest regulates development of both NSCs and mature neurons by controlling expression of key components of the ECM. My contributions in this paper include establishing embryonic stem cell-derived neural differentiation model, generating ideas, designing experiments, conducting experiments, supervising students to carry out some of experiments, writing manuscript for publication (as a corresponding author).

2.2.3.4 Defining the role of Nnat in neural induction

Knowledge of the mechanism underlying neural induction is primarily derived from studies in Xenopus, in which bone morphogenetic proteins (BMPs) act as a decisive inhibitory force during neural induction. This generates the neural default model, which postulates that in the absence of BMP signalling, ectodermal cells will adopt a neural fate (Hermmati-Brivanlou et al., 1994). However, the default model remains a debated issue (Stern, 2006; Munoz-Sanju et al., 2006). To date, several signalling pathways, including BMP (Lamb et al., 1993; SasaiY, 1994; Liem et al., 1995; Di-Gregorio et al., 2007), FGF (Streit et al., 2000; Wilson et al., 2000; Kuroda et al., 2005; Kunath et al., 2007; Stavridis et al., 2007; Chen et al., 2010; Cohen et al., 2010), $Ca2^{+}$ (Moreau et al., 1994; 2008), Wnt (Wilson et al., 2001; Aubert et al., 2002; Heeg-Truesdell et al., 2006; Tonge et al., 2010), and Shh (Maye et al., 2004) have been shown to play critical roles in neural induction in various species. BMP4, FGFs, Wnt, and Shh exert their regulatory roles in neural induction by binding to their receptors in the cell membrane of ectodermal cells, which in turn trigger intracellular signalling

cascades. These factors exert extrinsic influences on ectodermal cells to inhibit or induce neural induction. So far, no intrinsic factor (other than Smad7, if it can be considered as one) (de Almeida et al., 2008) has been identified and its role in neural induction is basically unknown.

In a wider study to screen for genes involved in neural induction (Fig. 4), I had identified a novel intrinsic neural initiator, Neuronatin (Nnat). Nnat is a maternal imprinted gene located on mouse chromosome 2 (Kagitani et al., 1997), which encodes a membrane protein in the endoplasmic reticulum (ER) (Kagitani et al., 1997) and is predominantly expressed in the developing brain (Kagitani et al., 1997; Joseph et al., 1994). Transcription processing of Nnat gene leads to the generation of two alternatively spliced isoforms (α and β mRNA) (Joseph et al., 1995) and their expression patterns suggest that Nnat plays a role in brain development (Wijnholds et al., 1995; Dou et al., 1996). However, its precise functions during central nervous system development remain to be elucidated. In this study, we address the role and mechanistic action of Nnat in neural induction and neuronal differentiation using an in vitro mammalian ESC-based neural lineage modelling system and an in vivo Xenopus neural induction system.

We found that Nnat acts as an intrinsic factor to promote neural fate in mammals and Xenopus. ESCs lacking this intrinsic factor fail to undergo neural induction despite the inhibition of the BMP pathway. We show that Nnat initiates neural induction in ESCs through increasing intracellular $Ca2^{+}$ ([$Ca2^{+}$]i) by antagonising $Ca2^{+}$-ATPase isoform 2 (sarco/endoplasmic reticulum $Ca2^{+}$-ATPase isoform 2) in the endoplasmic reticulum, which in turn increases the phosphorylation of Erk1/2 and inhibits the BMP4 pathway and leads to neural induction in conjunction with FGF/Erk pathway (Fig. 5).

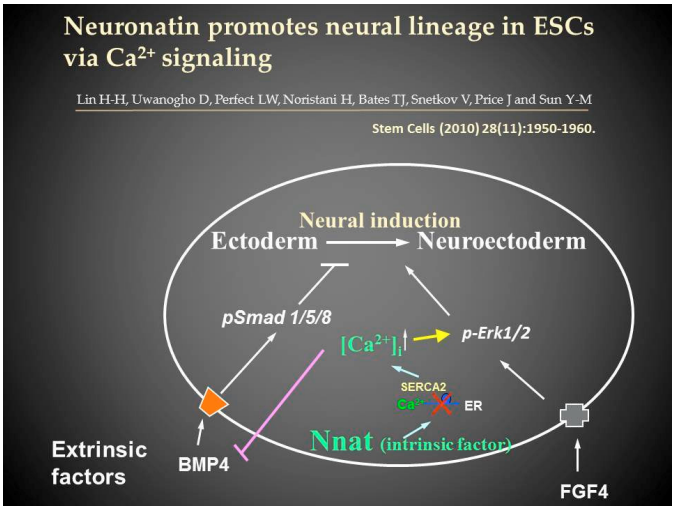

Fig. 5. A schematic diagramme depicts the Nnat-mediated neural induction in ESCs.

The results were published in STEM CELLS (2010);28:1950–1960 (the impact factor was 7.8 at the time of publication) (see Appendix 3). My contributions to this paper were generating ideas, designing experiments, supervising Master and PhD students to carry out experiments, managing the project, writing manuscript for publication (as a corresponding author) and obtaining funding. The major contribution of this paper is that we identified a novel or the first intrinsic factor that regulates neural induction in mammals.

2.2.4 Phase 4: the establishment of human ESC-based neural developmental modelling

After spending 8 years in the mouse ESC field, I was keen to get into translational research so I applied for the SoMoPro grant to come to learn more about human ESCs at the Department of biology, faculty of Medicine, Masaryk University.

First, I had to set up the human ESC-based neural developmental modelling from scratch, as no body in this Department is working on neural development. Second, adopted this modelling system, I embarked on a project to investigate the role of Activin in the early fate decision during hESC differentiation. Activin/Nodal, members of the transforming growth factor-β (TGF-β) superfamily, exhibit various roles during different stages of embryogenesis. The Activin/Nodal pathway maintains the undifferentiated status of the epiblast in mice (Mesnard et al., 2006), which coincides with the in vitro role of Activin in sustaining the pluripotency of mouse and human embryonic stem cells (ESCs) (Ogawa et al., 2007; Vallier et al., 2005). As development proceeds, the Activin/Nodal pathway plays a crucial role in lineage decisions. In vivo studies showed that different concentrations of Activin elicit distinct responses from Xenopus animal caps, ultimately producing a range of mesodermal fates (Green and Smith, 1990). Nodal-/- mice fail to form both the mesoderm and the definitive endoderm but show precocious neural differentiation (Camus et al., 2006), suggesting that the Activin/Nodal pathway promotes the mesendodermal lineage and inhibits neural fate. Furthermore, inhibition of Activin signaling has been shown to promote neural fate in human ESCs and induced pluripotent stem cells (iPSCs) (Smith et al., 2008; Chambers et al., 2009). The action in which the Activin/Nodal pathway promotes mesendodermal fate over neural fate has begun to be investigated. Chng et al. (2010) recently suggested that Activin/Nodal signaling acts through Smad-interacting protein 1 (SIP1) to regulate the cell-fate decision between neuroectoderm and mesendoderm fates. However, the precise molecular mechanisms underlying the specification of mesendodermal fate and the inhibition of neural fate by the Activin/Nodal pathway remain to be elucidated.

I supervised a PhD student and a technician to carry out the project. We found that the Activin/ALK4 pathway directly recruits protein tyrosine phosphatase 1B (PTP1B) and stimulates its release from the endoplasmic reticulum through ALK4-mediated cleavage. Subsequently, PTP1B suppresses p-ERK1/2 signalling to inhibit neural specification and promote mesendodermal commitment (Fig. 6, left panel). In summary, PTP1B keeps the balance between Activin/ALK4 and p-ERK1/2 signalling pathways. When PTP1B is high then the Activin/ALK4 pathway is in control and that drives ESC differentiation toward mesendodermal fate, whereas when PTP1B is low, the p-ERK1/2 pathway is dominant and that promotes ESC to adopt neural fate (Fig. 6, right panel). Our finding suggested a novel noncanonical Activin signalling pathway functions in lineage specification of mouse and human embryonic stem cells.

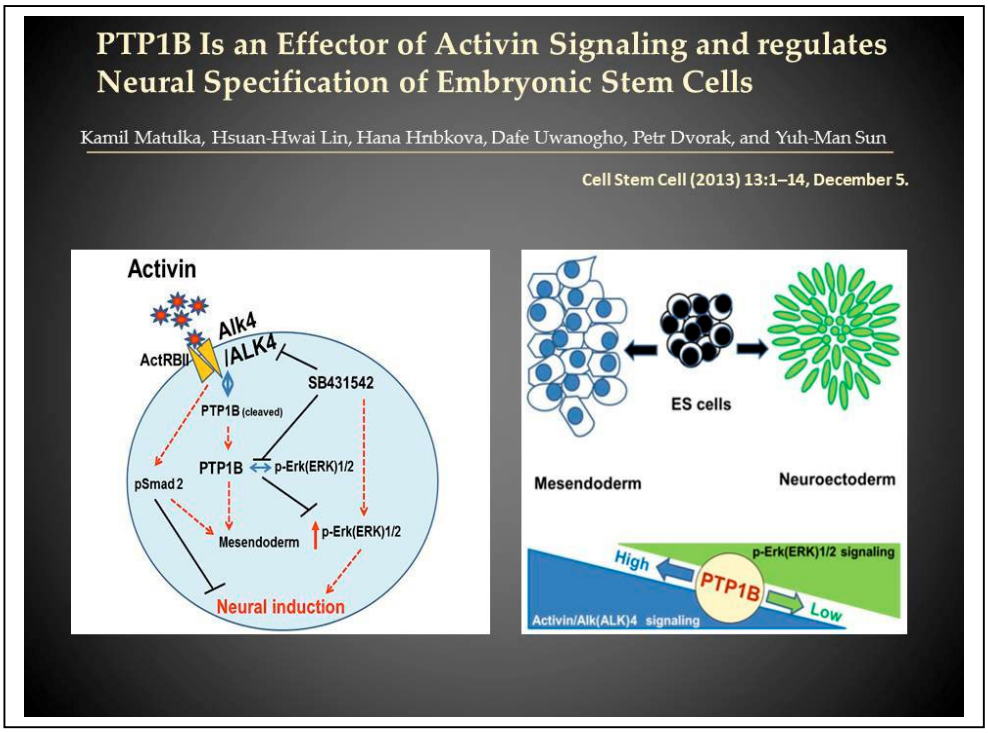

Fig. 6. Summaries of the role of PTP1B in Activin-mediated early fate descision during ESC differentiation. A) A schematic diagram depicts the Activin/ALK4/pSmad2 pathway promotes mesendo-dermal fate in ESCs, in part, via PTP1B that dephos-phorylates (or inactivates) p-ERK1/2 signalling, which leads to the inhibition of neural induction. B) A graphic summary to describe the balance between the Activin and p-ERK1/2 pathways by PTP1B.

This study has been published in Cell Stem Cell (2013) December 5; 13:1–14 (the impact factor was 25.911 at the time of publication) (see Appendix 4). My contributions to this paper were generating ideas, designing experiments, supervising Master and PhD students to carry out experiments, managing the project, writing manuscript for publication (as a corresponding author) and obtaining funding. The major contribution of this paper is that PTP1B acts as a switch within the ESC to choose mesendodermal or neuroectodermal fate by balancing the Activin and p-ERK1/2 pathways.

2.3 Future research directions

I divide my future research direction into two domains: basic research and translational research. In basic research, I will continue to investigate the molecular mechanism underling neural cell specification using the human ESC-based developmental modelling system. In translational research, I believe that fortunate people should contribute their abilities to help less fortunate people. Thus, I wish to contribute my expertise in stem cell work to explore the potential molecular mechanisms underlying psychiatry disorders (e.g. schizophrenia and autism) using human pluripotent stem cell (hPSC)-based psychiatric disorder modelling. I hope that my efforts can solicit more interest in developing tailored treatments for the patients who lost their thinking and control of their behaviour. To this end, I am the coordinator of a grant application to Horizon 2020 (H2020) and have recruited several top scientists in the EU (including UK, Norway, Sweden, Slovenia, Czech Republic) and in America. We have submitted an application (the first-step submission) for a H2020 grant in Oct. 2014.

2.4 Acknowledgements

I thank my beloved husband for his unconditional supports and help. Moreover, I would like to show my gratitude to my team members who are willing to look beyond their limitations.

2.5 References

Andres ME, Burger C, Peral-Rubio MJ, Battaglioli E, Anderson ME, Grimes J, Dallman J, Balls N, and Mandel G. (1999) CoREST: a functional corepressor required for regulation of neural-specific gene expression. Proc. Natl. Acad. Sci. USA *96*, 9873–9878.

Aubert J, Dunstan H, Chambers I et al. (2002) Functional gene screening in embryonic stem cells implicates Wnt antagonism in neural differentiation. Nat. Biotechnol. 20:1240–1245.

Ballas, N. et al. (2001) Regulation of neuronal traits by a novel transcriptional complex. Neuron 31:353–365.

Ballas N, Grunseich C, Lu DD, Speh JC, and Mandel G. (2005) REST and its corepressors mediate plasticity of neuronal gene chromatin throughout neurogenesis. Cell 121: 645–657.

Battaglioli E, Andres ME, Rose DW, Chenoweth JG, Rosenfeld MG, Anderson ME, and Mandel G. (2002) REST repression of neuronal genes requires components of the hSWI.SNF complex. J. Biol. Chem. 277: 41038–41045.

Bruce AW, Donaldson IJ, Wood IC, Yerbury SA, Sadowski MI, Chapman M, Gottgens B, and Buckley NJ. (2004) Genome-wide analysis of repressor element 1 silencing transcription factor/neuron-restrictive silencing factor (REST/NRSF) target genes. Proc. Natl. Acad. Sci. USA 101:10458–10463.

Camus A, Perea-Gomez A, Moreau A, and Collignon J. (2006) Absence of Nodal signaling promotes precocious neural differentiation in the mouse embryo. Dev. Biol. 295:743–755.

Chambers SM, Fasano CA, Papapetrou EP, Tomishima M, Sadelain M, and Studer L. (2009) Highly efficient neural conversion of human ES and iPS cells by dual inhibition of SMAD signaling. Nat. Biotechnol. 27:275–280.

Chen Z-F, Paquette AJ, and Anderson DJ. (1998) NRSF/REST is required in vivo for repression of multiple neuronal target genes during embryogenesis. Nat. Genet. 20:136–142.

Chen CW, Liu CS, Chiu IM et al. (2010) The signals of FGFs on the neurogenesis of embryonic stem cells. J. Biomed. Sci. 29:17–33.

Chng Z, Teo A, Pedersen RA, and Vallier L. (2010) SIP1 mediates cell-fate decisions between neuroectoderm and mesendoderm in human pluripotent stem cells. Cell Stem Cell 6:59–70.

Chong JA, Tapia-Ramirez J, Kim S, Toledo-Aral JJ, Zheng Y, Boutros MC, Altshuller Y-M, Frohman MA, Kraner SD, and Mandel G. (1995) REST: a mammalian silencer protein that restricts sodium channel gene expression to neurons. Cell 80:949–957.

Cimadamore F1, Fishwick K, Giusto E, Gnedeva K et al. (2011) Human ESC-derived neural crest model reveals a key role for SOX2 in sensory neurogenesis. Cell Stem Cell 8(5):538-551.

Cohen MA, Itsykson P, and Reubinoff BE. (2010) The role of FGF-signaling in early neural specification of human embryonic stem cells. Dev. Biol. 340:450–458.

Coucouvanis E and Martin GR. (1995) Signals for death and survival: a two-step mechanism for cavitation in the vertebrate embryo. Cell 83: 279–287.

de Almeida I, Rolo A, Batut J et al. (2008) Unexpected activities of Smad7 in Xenopus mesodermal and neural induction. Mech. Dev. 125: 421–431.

Di-Gregorio A, Sancho M, Stuckey DW et al. (2007) BMP signaling inhibits premature neural differentiation in the mouse embryo. Development 134:3359–3369.

Dou D and Joseph R. (1996) Cloning of human neuronatin gene and its localization to chromosome-20q 11.2–12: The deduced protein is a novel “proteolipid’. Brain Res. 723:8–22.

Gardner RL and Rossant J. (1979) Investigation of the fate of 4–5 day post-coitum mouse inner cell mass cells by blastocyst injection. J. Embryol. Exp. Morphol. 52:141–152.

Gilbert S.F. (2010) Developmental Biology, ninth edition, Sinauer.

Green JB and Smith JC. (1990) Graded changes in dose of a Xenopus activin A homologue elicit stepwise transitions in embryonic cell fate. Nature 347:391–394.

Hakimi MA, Bochar DA, Chenoweth J, Lane WS, Mandel G, and Shiekhattar R. (2002) A core-BRAF35 complex containing histone deacetylase mediates repression of neuronal-specific genes. Proc. Natl. Acad. Sci. USA 99:7420–7425.

Heeg-Truesdell E and LaBonne C. (2006) Neural induction in Xenopus requires inhibition of Wnt-beta-catenin signaling. Dev. Biol. 298:71–86.

Hermmati-Brivanlou A and Melton DA. (1994) Inhibition of activin receptor signaling promotes neuralization in Xenopus. Cell 77:273–281.

Huang Y, Myers SJ, and Dingledine R. (1999) Transcriptional repression by REST: recruitment of Sin3A and histone deacetylase to neuronal genes. Nat. Neurosci. 2: 867–872.

Joseph R, Dou D, and Tsang W. (1994) Molecular cloning of a novel mRNA (neuronatin) that is highly expressed in neonatal mammalian brain. Biochem. Biophys. Res. Commun. 201:1227–1234.

Joseph R, Dou D, and Tsang W. (1995) Neuronatin mRNA: Alternatively spliced forms of a novel brain-specific mammalian developmental gene. Brain Res. 690:92–98.

Kagitani F, Kuroiwa Y, Wakana S et al. (1997) Peg5/Neuronatin is an imprinted gene located on sub-distal chromosome 2 in the mouse. Nucleic Acids Res. 25:3428–3432.

Kershaw TR, Rashid-Doubell F, and Sinden JD. (1994) Immunocharacterization of H-2Kb-tsA58 transgenic mouse hippocampal neuroepithelial cells. Neuroreport 5:2197–2200.

Kunath T, Saba-El-Leil MK, Almousailleakh M et al. (2007) FGF stimulation of the Erk1/2 signaling cascade triggers transition of pluripotent embryonic stem cells from self-renewal to lineage commitment. Development 134:2895–2902.

Kuroda H, Fuentealba L, Ikeda A et al. (2005) Default neural induction: Neuralization of dissociated Xenopus cells is mediated by Ras/MAPK activation. Genes Dev. 19:1022–1027.

Lamb TM, Knecht AK, Smith WC et al. (1993) Neural induction by the secreted polypeptide noggin. Science 262:713–718.

Lawson KA and Pedersen RA. (1992) Clonal analysis of cell fate during gastrulation and early neurulation in the mouse. In Post-implantation Development in the Mouse. Chichester: Wiley (Ciba Found. Symp. 165). pp 3–26.

Liem KFJr, Tremml G, Roelink H et al. (1995) Dorsal differentiation of neural plate cells induced by BMP-mediated signals from epidermal ectoderm. Cell 82:969–979.

Maye P, Becker S, Siemen H et al. (2004) Hedgehog signaling is required for the differentiation of ES cells into neurectoderm. Dev. Biol. 265:276–290.

Mesnard D, Guzman-Ayala M, and Constam DB. (2006) Nodal specifies embryonic visceral endoderm and sustains pluripotent cells in the epiblast before overt axial patterning. Development 133:2497–2505.

Moreau M, Leclerc C, Gualandris-Parisot L et al. (1994) Increased internal $Ca2^{+}$ mediates neural induction in the amphibian embryo. Proc Natl Acad Sci USA 91:12639–12643.

Munoz-Sanju I and Brivanlou AH. (2002) Neural induction, the default model and embryonic stem cells. Nat. Rev. Neurosci. 3:271–280.

Moreau M, Neant I, Webb SE et al. (2008) Calcium signaling during neural induction in Xenopus laevis embryos. Philos. Trans. R. Soc. Lond. B. Biol. Sci. 363:1371–1375.

Ogawa K, Saito A, Matsui H, Suzuki H et al. (2007) Activin-Nodal signaling is involved in propagation of mouse embryonic stem cells. J. Cell Sci. 120:55–65.

Roopra A, Sharling L, Wood IC, Briggs T, Bachfischer U, Paquette AJ, and Buckley NJ. (2000) Transcriptional repression by neuron-restrictive silencer factor is mediated via the Sin3-histone deacetylase complex. Mol. Cell. Biol. 20:2147–2157.

Roopra A, Qazi R, Schoenike B, Daley TJ, and Morrison JF. (2004) Localized domains of G9a-mediated histone methylation are required for silencing of neuronal genes. Mol. Cell 14:727–738.

Rubenstein JLR and Shimamura K. (1998) Regionalisation of the prosencephalic neural plate. Ann. Rev. Neurosci. 21:445–477.

Sakurai H1, Inami Y, Tamamura Y, Yoshikai T, Sehara-Fujisawa A, Isobe K. (2009) Bidirectional induction toward paraxial mesodermal derivatives from mouse ES cells in chemically defined medium. Stem Cell Res. 3:157-169.

Sasai Y, Lu B, Steinbeisser H et al. (1994) Xenopus chordin:Anovel dorsalizing factor activated by organizer-specific homeobox genes. Cell 79:779–790.

Schoenherr CJ and Anderson DJ. (1995) The neuron-restrictive silencer factor (NRSF): a coordinate repressor of multiple neuron-specific genes. Science 267:1360–1363.

Schoenherr CJ, Paquette AJ, and Anderson DJ. (1996) Identification of potential target genes for the neuron-restrictive silencer factor. Proc. Natl. Acad. Sci. USA 93:9881–9886.

Shi Y, Lan F, Matson C, Mulligan P, Whetstine JR, Cole PA, Casero RA, and Shi Y. (2004) Histone demethylation mediated by the nuclear amine oxidase homolog LSD1. Cell 119:941–953.

Smith JR, Vallier L, Lupo G, Alexander M, Harris WA, and Pedersen RA. (2008) Inhibition of Activin/Nodal signaling promotes specification of human embryonic stem cells into neuroectoderm. Dev. Biol. 313:107–117.

Singh SK, Kagalwala MN, Parker-Thornburg J, Adams H, and Majumder S. (2008) REST maintains self-renewal and pluripotency of embryonic stem cells. Nature. pp 23. [Epub ahead of print].

Slawny N and O'Shea KS. (2013) Geminin promotes an epithelial-to-mesenchymal transition in an embryonic stem cell model of gastrulation. Stem Cells Dev. 22:1177-1189.

Stavridis MP, Lunn JS, Collins BJ et al. (2007) Discrete period of FGFinduced Erk1/2 signaling is required for vertebrate neural specification. Development 134:2889–2894.

Stern CD. (2006) Neural induction: 10 years on since the ‘default model’. Curr. Opin. Cell Biol. 18:692–697.

Streit A, Berliner AJ, Papanayotou C et al. (2000) Initiation of neural induction by FGF signaling before gastrulation. Nature 406:74–78.

Sun Y-M, Greenway DJ, Johnson R, Street M, et al. (2005) Distinct profiles of REST interactions with its target genes at different stages of neuronal development. Mol. Biol. Cell 16:5630–5638.

Sun Y-M, Cooper M, Finch S, Lin H-H, Chen Z-F, Williams B and Buckley NJ. (2008) REST-mediated regulation of extracellular matrix is crucial for neural development. PLoS ONE 3:e3656.

Tonge PD, and Andrews PW. (2010) Retinoic acid directs neuronal differentiation of human pluripotent stem cell lines in a non-cell-autonomous manner. Differentiation 80:20–30.

Vallier L, Alexander M, and Pedersen RA. (2005) Activin/Nodal and FGF pathways cooperate to maintain pluripotency of human embryonic stem cells. J. Cell Sci. 118:4495–4509.

Wijnholds J, Chowdhury K, and Wehr R. (1995) Segment-specific expression of the neuronatin gene during early hindbrain development. Dev. Biol. 171:73–84.

Wilson SI, Graziano E, Harland R et al. (2000) An early requirement for FGF signaling in the acquisition of neural cell fate in the chick embryo. Curr. Biol. 10:421–429.

Wilson SI, Rydstro¨m A, Trimborn T et al. (2001) The status of Wnt signaling regulates neural and epidermal fates in the chick embryo. Nature 411:325–330.

Appendix 1

Distinct Profiles of REST Interactions with Its Target Genes at Different Stages of Neuronal Development

Yuh-Man Sun, Deborah J. Greenway, Rory Johnson, Miyoko Street, Nikolai D. Belyaev, Jim Deuchars, Thomas Bee, Sandra Wilde, and Noel J. Buckley

Molecular Biology of the Cell (2005) 16:5630–5638.

Molecular Biology of the Cell
Vol. 16, 5630–5638, December 2005

Distinct Profiles of REST Interactions with Its Target Genes at Different Stages of Neuronal Development[D]

Yuh-Man Sun,*† Deborah J. Greenway,†‡ Rory Johnson,* Miyoko Street,* Nikolai D. Belyaev,* Jim Deuchars,§ Thomas Bee,* Sandra Wilde,* and Noel J. Buckley*§

*School of Biochemistry and Microbiology, §School of Biomedical Sciences, and ‡School of Biology, University of Leeds, Leeds LS2 9JT, United Kingdom

Submitted July 28, 2005; Revised September 15, 2005; Accepted September 20, 2005
Monitoring Editor: Marianne Bronner-Fraser

Differentiation of pluripotent embryonic stem (ES) cells through multipotent neural stem (NS) cells into differentiated neurons is accompanied by wholesale changes in transcriptional programs. One factor that is present at all three stages and a key to neuronal differentiation is the RE1-silencing transcription factor (REST/NRSF). Here, we have used a novel chromatin immunoprecipitation-based cloning strategy (SACHI) to identify 89 REST target genes in ES cells, embryonic hippocampal NS cells and mature hippocampus. The gene products are involved in all aspects of neuronal function, especially neuronal differentiation, axonal growth, vesicular transport and release, and ionic conductance. Most target genes are silent or expressed at low levels in ES and NS cells, but are expressed at much higher levels in hippocampus. These data indicate that the REST regulon is specific to each developmental stage and support the notion that REST plays distinct roles in regulating gene expression in pluripotent ES cells, multipotent NS cells, and mature neurons.

INTRODUCTION

Neural development proceeds via a series of commitments whereby pluripotent embryonic stem (ES) cells give rise to more restricted multipotent neural stem (NS) cells, which in turn generate differentiated neurons. This is orchestrated and accompanied by wholesale changes in transcriptional programs and patterns of gene expression. One factor that has emerged as a key player is a Krüppel-type zinc-finger transcription factor, RE1-silencing transcription factor (REST; also known as the neuron-restrictive silencing factor, NRSF). Understanding the molecular mechanism underlying the REST regulatory roles during neuronal differentiation will shed light on the process of neuronal development. The first step in decoding the REST-directed mechanism is to profile its immediate target genes, which elucidate REST's possible biological functions.

REST interacts with RE1 sites and recruits corepressors including mSin3A (Huang *et al.*, 1999, Roopra *et al.*, 2000) and CoREST (Andrés *et al.*, 1999, Ballas *et al.*, 2001), which in turn, recruit multiple cofactors and transcriptional regulators including histone deacetylases 1 and 2, G9a histone methyltransferase (Roopra *et al.*, 2004), H3 lysine 4 demethylase LSD1 (Shi *et al.*, 2004), and chromatin remodeling machinery, including BRG1, BAF57, and BAF170 (Battaglioli *et al.*, 2002) and BRAF35 (Hakimi *et al.*, 2002). There are over 1300 RE1 sites in the human and murine genomes (Bruce *et al.*, 2004; www.bioinformatics.leeds.ac.uk/group/online/RE1db/re1db_home.htm) and the majority encode ion channels, neurotransmitters, growth factors and hormones, and factors involved in axonal guidance and vesicle trafficking, and molecules involved in maintenance of the cytoskeleton and extracellular matrix (Schoenherr *et al.*, 1996; Bruce *et al.*, 2004). Because many of these target genes are expressed by postmitotic neurons, the role of REST was originally perceived as that of silencer of neuron-specific genes in non-neuronal cells (Chong *et al.*, 1995; Schoenherr and Anderson, 1995). However, several observations have tempered this view. First, REST is expressed in many adult postmitotic neurons, most notably those of the hippocampus, where both REST and its target genes are modulated in the adult hippocampus in response to ischemic or epileptic insults (Palm *et al.*, 1998; Calderone *et al.*, 2003). Second, we have shown that, in most neural and nonneural cell lines, REST principally acts as a repressor of active gene transcription rather than as a silencer (Wood *et al.*, 2003; Belyaev *et al.*, 2004; Bruce *et al.*, 2004). Third, REST has been shown to be sufficient to drive neuronal differentiation of adult neural stem cells (Kuwabara *et al.*, 2004; Su *et al.*, 2004) and even myoblasts (Watanabe *et al.*, 2004). Fourth, REST is present at all stages of neural development from the blastocyst, through embryonic development in most tissues including the neuroepithelium. Finally, $REST^{-/-}$ mice are embryonic lethal around E10 and do not show widespread precocious expression of REST target genes and introduction of a dominant-negative REST construct into chick myotome caused up-regulation of some, but not all, REST target genes (Chen

This article was published online ahead of print in *MBC in Press* (http://www.molbiolcell.org/cgi/doi/10.1091/mbc.E05–07–0687) on September 29, 2005.

[D] The online version of this article contains supplemental material at *MBC Online* (http://www.molbiolcell.org).

† These authors contributed equally to this work.

Address correspondence to: Yuh-Man Sun (y.sun@bmb.leeds.ac.uk).

Abbreviations used: RE1, repressor element 1; NRSE, neuron-restrictive silencer element; REST, repressor element 1 silencing transcription factor; NRSF, neuron-restrictive silencing factor; ES, embryonic stem cell; NS, neural stem cell; EMSA, electrophoretic mobility shift assay.

Supplemental Material can be found at:
http://www.molbiolcell.org/content/suppl/2005/09/23/E05-07-0687.DC1.html

© 2005 by The American Society for Cell Biology

et al., 1998), whereas constitutive expression of REST down-regulated some target genes and caused axon pathfinding errors (Paquette *et al.*, 2000). Taken together, these observations suggest that REST plays distinct roles in embryonic and adult cells and that this complexity might be reflected in the range of target genes that REST interacts with at different developmental stages.

In this study, we directly investigate this hypothesis by using a novel chromatin immunoprecipitation (ChIP) cloning strategy based on selective amplification of ChIP (SACHI) to identify REST target gene interactions in ES cells, hippocampal NS cell line, MHP36 (Kershaw *et al.*, 1994) and mature hippocampus, all of which represent distinct stages of neuronal development. Using this technique, we identify 81 novel REST targets and further, we show that REST occupies a unique subset of target genes in each cell type.

MATERIALS AND METHODS

Preparation of Cells, Tissues, and cDNA

Embryonic stem cells, HM-1 (a gift from Dr. J. McWhir, the Roslin Institute), were cultured in Glasgow minimum essential medium (Sigma, St. Louis, MO) supplemented with 5% fetal calf serum, 5% new born calf serum, 1000 U/ml leukemia inhibitory factor (Chemicon, Temecula, CA), and the following reagents: 2 mM L-glutamine, 1% nonessential amino acids, 1 mM sodium pyruvate and 1% β-mercaptoethanol (Invitrogen, Carlsbad, CA). Neural stem cells, MHP36 (a gift from Prof. J. Price, King's College London), were plated out in 10-cm dishes precoated with 10 μl/ml fibronectin and cultured in DMEM/F12 medium in the presence of 47 μg/ml gentamicin and 200 μg/ml geneticin (Invitrogen). The medium was supplemented with 0.03% bovine serum albumin (BSA) Pathocyte (ICN, Costa Mesa, CA), 94 μg/ml human apo-transferrin, 15 μg/ml human putrescine dihydrochloride, 4.7 μg/ml bovine pancreatic insulin, 380 ng/ml L-thyroxine, 317 ng/ml tri-iodo-L-thyronine, 58 ng/ml progesterone, 1.9 mM L-glutamine, 38 ng/ml sodium selenite, 9.4 U/ml heparin sodium salt (all from Sigma), 10 ng/ml human bFGF, and 10 ng/ml murine interferon (PeproTech, Rocky Hill, NJ). Hippocampal tissues were collected by gross dissection from F1 mice (FVB/N $\times$ C57BL6) aged between 16 and 20 d. RNA was extracted using Tri reagent (Sigma) from cells or tissues. RNA was treated with DNAse (Ambion, Austin, TX) and cDNA was made from 2 μg RNA using MMLV (H-point mutant) reverse transcriptase and oligo dT and random hexamers as primers. cDNA was then purified through spin columns (Qiagen, Santa Clarita, CA) using ultra centrifugation and eluted in 50 μl of elution buffer.

Neuronal Differentiation

MH-1 ES cells were differentiated to NS cells and subsequently to mature neurons using monolayer culture in N2B27 medium (Ying *et al.*, 2003). ES cells were plated onto 0.1% gelatin-coated cover slips in 24-well plates at a density of $1 \times 10^4/cm^2$ in ES cell medium. The next day, the ES cell medium was replaced with N2B27 medium, which is a 1:1 mixture of DMEM/F12 medium supplemented with N2 and Neurobasal medium supplemented with B27 (all from Invitrogen). N2 consisted of 25 μg/ml insulin, 100 μg/ml apotransferrin, 6 ng/ml progesterone, 16 μg/ml putrescine, 30 nM sodium selenite, and 50 μg/ml BSA fraction V. Medium was changed every 2 d. Cells were processed for immunocytochemistry at day 0 (prior differentiation) and days 6, 9, and 18 after differentiation.

Immunostaining

Mice (C57BL6) were anesthetized with intraperitoneal Sagatal (60 mg/kg) and transcardially perfused with 4% paraformaldehyde (in 0.1 M phosphate buffer PB; pH 7.4). The brains were removed and postfixed in the same solution for 2 h at 4°C. Transverse sections (50 μm) were then cut on a vibrating microtome (Leica, Milton Keynes, United Kingdom) and collected into phosphate-buffered saline (PBS; pH 7.2). After 10-min washes three times in PBS, the sections were incubated with rabbit anti-REST primary antibody P18 (Santa Cruz Biotechnology, Santa Cruz, CA) for 12–18 h at 4°C. After 10-min washes three times in PBS, sections were incubated with a Cy3-conjugated anti-rabbit secondary antibody (1:1000 in PBS; Jackson ImmunoResearch, Luton, United Kingdom) for $\sim$ 4 h at room temperature. These sections were then washed 10 min three times in PBS, air-dried onto glass slides, and mounted under a coverslip using VectaMount mounting medium (Vector Laboratories, Peterborough, United Kingdom). The sections were viewed under a Nikon E600 microscope (Melville, NY) equipped with epifluorescence and images obtained via an integrating analogue CCD camera (JVC KYF 55B) attached to an Acquis image capture system (Synoptics Ltd, Cambridge, United Kingdom). The fluorescent images were converted to greyscale, inverted and adjusted for brightness/contrast/intensity and color balance using CorelDraw 11 (Corel Systems, Ottawa, Ontario, Canada).

ES cells, derived NS cells and neurons, and MHP36 cells were fixed in 3.5% paraformaldehyde for 20 min and stained with REST antibody (1: 300; Santa Cruz Biotechnology) alone or in combination with Sox1 (1:1000; Chemicon), Tuj1 (1:200; COVANCE, Princeton, NJ) and NeuN (1:500; Chemicon) antibodies overnight at 4°C.

Chromatin Immunoprecipitation

Cells (1×10^8 cells) or tissues (minced, 100 mg wet weight) were fixed for 10 min in 0.37% or 15 min in 1% formaldehyde, respectively. The fixation reaction was quenched with 0.125 M glycine. Nuclei were isolated by incubation on ice for 10 min in cell lysis buffer (10 mM Tris-HCl, pH 8.0, 10 mM NaCl, 0.2% NP40, 10 mM sodium butyrate, and protease inhibitors) and lysed in nuclei lysis buffer (50 mM Tris-HCl, pH 8.1, 10 mM EDTA, 1% SDS, 10 mM sodium butyrate, and protease inhibitors) for 10 min on ice. The lysate was then sonicated to shear the chromatin, cell debris was removed by centrifugation, and IP dilution buffer was added (20 mM Tris-HCl, pH 8.1, 150 mM NaCl, 2 mM EDTA, 1% Triton-X-100, 0.01% SDS, 10 mM sodium butyrate, and proteinase inhibitors). Chromatin was precleared for 3 h at 4°C with 200 μl of protein G-Sepharose blocked with 5% BSA. Whole cell extract was divided into aliquots: 270 μl kept as input chromatin and equal aliquots were incubated separately with anti-REST (P-18) and anti-HA (as a negative control) antibodies (Santa Cruz Biotechnology). Immune complexes were collected by rotation at 4°C for 3 h with 100 μl blocked protein G-Sepharose. Beads were washed twice with wash buffer 1 (20 mM Tris-HCl, pH 8.1, 50 mM NaCl, 2 mM EDTA, 1% Triton-X-100, and 0.1% SDS), once with wash buffer 2 (10 mM Tris-HCl, pH 8.1, 250 mM LiCl, 1 mM EDTA, 1% NP-40, 1% deoxycholic acid), and twice with TE buffer. Immune complexes were eluted with elution buffer (100 mM $NaHCO_3$, 1% SDS) and cross-links were reversed by incubation at 65°C for 6 h in the presence of 5 μg RNase A and 0.3 M NaCl. Proteinase K, 90 μg, was added and samples were incubated overnight at 45°C. DNA was purified using phenol:chloroform extraction and ethanol precipitation. DNA from input sample was resuspended in 200 μl water, and DNA was pulled down by REST and HA antibodies in 100 μl water. Two-microliter aliquots were analyzed in real time PCR using primers designed adjacent to the RE1 regions.

ChIP Cloning

A cloning protocol was devised to specifically amplify RE1 containing sequences from the DNA output of anti-REST immunoprecipitated DNA. The principal of this procedure was to enrich target sequences by a nested PCR strategy using primers corresponding to the RE1 sequence and to end-ligated adaptors. The detailed procedure is summarized in Figure 1. After immunoprecipitation of fixed, sonicated chromatin but before elution of DNA from protein G-Sepharose, the sheared DNA ends were blunt-ended using mung bean nuclease, followed by adding phosphate to the 5′-ends of DNA using T4 polynucleotide kinase (BioLabs, St. Paul, MN). ChIP DNA was ligated with a specific adaptor [5′-CTAATACGACTCACTATAGGGCTCGAGCGGCCGCC-CGGGCAGGT-3′]. The RE1-containing fragments were amplified from the enriched ChIP DNA by two rounds of PCR with primer pairs. First-round PCR used an RE1 degenerate primer 5′-[TT(C)AGA(C)G(A)CCA(T)A(T)G-GACAG-3′] and adaptor primer A [CTAATACGACTCACTATAGGGC-3′]. PCR cycling parameters were 95°C $\times$ 5 min; 94°C $\times$ 10 s, 52°C $\times$ 20 min, 72°C $\times$ 2 min, for 10 cycles; 94°C $\times$ 10 s, 56°C $\times$ 20 min, 72°C $\times$x 2 min, for 25 cycles. Second-round PCR used the RE1 degenerate primer and a nested adaptor primer B [5′-TCGAGCGGCCGCCCGGGCAGGT-3′]. Cycling conditions were 95°C $\times$ 5 min; 94°C $\times$ 10 s, 58°C $\times$ 20 min, 72°C $\times$ 2 min, for 35 cycles. Second-round PCR-products were size selected at 200–800 base pairs and cloned into the pGEM-easy vector. Seven hundred clones from each cell line were isolated and sequenced. We found that the crucial factor for designing an effective RE1 degenerate primer was to contain no degeneracy within the first six base pairs of the 3′-end.

Electrophoretic Mobility Shift Assay

The ability of predicted RE1s obtained from the ChIP cloning protocol to bind REST was assayed by electrophoretic mobility shift assay (EMSA), performed as previously described (Bruce *et al.*, 2004). Nuclear protein extract from U373 expressing the REST DNA-binding domain was mixed with a ^{32}P-labeled *NaV1.2* consensus RE1 probe and 100-fold molar excess unlabeled 24–28-base pair oligonucleotides, derived from cloned REST target genes, were used to compete the gel shift.

Quantitative Real-time PCR

Primers were designed using the primer3 (http://frodo.wi.mit.edu/cgi-bin/primer3/primer3_www_slow.cgi) and "mfold" (http://www.bioinfo.rpi.edu/applications/mfold/old/dna) programs to obtain amplicons using the following parameters: Tm between 58 and 62°C, devoid of secondary structure at Tm 60°C and amplicon size of 50–150 base pairs. ChIP primers were derived from sequence within 500 base pairs of the RE1. Real-time PCR was carried out using SYBR green containing Supermix (Bio-Rad, Hercules,

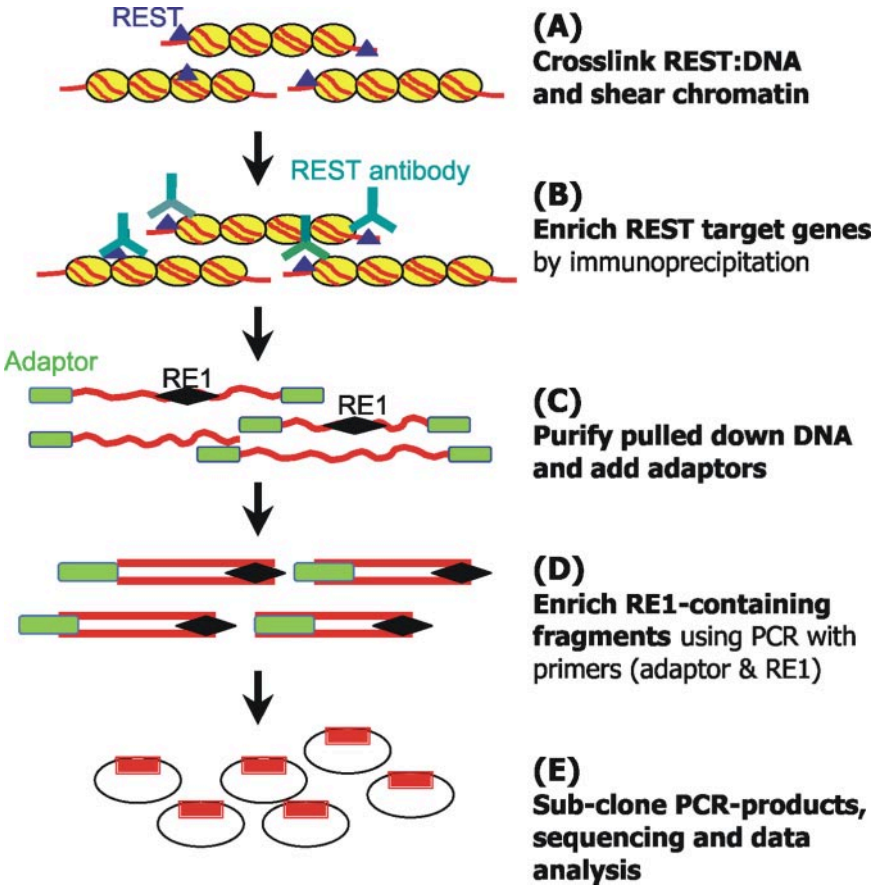

Figure 1. Schematic diagram of ChIP cloning (SACHI) procedure. The technology consists of five steps (A–E). Details are given in *Materials* and *Methods*. Briefly, chromatin is cross-linked (A) and immunoprecipitated (B) to enrich for chromatin fragments containing RE1 binding sites. DNA is then purified and polished, and adaptors are ligated (C). RE1 containing fragments are further enriched by nested PCR (D) before subcloning and analysis (E).

CA) on a Bio-Rad iCycler. All reactions were performed in duplicate. PCR cycle parameters were 95°C for 3 min, followed by 45 cycles of 95°C for 30 s, 60°C for 30 s, and 72°C for 30 s. At the end of the program, the temperature was reduced to 50°C and then gradually increased by 1°C for 10 s up to 96°C, to produce a melt curve. Gene expression was normalized to cyclophilin using the formula $1/2^{\Delta Ct}$, where ΔCt = average unknown gene threshold cycle-average cyclophilin threshold cycle. The expression levels of cyclophilin in ES, MHP cells, and hippocampus showed no significant differences (Supplementary Figure 1).

Data Analysis

The sequences of clones obtained from ChIP cloning were blast-searched against Ensembl mouse database (http://www.ensembl.org/Multi/blastview?Species = Mus_musculus). Homologous sequences were investigated to identify the RE1 consensus: 5′-TY(TC)AGM(AC)R(AG)CCN(ACGT)NRGMCAG-3′ (Bruce *et al.*, 2004). Sequences were classified according to 0, 1, 2, 3, or 4 base pairs mismatch to the consensus RE1. All fragments showing no deviation from the consensus RE1 were then annotated according to the closest genes.

RESULTS

REST Expression Profile during Neuronal Development In Vitro and In Vivo

To establish the involvement of REST in neuronal development, we investigated REST expression profiles in neuronal differentiation in vitro and in vivo. The results showed that REST was expressed in both ES cells (Figure 2A) and its derived NS cells, identified by coexpression of the NS marker Sox1 (Figure 2B). Interestingly, no evident REST staining was seen in differentiated neurons either Tuj1$^+$ or NeuN$^+$ cells (Figure 2, C and D). REST was down-regulated in Tuj1$^+$ cells (Figure 2C). We considered these cells as early neurons because some Tuj1$^+$ cells were also nestin$^+$ (unpublished data). The down-regulation of REST persisted in NeuN$^+$ cells (Figure 2D). These observations contrast with the previous report that REST is initially down-regulated in neural stem cell, but are consistent with the observation that REST is down-regulated in early and mature neurons (Ballas *et al.*, 2005). Our results suggest that, during ES cell differentiation, the expression profile of REST declines as neuronal differentiation proceeds.

However, REST mRNA and protein have been reported to be expressed in both hippocampal neurons and Tuj1$^+$ cells derived from adult hippocampal NS cells, respectively (Kuwabara *et al.*, 2004). Accordingly we examined REST expression in an embryonic hippocampal NS cell line (MHP36 cells) and in hippocampal neurons. In MHP36 cells, nuclear REST was evident (Figure 3A). MHP36 cells are homogenous with regard to both the expression of REST and the progenitor marker, nestin (unpublished data). Furthermore, in hippocampus, REST was restricted to neuronal cell bodies throughout the pyramidal cell layer and the granular layer of the dentate gyrus (Figure 3B), a distribution that is consistent with the REST mRNA expression profile (Kuwabara *et al.*, 2004). These results are different from those reported in early cortical neurons (Ballas *et al.*, 2005). This is a key difference because it illustrates heterogeneity of REST expression within both progenitors and within differentiated postmitotic neurons. Accordingly, we used immunocytochemistry to demonstrate that REST was expressed in HM-1 ES cells, ES-derived NS cells, MHP36 NS cells, and in neurons of the mature hippocampus.

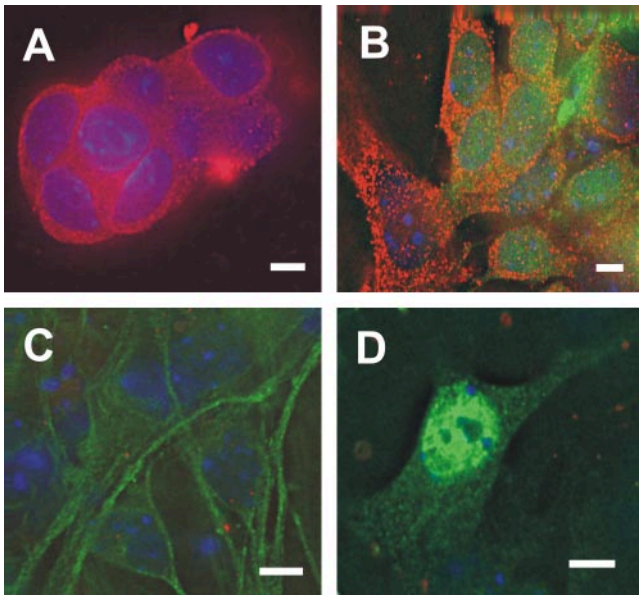

Figure 2. REST expression during embryonic stem (ES) cell differentiation into neurons. (A) REST (red) is expressed in both nuclei and cytoplasm of ES cells before differentiation. (B) REST (red) continues to be expressed in ES-derived neural stem cells identified by $Sox1^+$ immunoreactivity (green). REST is down-regulated in differentiated early and mature neurons identified by $Tuj1^+$ (C) and $NeuN^+$ immunoreactivity (D; green). Nuclei are stained with DAPI (blue). Scale bar, 10 μm.

ChIP Cloning

ChIP has become increasingly the method of choice to identify specific targets of transcription factors. However, the relatively poor enrichment afforded by ChIP means that the vast majority of isolated DNA is not specifically bound to the transcription factor. This massive background precludes any direct cloning approach aimed at identifying novel targets. Here, we have used a selection strategy based on the use of nested PCR to specifically amplify bona fide targets. By using a degenerate RE1 sequence as one PCR primer and two nested linker primers, we were able to amplify those genomic fragments that contained RE1 consensus sequences. Next, we distinguished those sequences that represented bona fide REST targets with EMSAs using unlabeled candidate RE1s to compete the gel shift produced by incubation of the *NaV1.2* consensus RE1 with U373 nuclear extract. This analysis showed that all consensus RE1s inhibited the *NaV1.2* gel shift with varying affinities, whereas only 30% of those sequences containing more than 1-base pair mismatches were bound by REST (Figure 4). Accordingly, in this study, we have focused only on those REST target genes adjacent to consensus RE1s.

Identification of REST Target Genes in Embryonic Stem Cells, Neural Stem Cells, and Hippocampus

Ninety-three independent clones containing consensus RE1s were isolated from ES, NS, and hippocampus using our ChIP cloning procedure. Eighty-nine of these sequences were proximal to a known or predicted transcriptional unit. Sixty RE1 sites were located within intragenic regions, of which 50% were located in the first intron. Another 25 (28%) and 7 (7.8%) RE1s were located in the 5′flanking and 3′flanking regions, respectively (Tables 1 and 2). Four genes comprising *L1cam*, *Syt2*, *GEF1*, and ENSMUSG00000041339 were adjacent to, or contained, two RE1 sites. Thirty-eight genes (42%) were annotated in the Ensembl database (Supplementary Table 1) and were classified into six groups according to their biological functions (Table 1), whereas the remaining 51 genes (58%) corresponded to novel, predicted transcriptional units (Table 2). Of the annotated genes, 24 (65%) are expressed specifically or selectively in the nervous system (Table 1), including those concerned with neurite outgrowth, axonal guidance, vesicle trafficking, signaling, and transcription, consonant with the role of REST in regulating neuronal gene expression. The fact that more than 85% of these genes have not previously been shown to be direct targets of REST is testament to the power of this ChIP cloning protocol to reveal novel target genes.

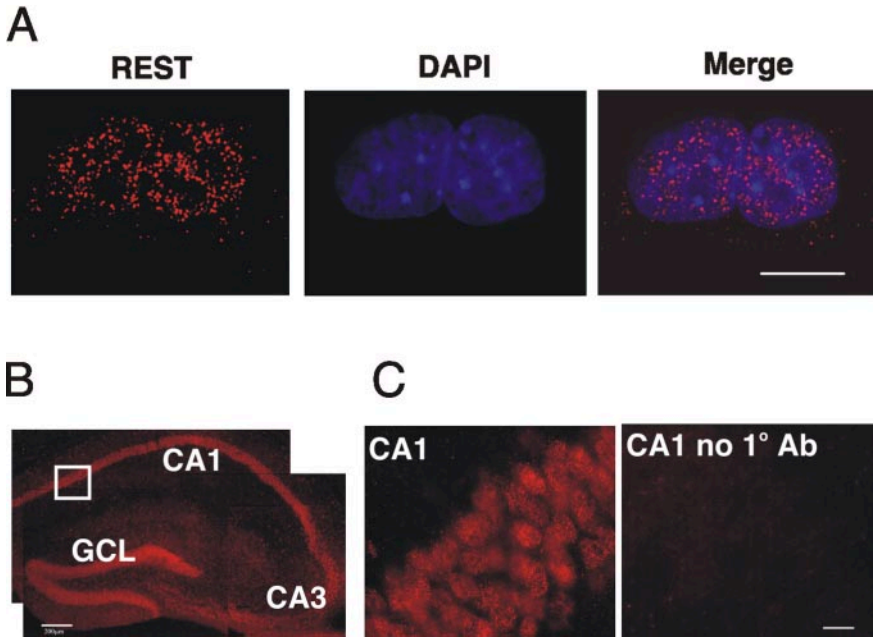

Figure 3. REST immunoreactivity in embryonic hippocampal neural stem (NS) cells and in hippocampus (red). (A) REST is expressed in MHP36 NS cells. Nuclei are stained with DAPI in blue. Scale bar, 10 μm. (B) REST is expressed in CA1, CA2, and CA3 regions and the granule cell layer of the dentate gyrus (GCL) of hippocampus (Scale bar, 250 μm). (C) Higher magnification view of the boxed region in B. A negative control of the CA1 region is included (CA1 no 1° antibody). Scale bar, 25 μm.

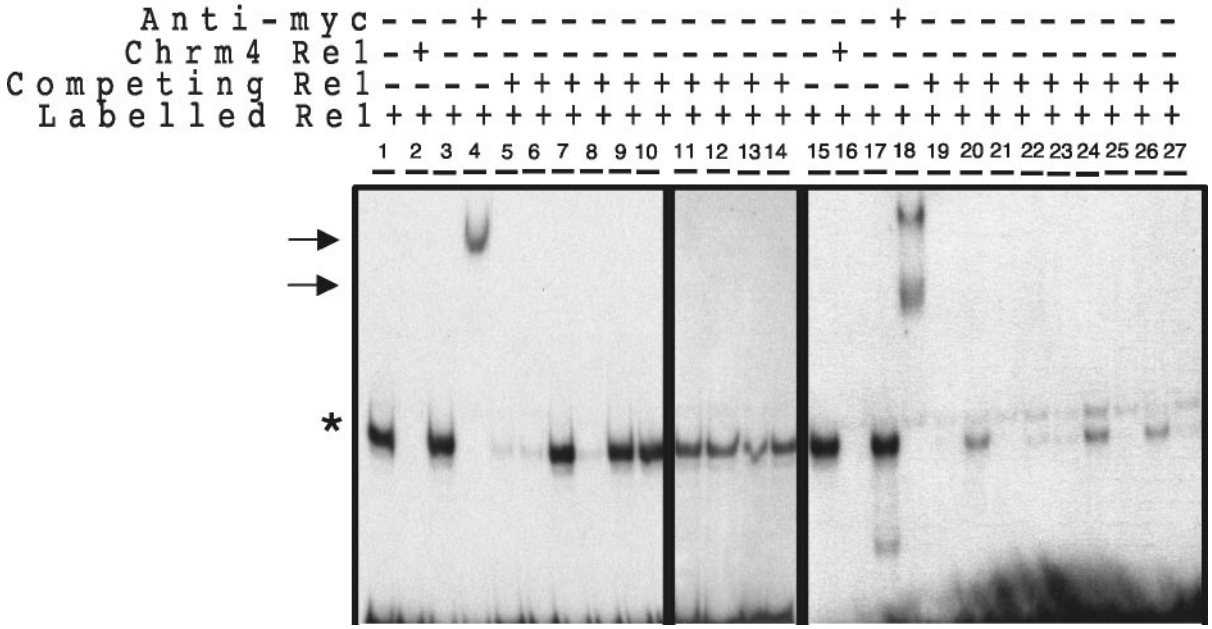

Figure 4. In vitro binding of predicted RE1s using EMSA. The ability of putative RE1 sequences to bind REST was judged by their ability to compete the shift produced by incubation of a radiolabeled rat *NaV1.2* promoter RE1 with a myc-tagged REST DNA binding domain construct (REST DBD), when used at 100-fold molar excess. Lanes 5–14 represent RE1s diverging by more than 1 base pairs mismatch, while lanes 19–27 represent perfect-match consensus RE1s. Specific REST DBD:RE1 complexes are indicated by an asterisk (*). Arrows indicate complexes supershifted by an anti-c-Myc antibody. Lanes 2 and 16 represent the EMSA conducted in the presence of excess *Chrm4* RE1, used as a positive control. Lanes 3 and 17 are EMSAs conducted in the presence of excess nonspecific ds oligonucleotide as a negative control. Lanes 4 and 18 are EMSAs conducted in the presence of an anti-myc antibody.

Validation of Bona Fide REST Target Genes

Validation of REST target genes isolated from ChIP cloning was carried out using conventional ChIP analysis. Thirty-three genes were randomly selected for testing from the isolated 89 genes and included 23 annotated genes and 10 predicted genes. Thirty-two genes (97%) were occupied by REST and showed greater than 1.5-fold enrichments in ChIP assays, in at least one of the three cell types (Figure 5). Four genes comprising *Resp18* and ENSMUSG00000038457 in NS cells, *Zfm1* in ES cells, and NM_173446 in NS cells and hippocampus exhibited markedly high enrichments of 18-, 20-, 46-, 36-, and 12.6-fold, respectively.

The results showed that the equivalent RE1 sites were differentially bound by REST in ES, NS cells, and hippocampus. RE1 sites associated with *Ntrk3*, ENMUSG00000041339/17k, *Olfr1336*, ENSMUSESTG00000031508, *CREBBP/EP300* inhibitory protein 2, *Accn1*, *Arc*, *Atp2b2*, and *Zfm1* genes were bound by REST in ES and NS cells, but not in hippocampus, whereas the RE1 sites associated with *Drd2*, ENSMUSG00000028804, *Syt2*, ENSMUSG00000015719, and *Kirrel3* genes were bound by REST in ES and hippocampus, but not in NS cells. Conversely, RE1 sites associated with NM_175461, *Apba2*, and NM_173446 genes were bound by REST in NS cells and hippocampus, but not in ES cells. Furthermore, some RE1 sites were bound by REST in only one cell type including *Pkd1l3* and *Mbp* genes in ES cells, the *Cacna2d3* gene in NS cells, and *Kcnh1* and *Cspg3* genes in hippocampus. Only one RE1 site, which was located 30 kb upstream from the coding region of *Cspg4* gene, failed to show any occupancy by REST in any cell type. Collectively, these data show that each cell type bears a unique REST occupancy signature.

Gene Expression Profile of the REST Differentially Targeted Genes

To examine the relationship between REST occupancy and expression of the corresponding gene, we carried out real-time quantitative PCR to determine the expression profile of REST target genes in each cell type. Of the 33 verified REST target genes, 20 were randomly selected to determine their expression pattern. One striking difference was evident in the contrast of the expression profile seen in ES and NS cells compared with that seen in the hippocampus. Although most genes were either silent or expressed at relatively low level in both ES and NS cells, with one exception, all genes were expressed at relatively high levels in hippocampus (Table 3). In ES cells, only the *Olfr1336* was silent. In NS cells, 10 of the 20 genes were silent, whereas *CREBBP/EP300* inhibitory protein 2, *Kirrel3*, and ENSMUSG00000051719 genes were expressed at relatively high levels. In hippocampus, only the olfactory receptor gene, *Olfr1336*, was silent. All other genes, including the five unannotated predicted genes were expressed at high levels relative to ES and NS cells.

Most of these target genes are reported to be specifically or selectively expressed in neurons. Exceptions include *CREBBP/EP300* inhibitory protein 2 and *Zfm1*, which are widely expressed and *Kirrel3*, which is expressed in both neural and stromal cells. The fact that REST and so many target genes are coexpressed in the hippocampus, further underscores the principle role of REST in the adult CNS as a regulator, but not a silencer of neuronal gene expression.

DISCUSSION

Transcription factors play crucial roles in all aspects of cellular function including cell proliferation, differentiation,

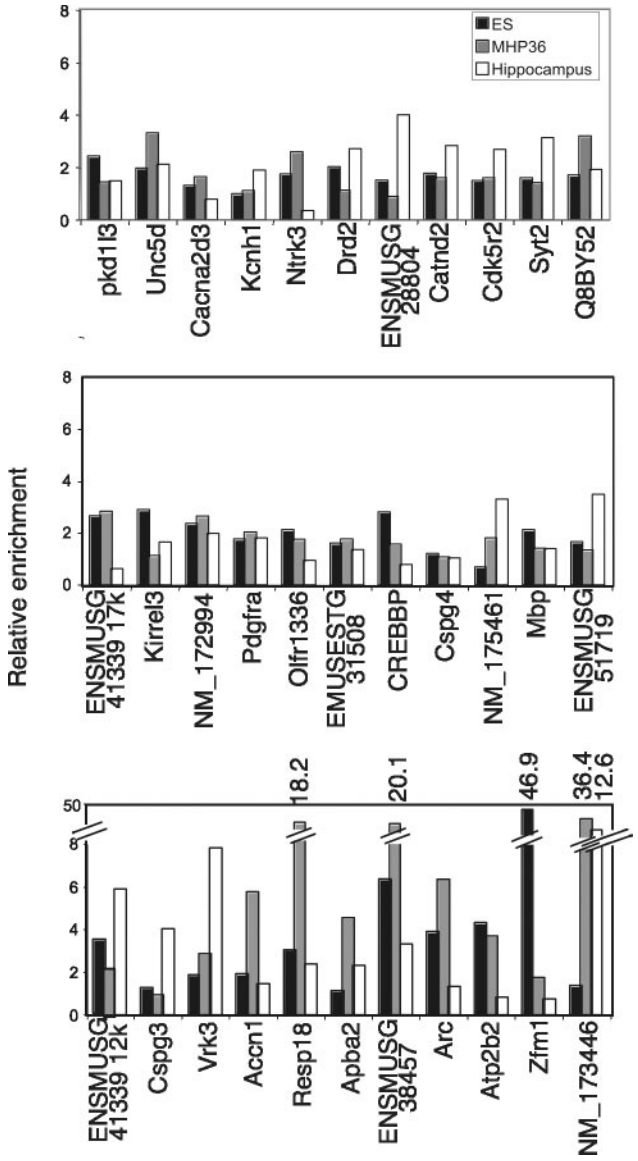

Figure 5. Validation of the isolated RE1 sites from ChIP cloning using in vivo ChIP assay. Thirty-three RE1 containing regions were tested in conventional ChIP for REST occupancy in ES cells (black bars), NS cells (gray bars), and hippocampus (white bars). Only the RE1 associated with *Cspg4* showed no enrichment for REST over background in any cell types, demonstrating the high efficiency of SAHI to identify *bona fide* REST targets.

and survival. Yet, a key issue remains identification of their target genes. It is anticipated that the repertoire of target genes operated on by any given transcription factor will vary according to cell type and developmental stage. Despite this assumption, we have very little knowledge of the cell-specific regulon for any transcription factor in the genome of higher eukaryotes. Several strategies have evolved to identify transcription factor targets including ChIP-chip (Lee *et al.*, 2002), ChIP Display (Barski and Frenkel, 2004), SACO (Impey *et al.*, 2004), GMAT (Roh *et al.*, 2005), and STAGE (Kim *et al.*, 2005). All of these methodologies combine ChIP with SAGE, differential display or microarray to reduce the overwhelming contribution of nonspecific products to ChIP pulldown. Their success rate in identifying validated target genes ranged from 60 to 85%. In this study, we have developed a novel strategy that uses a selective amplification of ChIP (SACHI) to identify cell and stage specific interactions of REST with its target genes with a success rate up to 97%. Among the isolated REST target genes, *Crhr2*, *Cdk5r2*, *Syt2*, *Syt7*, *Kcnh1*, *Cspg3*, *L1cam*, and *Ntrk3* have been identified in our previous study (Bruce *et al.*, 2004). We have used this new strategy to identify 81 additional REST target genes from ES, NS, and hippocampus. This new protocol could also be used to isolate the target genes of other transcription factors as long as the length of their DNA binding sites exceeds five base pairs.

REST Target Genes and Neuronal Function

Many REST target genes involved in regulating core aspects of neuronal phenotype such as vesicular transport and release, signaling, and neurite outgrowth. Several known REST target genes are involved in neurite outgrowth and/or axonal guidance through regulation of intercellular and cell matrix interactions and of the intracellular cytoskeleton and include *L1cam*, *Cdh4*, *Adam23*, *Catnd2*, *Ppp2r2c*, and *Unc5d* (Gerhardt *et al.*, 2000; Kim *et al.*, 2002, Strack, 2002; Nishimura *et al.*, 2003; Frappé *et al.*, 2004; Goldsmith *et al.*, 2004; Liu *et al.*, 2004). This list can now be expanded by the addition of a further four REST target genes, *Cspg3*, *Shank2*, *Extl3*, and *Arc*, all of which are involved in regulation of cell adhesion or modulation of the cytoskeleton (Fujimoto *et al.*, 2004; Osman *et al.*, 2004; Qualmann *et al.*, 2004). This cohort of target genes lends mechanistic insight into the axon pathfinding errors resulting from constitutive expression of REST (Paquette *et al.*, 2000). Two new targets regulating vesicular trafficking and release include *Rab4a* and *Apba2*. These add to the known REST targets, *Snap25*, *Syt2*, *Syt7*, *synapsin 1*, and *synaptophysin* and illustrate the ability of REST to regulate every step of neurosecretion from trafficking, through docking to fusion and release.

REST Interacts with the Chromatin of Transcriptionally Active Genes in Differentiated Neurons

Our results show that REST occupies distinct subsets of target genes in ES cells, NS cells and hippocampus. A total of 89 genes were identified in this study, 38 of which are annotated, whereas 51 have no annotation and represent hypothetical genes. Of the 38 annotated REST target genes 24 (65%) encode gene products that are specifically or selectively expressed in neural tissue. Most target genes are transcribed at high levels in the hippocampus compared with ES and NS cells.

All target genes selected for expression analysis were transcribed in hippocampus, with the exception *of Olfr1336*. Most of the RE1 sites of these genes are occupied by REST. How does REST act principally as a repressor and become an activator in hippocampus? A previous study showed that NRSE dsRNA (RE1 dsRNA) appeared in the early stage of neurogenesis and in hippocampus. During the differentiation of NS cell to neurons, NRSE dsRNA triggered gene expression of neuron-specific genes through interaction with REST transcriptional machinery, by which REST was converted from a repressor to an activator (Kuwabara *et al.*, 2004). If this is the case, why are not all the REST target genes occupied by REST? For example, five genes comprising *Atp2b2*, *Cacna2d3*, *Ntrk3*, *Zfm1*, and *CREBBP/EP300* inhibitory protein 2 are actively transcribed but not occupied by REST in hippocampus. This indicates that existence of NRSE dsRNA cannot explain all facets of REST interaction with its target genes. Equally clear, is that REST cannot operate purely as an "on/off" switch whereby REST acts as a silencer.

Table 1. Categorization of REST target genes from embryonic stem cells, embryonic hippocampal neural stem cells, and hippocampus

Gene (Protein)	RE1 location	Biological process	Expression
Syt7 (Synaptotagmin-7)	(Intron 1)	Vesicular transport/release	Neuronal
Syt2 (Synaptotagmin-2)	(Intron 1 and 42 kb 5')	Vesicular transport	Neuronal
Rab4a (Ras-related protein Rab-4A)	(3.2 kb 3′)	Vesicular transport	?
Apba2 (Amyloid β A4 precursor protein-binding family A member 2)	(Intron 4)	Vesicular release	Neuronal
Foxp4 (Foxp4 protein)	(53 kb 5′)	Transcription	Neuronal
Fev (ETS-domain transcription factor)	(6.4 kb 5′)	Transcription	Neuronal
CREBBP/EP300 inhibitory protein 2 (E1A-like inhibition of differentiation 2)	(3.9 kb 5′)	Transcription	Widely expressed
Zfm1 (Nuclear protein, NP220)	(Intron I)	Transcription	?
ENSMUSG00000058422 (human homolog LMTK2 kinase)	(1.7 kb 5′)	Signalling	?
Resp18 (Regulated endocrine-specific protein 18 precursor)	(Intron 1)	Signalling	Neuronal
NM_172994 (human homolog PP2A, subunit B, B-γ isoform, Ppp2r2c)	(Intron 1)	Signal transduction	Neuronal
Cdk5r2 (Cyclin-dependent kinase 5 activator 2 precursor)	(2.9 kb 3′)	Signal transduction	Neuronal
Q8BY52 (BFA-resistant GEF1)	(0.7 kb 5′ and ex6/in5)	Signal transduction	Ubiquitous
Vrk3 (Serine/threonine-protein kinase VRK3)	(Intron 12)	Signal transduction	Non-neuronal
Pdgfra (α platelet-derived growth factor receptor precursor)	(40 kb 5′)	Organogenesis	Widely expressed
Drd2 (D(2) dopamine receptor)	(Intron 1)	Neurotransmission	Neuronal
Olfr1336 (Olfactory receptor MOR103-7)	(4.5 kb 5′)	Neurotransmission	Neuronal
Ntrk3 (Neurotrophin-3 receptor non-catalytic isoform 2)	(Intron 2)	Neuronal differentiation	Neuronal
Catnd2 (catenin δ-2, neurojungin)	(Intron 13)	Neurite outgrowth/cell adhesion	Neuronal
Cdh4 (Cadherin-4 precursor)	(Intron 1)	Neurite outgrowth/cell adhesion	Neuronal
Shank2 (SH3 and multiple ankyrin repeat domains protein 2)	(Intron 7)	Neurite outgrowth	Neuronal
L1cam (Neural cell adhesion molecule L1 precursor)	(15 kb 5′ and intron 1)	Neurite outgrowth	Neuronal
Extl3 (Exostosin-like 3)	(Exon 4)	Neurite outgrowth	Ubiquitous
Arc (Growth factor ARC)	(15 kb 5′)	Neurite outgrowth/cell-matrix	Neuronal
Cspg3 (Neurocan core protein precursor)	(Intron 1)	Neurite outgrowth/cell adhesion	Neuronal
Unc5d (Netrin receptor UNC5D precursor)	(Intron 1)	Neurite outgrowth/cell adhesion	Mesenchymal
Mbp (Myelin basic protein)	(63 kb 5′)	Myelination	Glial
Pkd1l3 (Polycystic kidney disease 1-like 3)	(Intron 14)	Ion channel	?
Accn1 (Amiloride-sensitive cation channel 1, neuronal)	(Intron 1)	Ion channel	Neuronal
Cacna2d3 (Calcium channel α-2-δ-C subunit)	(Intron 1)	Ion channel	Neuronal
Kcnh1 (Potassium voltage-gated channel subfamily H member 1)	(Intron 10)	ion channel	Neuronal+muscle
Atp2b2 (Plasma membrane calcium-transporting ATPase 2)	(Intron 2)	Ion channel	Neuronal
Hcn3 (K/Na hyperpolarization-activated cyclic nucleotide-gated channel 3)	(Intron 1)	Ion channel	Neuronal
Kirrel3 (Kin of IRRE-like protein 3 precursor)	(74 kb 5′)	Hemopoeisis	Neuronal+stromal
Adam23 (ADAM 23 precursor)	(22 kb 3′)	Cell-matrix interaction	Neuronal
Crhr2 (Corticotropin-releasing factor receptor 2 precursor)	(Intron 3)	Angiogenesis	Widely expressed
ENSMUSG00000028804 (human homolog cub and sushi multiple domain 2)	(Intron 1)	?	?
Fndc1 (fibronectin type III domain containing 1)	(Intron 1)	?	?

REST Interaction with Target Genes in Stem Cells

In contrast to the hippocampus, the majority of target genes are silent in MHP36 neural stem cells and most are occupied by REST, irrespective of their transcriptional status. The only unoccupied sites lie within the *Cspg3*, *Kcnh1*, *Drd2*, and *Kirrel 3* genes. The profile of REST occupancy in ES cells is very similar to that of MHP36 cells but unlike MHP36 cells, most REST target genes are transcribed in ES cells, albeit at low levels compared with the hippocampus. As with MHP36 cells, *Cspg3*, and *Kcnh1* are both silent and occupied by REST. This low level of transcription likely reflects a transcriptionally poised state whereby the chromatin is an open configuration before full transcriptional activation upon differentiation (Schubeler *et al.*, 2000; Ragoczy *et al.*, 2003). In general, this study shows that many REST target genes are either silent or weakly expressed in ES and MHP36 cells but are strongly expressed in hippocampus. This may imply that REST is acting to silence or strongly repress these genes in both multipotent and pluripotent cells and then switches to become a regulator in postmitotic differentiated neurons.

A recent study reported that REST was present in ES cells but upon retinoic acid differentiation into neurons, REST was rapidly down-regulated in NS cells and was absent

Table 2. Hypothetical genes isolated by ChIP cloning using REST antibody

NM_177374 (intron 1)[a]	GENSCAN00000142787 (intron 4)
NM_175461 (intron 2)	GENSCAN00000090077 (intron 1)
NM_198617 (17.6 kb 5′)	GENSCAN00000117131 (8.8 kb 5′)
NM_153584 (intron 1)	GENSCAN00000131824 (intron 4)
NM_173446 (intron 1)	GENSCAN00000072415 (intron 8)
Q8BS13 (8.9 kb 3′)	GENSCAN00000099949 (intron 2)
Q8BMM4 (54 kb 3′)	GENSCAN00000005818 (intron 1)
Q8BPU5 (intron 2)	GENSCAN00000001446 (intron 4)
Q8C817 (3.2 kb 5′) (human KIAA1913)	GENSCAN00000133834 (intron 2)
Q80T91 (intron 4)	GENSCAN00000123398 (intron 4)
ENSMUSG00000039098 (3 kb 5′)	GENSCAN00000164262 (2 kb 3′)
ENSMUSG00000034324 (intron 3)	GENSCAN00000161449 (0.6 kb 5′)
ENSMUSG00000041544 (5.6 kb 5′)	GENSCAN00000165253 (7 kb 5′)
ENSMUSG00000064130 (38.1 kb 5′)	GENSCAN00000119112 (intron 1)
ENSMUSG00000046182 (intron 2)	GENSCAN00000152268 (intron 1)
ENSMUSG00000061706 (17 kb 5′)	GENSCAN00000017182 (intron 1)
ENSMUSG00000028804 (intron 1)	GENSCAN00000180246 (intron 1)
ENSMUSG00000051719 (intron 1)	GENSCAN00000023281 (intron 3)
ENSMUSG00000038457 (intron 5)	GENSCAN00000123398 (intron 4)
ENSMUSG00000041339 (12 kb and 17 kb 5′)	GENSCAN00000149179 (5 kb 5′)
ENSMUSG00000051978 (intron 1)	GENSCAN00000134958 (intron 1)
ENSMUSESTG00000031508 (intron 1)	GENSCAN00000137792 (12 kb 5′)
ENSMUSESTG00000025135 (intron 2)	GENSCAN00000126950 (intron 9)
ENSMUSESTG00000018966 (intron 1)	GENSCAN00000129663 (intron 1)
ENSMUSESTG00000020906 (10 kb 5′)	GENSCAN00000057808 (intron 3)
	GENSCAN00000103896 (17 kb 3′)

[a] The locations of RE1 sites are indicated in parentheses.

from both cultured cortical progenitors and cortical neurons (Ballas *et al.*, 2005). However, in our study, REST continues to be expressed in NS cells, embryonic hippocampal stem cells, and ES cell-derived NS cells. In vivo, REST is expressed widely throughout the ventricular neuroepithelium (Schoenherr *et al.*, 1995) and is present in many adult cortical neurons (Palm *et al.*, 1998). In the hippocampus, most neurons of the pyramidal and granular layers express REST. In fact, REST levels and REST target gene levels are dynamically regulated in response to ischemic or epileptic insults (Palm *et al.*, 1998; Calderone *et al.*, 2003). Here, we have used the MHP36 neural stem cell line, derived from embryonic mouse hippocampus and which is capable of differentiating into neurons and glia both in vitro and in vivo (Mellodew *et al.*, 2004; Hugnot *et al.*, 2001). As such it represents a homogenous, tractable system to examine REST interactions with its target genes at the neural stem cell stage. In contrast to the study of Ballas *et al.* (2005) on cortical progenitors and neurons, we find REST is expressed in both hippocampal stem cells and neurons. This difference probably indicates diversity of REST actions in different populations of CNS progenitors and neurons but may also reflect differences in developmental stage.

Table 3. Quantitative PCR analysis of REST target gene expression levels in embryonic stem (ES) cells, embryonic hippocampal neural stem (NS) cells, and hippocampus

REST target genes	ES	NS	Hippocampus
Cspg3	0.3	0	230.8
Arc	82.0	19.0	276.0
Syt2	4.0	0.4	115.0
Apba2	48.0	0.7	6684.0
Kcnh1	0.1	0	22.0
Atp2b2	48.0	0	2179.0
Accn1	12.0	0	1858.0
Cacna2d3	14.0	10.0	468.0
Drd2	5.0	0	101.0
Olfr1336	0	2.0	0
Ntrk3	0.6	0	2330.0
Mbp	7.0	0	39473.0
Zfm1	727.6	5.5	5048.0
CREBBP/EP300 inhibitory protein 2	239.1	214.5	1120.1
Kirrel3	0.1	231.0	434.0
NM_175461	9.0	6.0	1385.0
NM_173446	0.3	0	2700.0
ENSMUSG00000051719	4.0	688	21234.0
ENSMUSG00000028804	1.0	0	741.0
ENSMUSESTG00000031508	2.0	0	1773.0

Expression levels are shown relative to cyclophilin ($\times 10^{-5}$).

In summary, we have used a novel ChIP cloning protocol (SACHI) to identify 89 REST target genes. We show that the REST occupies a distinct set of target genes in ES cells, NS cells and hippocampal neurons and that occupancy is not simply related to expression levels. The results suggest that the REST-directed mechanism in the gene expression of its target genes extends beyond the simple "on/off" model and the mechanism may be compounded by combinatorial regulation from other transcription factors or corepressors.

ACKNOWLEDGMENTS

This work was funded by the Wellcome Trust.

REFERENCES

Andrés, M. E., Burger, C., Peral-Rubio, M. J., Battaglioli, E., Anderson, M. E., Grimes, J., Dallman, J., Balls, N., and Mandel, G. (1999). CoREST: a functional corepressor required for regulation of neural-specific gene expression. Proc. Natl. Acad. Sci. USA *96*, 9873–9878.

Ballas, N. *et al.* (2001). Regulation of neuronal traits by a novel transcriptional complex. Neuron *31*, 353–365.

Ballas, N., Grunseich, C., Lu, D. D., Speh, J. C., and Mandel, G. (2005). REST and its corepressors mediate plasticity of neuronal gene chromatin throughout neurogenesis. Cell *121*, 645–657.

Barski, A., and Frenkel, B. (2004). ChIP Display: novel method for identification of genomic targets of transcription factors. Nucleic Acids Res. *32*, e104–112.

Battaglioli, E., Andres, M. E., Rose, D. W., Chenoweth, J. G., Rosenfeld, M. G., Anderson, M. E., and Mandel, G. (2002). REST repression of neuronal genes requires components of the hSWI.SNF complex. J. Biol. Chem. *277*, 41038–41045.

Belyaev, N. D., Wood, I. C., Bruce, A. W., Street, M., Trinh, J-B., and Buckley, N. J. (2004). Distinct RE-1 silencing transcription factor-containing complexes interact with different target genes. J. Biol. Chem. *279*, 556–561.

Bruce, A. W., Donaldson, I. J., Wood, I. C., Yerbury, S. A., Sadowski, M. I., Chapman, M., Göttgens, B., and Buckley, N. J. (2004). Genome-wide analysis of repressor element 1 silencing transcription factor/neuron-restrictive silencing factor (REST/NRSF) target genes. Proc. Natl. Acad. Sci. USA *101*, 10458–10463.

Calderone, A., Jover, T., Noh, K. M., Tanaka, H., Yokota, H., Lin, Y., Grooms, S. Y., Regis, R., Bennett, M. V., and Zukin, R. S. (2003). Ischemic insults derepress the gene silencer REST in neurons destined to die. J. Neurosci. *23*, 2112–2121.

Chen, Z-F., Paquette, A. J., and Anderson, D. J. (1998). NRSF/REST is required *in vivo* for repression of multiple neuronal target genes during embryogenesis. Nat. Genet. *20*, 136–142.

Chong, J. A., Tapia-Ramirez, J., Kim, S., Toledo-Aral, J. J., Zheng, Y., Boutros, M. C., Altshuller, Y. M., Frohman, M. A., Kraner, S. D., and Mandel, G. (1995). REST: a mammalian silencer protein that restricts sodium channel gene expression to neurons. Cell *80*, 949–957.

Frappé, I., Wang, C., Caines, G., Rideout-Gros, S., and Aubert, I. (2004). Cell adhesion molecule L1 promotes neurite outgrowth of septal neurons. J. Neurosci. Res. *75*, 667–677.

Fujimoto, T., Tanaka, H., Kumamaru, E., Okamura, K., and Miki, N. (2004). Arc interacts with microtubules/microtubule-associated protein 2 and attenuates microtubule-associated protein 2 immunoreactivity in the dendrites. J. Neurosci. Res. *76*, 51–63.

Gerhardt, H., Rascher, G., Schuck, J., Weigold, U., Reidies, C., and Wolburg, H. (2000). R- and B-cadherin expression defines subpopulations of glial cells involved in axonal guidance in the optic nerve head of the chicken. Glia *31*, 131–143.

Goldsmith, A. P., Gossage, S. J., and ffrench-Constant, C. (2004). ADAM23 is a cell-surface glycoprotein expressed by central nervous system neurons. J. Neurosci. Res. 78, 647–658.

Hakimi, M. A., Bochar, D. A., Chenoweth, J., Lane, W. S., Mandel, G., and Shiekhattar, R. (2002). A core-BRAF35 complex containing histone deacetylase mediates repression of neuronal-specific genes. Proc. Natl. Acad. Sci. USA *99*, 7420–7425.

Huang, Y., Myers, S. J., and Dingledine, R. (1999). Transcriptional repression by REST: recruitment of Sin3A and histone deacetylase to neuronal genes. Nat. Neurosci. *2*, 867–872.

Hugnot, J. P., Pilcher, H., Rashid-Doubell, F., Sinden, J., and Price, J. (2001). Regulation of glial differentiation of MHP36 neural multipotent cell line. Neuroreport *12*, 2237–2241.

Impey, S., McCorkle, S. R., Cha-Molstad, H., Dwyer, J. M., Yochum, G. S., Boss, J. M., McWeeney, S., Dunn, J. J., Mandel, G., and Goodman, R. H. (2004). Defining the CREB regulon: a genome-wide analysis of transcription factor regulatory regions. Cell *119*, 1041–1054.

Kershaw, T.R., Rashid-Doubell, F., and Sinden, J. D. (1994). Immunocharacterization of H-2Kb-tsA58 transgenic mouse hippocampal neuroepithelial cells. Neuroreport *5*, 2197–2200.

Kim, K., Sirota, A., Chen, Y-H., Jones, S. B., Dudek, R., Lanford, G. W., Thakore, C., and Lu, Q. (2002). Dendrite-like process formation and cytoskeletal remodeling regulated by delta-catenin expression. Exp. Cell Res. *275*, 171–184.

Kim, J., Bhinge, A. A., Morgan, X. C., and Iyer, V. R. (2005). Mapping DNA-protein interactions in large genomes by sequence tag analysis of genomic enrichment. Nat. Methods *2*, 47–53.

Kuwabara, T., Hsieh, J., Nakashima, K., Taira, K., and Gage, F. H. (2004). A small modulatory dsRNA specifies the fate of adult neural stem cells. Cell *116*, 779–793.

Lee, T. I. *et al.* (2002). Transcriptional regulatory networks in *Saccharomyces cerevisiae*. Science *298*, 799–804.

Liu, G., Beggs, H., Jürgensen, C., Park, H-T., Gorski, J., Jones, K., Reichardt, L., Wu, J., and Rao, Y. (2004). Netrin requires focal adhesion kinase and Src family kinases for axon outgrowth and attraction. Nat. Neurosci. *7*, 1222–1232.

Mellodew, K., Suhr, R., Uwanogho, D. A., Reuter, I., Lendahl, U., Hodges, H., and Price, J. (2004). Nestin expression is lost in a neural stem cell line through a mechanism involving the proteasome and Notch signalling. Brain Res. Dev. Brain Res. *151*, 13–23.

Nishimura, K., Yoshihara, F., Tojima, T., Ooashi, N., Yoon, W., Mikoshiba, K., Bennett, V., and Kamiguchi, H. (2003). L1-dependent neuritogenesis involves ankyrinB that mediates L1-CAM coupling with retrograde actin flow. J. Cell Biol. *163*, 1077–1088.

Osman, N.M.S., Naora, H., and Otani, H. (2004). Glycosyltransferase encoding gene EXTL3 is differentially expressed in the developing and adult mouse cerebral cortex. Brain Res. Dev. Brain Res. *151*, 111–117.

Ragoczy, T., Telling, A., Sawado, T., Groudine, M., and Kosak, S. T. (2003). A genetic analysis of chromosome territory looping: diverse roles for distal regulatory elements. Chromosome Res. *11*, 513–525.

Roh, T. Y., Cuddapah, S., and Zhao, K. (2005). Active chromatin domains are defined by acetylation islands revealed by genome-wide mapping. Genes Dev. *19*, 542–552.

Roopra, A., Sharling, L., Wood, I. C., Briggs, T., Bachfischer, U., Paquette, A. J., and Buckley, N. J. (2000). Transcriptional repression by neuron-restrictive silencer factor is mediated via the Sin3-histone deacetylase complex. Mol. Cell. Biol. *20*, 2147–2157.

Roopra, A., Qazi, R., Schoenike, B., Daley, T. J., and Morrison, J. F. (2004). Localized domains of G9a-mediated histone methylation are required for silencing of neuronal genes. Mol. Cell *14*, 727–738.

Palm, K., Belluardo, N., Metsis, M., and Timmusk, T. (1998). Neuronal expression of zinc finger transcription factor REST/NRSF/XBR gene. J. Neurosci. *18*, 1280–1296.

Paquette, A. J., Perez, S. E., and Anderson, D. J. (2000). Constitutive expression of the neuron-restrictive silencer factor (NRSF)/REST in differentiating neurons disrupts neuronal gene expression and causes axon pathfinding errors *in vivo*. Proc. Natl. Acad. Sci. USA *97*, 12318–12323.

Qualmann, B., Boeckers, T. M., Jeromin, M., Gundelfinger, E. D., and Kessels, M. M. (2004). Linkage of the actin cytoskeleton to the postsynaptic density via direct interactions of Abp1 with the ProSAP/Shank family. J. Neurosci. *24*, 2481–2495.

Schoenherr, C. J., and Anderson, D. J. (1995). The neuron-restrictive silencer factor (NRSF): a coordinate repressor of multiple neuron-specific genes. Science *267*, 1360–1363.

Schoenherr, C. J., Paquette, A. J., and Anderson, D. J. (1996). Identification of potential target genes for the neuron-restrictive silencer factor. Proc. Natl. Acad. Sci. USA *93*, 9881–9886.

Schubeler, D., Francastel, C., Cimbora, D. M., Reik, A., Martin, D. I., and Groudine, M. (2000). Nuclear localization and histone acetylation: a pathway for chromatin opening and transcriptional activation of the human beta-globin locus. Genes Dev. *14*, 940–950.

Shi, Y., Lan, F., Matson, C., Mulligan, P., Whetstine, J. R., Cole, P.A., Casero, R. A., and Shi, Y. (2004). Histone demethylation mediated by the nuclear amine oxidase homolog LSD1. Cell *119*, 941–953.

Strack, S. (2002). Overexpression of the protein phosphatase 2A regulatory subunit Bgamma promotes neuronal differentiation by activating the MAP kinase (MAPK) cascade. J. Biol. Chem. *277*, 41525–41532.

Su, X., Kameoka, S., Lentz, S., and Majumder, S. (2004). Activation of REST/NRSF target genes in neural stem cells is sufficient to cause neuronal differentiation. Mol. Cell. Biol. *24*, 8018–8025.

Watanabe, Y., Kameoka, S., Gopalakrishnan, V., Aldape, K. D., Pan, A. A., Lang, F. F., and Majumder, S. (2004). Conversion of myoblasts to physiologically active neuronal phenotype. Genes Dev. *18*, 889–900.

Wood, I. C., Belyaev, N. D., Bruce, A. W., Jones, C., Mistry, M., Roopra, A., and Buckley, N. J. (2003). Interaction of the repressor element 1-silencing transcription factor (REST) with target genes. J. Mol. Biol. *334*, 863–874.

Ying, Q. L., Stavridis, M., Griffiths, D., Li, M., and Smith, A. (2003). Conversion of embryonic stem cells into neuroectodermal precursors in adherent monoculture. Nat. Biotechnol. *21*, 183–186.

Appendix 2

Rest-Mediated Regulation of Extracellular Matrix Is Crucial for Neural Development

Yuh-Man Sun, Megan Cooper, Sophie Finch, Hsuan-Hwai Lin, Zhou-Feng Chen, Brenda P. Williams, Noel J. Buckley

PLoS ONE (2008) 3 (11):e3656-e3668.

OPEN ACCESS Freely available online

PLoS one

Rest-Mediated Regulation of Extracellular Matrix Is Crucial for Neural Development

Yuh-Man Sun[1]*, Megan Cooper[1☯], Sophie Finch[1☯], Hsuan-Hwai Lin[1☯], Zhou-Feng Chen[2], Brenda P. Williams[1], Noel J. Buckley[1]

1 Centre for the Cellular Basis of Behaviour (CCBB), The James Black Centre, Institute of Psychiatry, King's College London, London, United Kingdom, **2** Departments of Anesthesiology, Psychiatry, and Developmental Biology, Washington University School of Medicine Pain Center, Saint Louis, Missouri, United States of America

Abstract

Neural development from blastocysts is strictly controlled by intricate transcriptional programmes that initiate the down-regulation of pluripotent genes, *Oct4*, *Nanog* and *Rex1* in blastocysts followed by up-regulation of lineage-specific genes as neural development proceeds. Here, we demonstrate that the expression pattern of the transcription factor *Rest* mirrors those of pluripotent genes during neural development from embryonic stem (ES) cells and an early abrogation of Rest in ES cells using a combination of gene targeting and RNAi approaches causes defects in this process. Specifically, Rest ablation does not alter ES cell pluripotency, but impedes the production of Nestin$^+$ neural stem cells, neural progenitor cells and neurons, and results in defective adhesion, decrease in cell proliferation, increase in cell death and neuronal phenotypic defects typified by a reduction in migration and neurite elaboration. We also show that these Rest-null phenotypes are due to the dysregulation of its direct or indirect target genes, *Lama1*, *Lamb1*, *Lamc1 and Lama2* and that these aberrant phenotypes can be rescued by laminins.

Citation: Sun Y-M, Cooper M, Finch S, Lin H-H, Chen Z-F, et al. (2008) Rest-Mediated Regulation of Extracellular Matrix Is Crucial for Neural Development. PLoS ONE 3(11): e3656. doi:10.1371/journal.pone.0003656

Editor: Patrick Callaerts, Katholieke Universiteit Leuven, Belgium

Received July 11, 2008; **Accepted** October 10, 2008; **Published** November 6, 2008

Copyright: © 2008 Sun et al. This is an open-access article distributed under the terms of the Creative Commons Attribution License, which permits unrestricted use, distribution, and reproduction in any medium, provided the original author and source are credited.

Funding: This work was supported by a start up fund (Y-M. Sun) from Neuroscience, IOP, King's College London, UK and Wellcome Trust grants (N. J. Buckley).

Competing Interests: The authors have declared that no competing interests exist.

* E-mail: yuh-man.sun@iop.kcl.ac.uk

☯ These authors contributed equally to this work.

Introduction

During mouse embryo development, the blastocyst differentiates into pluripotent primitive ectoderm and gives rise to a structure known as the epiblast [1]. The epiblast responds to extrinsic signals and generates three primary germ layers (ectoderm, mesoderm and endoderm) [2]. During neurulation, the ectoderm gives rise to the neuroectoderm in the form of a neural plate, which subsequently folds to generate the neural tube, composed of a single layer of neuroepithelial cells or neural stem cells (NSCs), where a series of ring-like constrictions mark the boundaries between the primordia of the major brain regions [3–4]. This process of neural development is orchestrated and accompanied by wholesale changes in transcriptional programmes and patterns of gene expression. However, due to the difficulties in accessing and manipulating early embryos, the transcriptional network that regulates neural development is poorly understood, especially in mammals. Embryonic stem (ES) cells derived from blastocysts retain the ability to recapitulate neural development *in vitro*, and offer an invaluable model to study early events in embryogenesis. The RE1 Silencing Transcription Factor / Neuron Restrictive Silencer Factor (Rest/Nrsf) is a zinc finger transcription repressor that has been postulated to act as a master regulator of neuronal gene expression in both the developing and mature nervous systems [5–6]. We and others have shown that Rest is highly expressed in blastocysts and ES cells, but that expression decreases as neural development proceeds [7–8]. In fact, down-regulation of Rest has been proposed to be obligate for differentiation of neural progenitors [8] and more recently, it has been proposed that Rest haplodeficiency results in loss of pluripotency markers and a reciprocal gain in differentiation markers [9]. Taken together, these observations suggest that Rest may play a crucial role at several stages of neural development. Here, we determine the function of Rest during neural development from ES cells through NSCs and neural progenitor cells (NPCs) to mature neurons using an *in vitro* ES cell-derived neural differentiation model.

Rest exerts its function by binding to both canonical and non-canonical RE1-sites identified at over 2000 loci in the mammalian genome [10–11] and is implicated in the regulation of both coding and non-coding genes [10,12], many of which represent neuron-specific transcriptional units. The observation that many of these target genes are expressed by differentiated neurons, including ion channels, neurotransmitter receptors, neurotrophins, synaptic vesicle associated proteins, cell adhesion molecules, growth-associated and cytoskeletal proteins, gave rise to the initial perception that Rest acted as a silencer of neuron-specific genes in NPCs and non-neural cells to prevent precocious expression of neuronal characteristics. However, recent studies emerge that Rest has more versatile roles and can regulate its target genes either by activation, repression or silencing, depending upon the developmental stage and cell type [7,13]. Rest recruits multiple cofactors, histone modifying and chromatin remodelling activities, all of which underwrite the complexity of Rest activity [14–16]. The diverse roles of Rest have been shown in both neural and non-neural pathologies including Huntington's disease, cardiac hypertrophy, medulloblastoma, malignant rhabdoid tumor, small cell lung cancer, ovarian cancer, and ischemia (see review for references [13]).

Despite the wealth of knowledge in identifying target genes [10–12] and in delineating the mechanistic actions of Rest [14–16], the biological function of Rest during neural development remains unclear. *Rest*−/− mice die around embryonic day (E)11.5, with embryo degeneration, neural tube malformations and widespread apoptosis evident from E9.5 [6]. Constitutive expression of Rest in chick spinal cord does not cause defects in neurogenesis but does result in axon pathfinding errors [17]. However, in Xenopus, disruption of Rest function disturbs ectoderm patterning and expands the neural plate [18], suggesting that Rest is indeed required for normal neural plate formation and neurogenesis. Collectively, these studies paint a somewhat ambiguous picture of the role of Rest in the development of NSCs and neurons. We have sought to address this issue by using a combination of gene targeting and RNAi to create ES lines expressing a range of Rest concentrations, which we have used to investigate the effect of Rest deficiency during ES cell-derived neural development. Importantly, in contrast to a recent study [9], we find that deletion of a single *Rest* allele does not result in any change in neural differentiation. Instead, we find that Rest levels have to be decreased by more than 92% to precipitate any phenotype. Rest ablation impairs the extracellular matrix (ECM) components and impedes the production of Nestin^{+} NSCs, NPCs and neurons. Furthermore, neurons derived from REST-null ES cells are devoid of elaborate processes, have defects in migration and undergo increased cell death. Importantly, all of these phenotypic effects of Rest ablation were rescued by treatment with laminins, a key component of the ECM that has been implicated in neuronal migration and more latterly in development of the neural plate. We propose a novel mechanism by which Rest regulates development of both NSCs and mature neurons by controlling expression of key components of the ECM.

Results

Rest expression during NSC and Neuron Development

We investigated the role of Rest in neural development using an *in-vitro* ES cell-derived neural differentiation model, which recapitulates events during neural development in vivo. ES cells firstly differentiate into neuroepithelial cells (early NSCs), which peak around 4–6 days of differentiation and express Sox1 and Nestin (about 80% of population), and then differentiate further into more restricted NSCs that peak around 10 days of differentiation and express either Ngn1 or Mash1 (about 80% of population) (Fig. 1C–D and Fig. S2B–C). In this paper, we refer to early NSCs as NSCs and late more restricted NSCs as NPCs. To

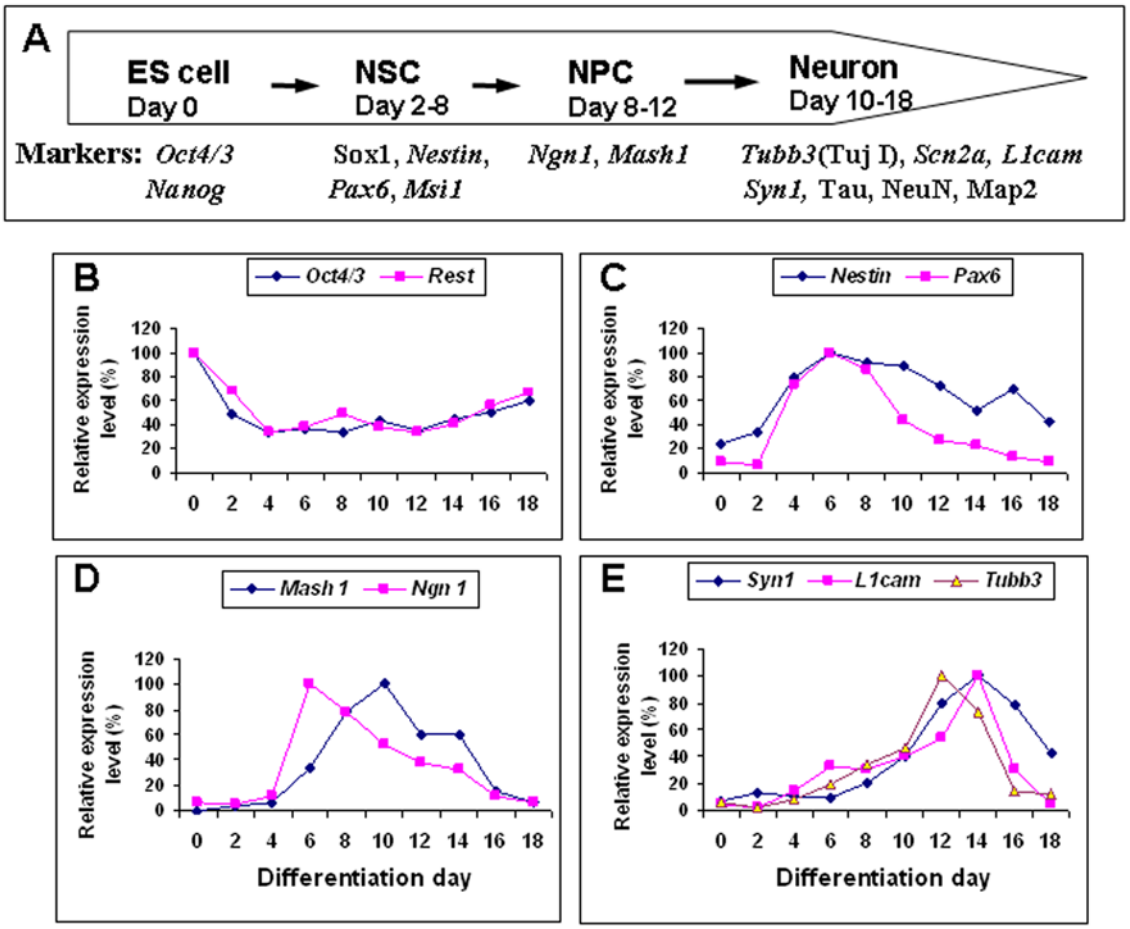

Figure 1. Time course of stage-specific marker expression during neural differentiation of HM1 embryonic stem (ES) cells. (A) Summary of neural stage-specific markers used in this study. NSC: neural stem cells; NPC: neural progenitor cells. (B) Down-regulation of *Oct4* and *Rest* was observed as neural differentiation proceeded. (C) From day 2–8, the expression of NSC markers, *Nestin and Pax6* is observed. (D) NPC markers, *Mash1* and *Ngn1*, appeared in an overlapping but slightly later wave than NSC markers. (E) After 10 days of differentiation, markers of early (*Tubb3*) *and* mature neurons (*Syn*1 and *L1cam*) appeared.
doi:10.1371/journal.pone.0003656.g001

establish the time course during which NSCs, NPCs and neurons are formed from HM1 and 46C ES cells, we examined gene expression patterns for NSC markers (*Nestin* and *Pax6*), NPC markers (*Mash1* and *Ngn1*) and neuronal markers (*Tubb3*, Syn*1* and *L1cam*) during ES cell-derived neural differentiation (Fig. 1A). We found that *Rest* expression mirrored that of the pluripotent ES cell marker *Oct4*, and was expressed at highest level in ES cells with its expression level declining as differentiation proceeded; reaching its lowest level 4 days after differentiation just before NSC production reached its peak (Fig. 1B and Fig. S2A). *Rest* levels were maintained at low levels throughout neuron formation. Conversely, the expression patterns of *Nestin* and *Pax6* reciprocated those of *Rest* and *Oct4* indicating that NSC production started 1- or 2-days after differentiation, reached a peak around 6 days, and thereafter declined (Fig. 1C and Fig. S2B). Mash1 and *Ngn1* expression indicated that NPCs started to be produced after 6-days of differentiation and peaked between 6 and 10 days (Fig. 1D and Fig. S2C). The early neuronal marker *Tubb3* was observed around the same time but did not peak until 12 days of differentiation whereas the peak of mature neuron marker expression (*Syn1* and *L1cam*) occurred at 14–16 days of differentiation (Fig. 1E and Fig. S2D). This time course closely recapitulates the sequential generation of NSCs, NPCs and neurons observed *in vivo* (Fig. 1A).

Rest ablation inhibits development of NSC and NPC

Next we examined the effects of Rest ablation on the development of NSCs and NPCs. The control REST-100, REST/KD-50 and REST-null ES cells, which express 100%, 50% and 0% wild-type Rest levels respectively (Fig. S1B and S1D), were differentiated into NSCs and then into NPCs identified using an array of NSC and NPC markers (Fig. 1A). We assessed the effects of Rest ablation on gene and protein expression of these markers using quantitative Real-time PCR, FACS and immunocytochemical analysis. In REST-100 ES cells, the expression profiles of *Pax6, Msi1 and Nestin* were similar to one another, with expression peaking around 4 days and thereafter gradually declining (Fig. 2A–2C). REST/KD-50 ES cells showed no significant difference in the expression level and pattern of these genes as compared to the control REST-100 cells (Fig. 2A–2C). Similarly, no change in the number of $Sox1^+/Nestin^+$ NSCs was seen (Table 1 and Fig. S3B–3C). However, in REST-null ES cells, the peak expression of *Pax6* and *Msi1* was significantly ($P<0.01$) reduced to 40% of control levels whilst expression of *Nestin* was reduced to 60% of control levels (Fig. 2A–2C). This mutant generated significantly ($P<0.01$) fewer $Sox1^+/Nestin^+$ NSCs (52%) as compared to the REST-100 (77%) and REST/KD-50 ES cells (76%), but generated double the number of $Sox1^+/ Nestin^-$ NSCs compared with the control cells ($P<0.01$) (Table 1 and Fig. S3D). Moreover, REST-null ES cells produced lower levels of *Mash1* and *Ngn1* expression ($P<0.01$) and this was reflected in a parallel reduction in the number of $Mash1^+$ NPCs (~50%) as compared to the control (87%) ($P<0.05$) (Fig. 2D–2E; Table 1; Fig. S4B and 4D). Our results suggest that a 50% depletion of Rest shows no discernible effect on the production of NSCs and NPCs from ES cells. In fact, the production of early $Sox1^+/Nestin^-$ NSCs from REST-null ES cells remained unaffected but formation of late $Sox1^+/Nestin^+$ NSCs and subsequent production of NPCs was inhibited.

Rest ablation impedes neuronal differentiation

Since Rest is known to be a repressor of neuronal gene expression and has been implicated in neurogenesis, we proceeded to examine the role of Rest in the generation of neurons from NSCs by assessing the expression of early and late neuronal markers (Fig. 1A). Similar to our studies on the generation of

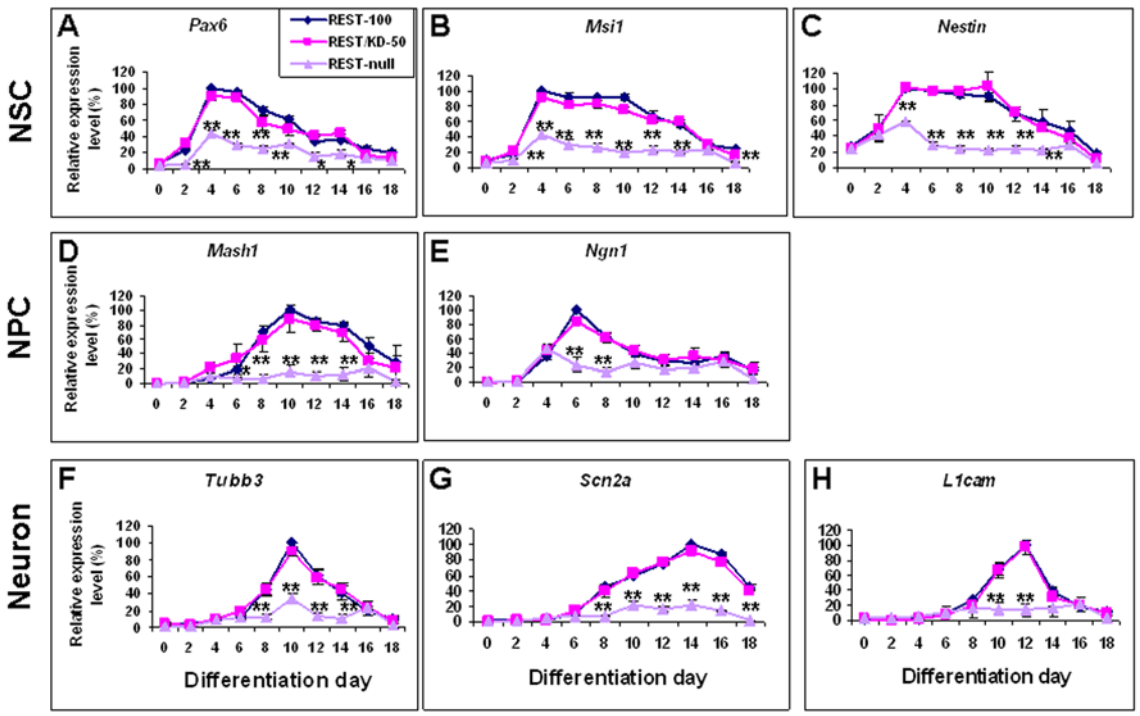

Figure 2. The effect of Rest ablation on the expression of stage-specific neural markers. The ability of control (REST-100) and Rest mutant ES cells (REST/KD-50 and REST-null) to generate the different neural cell populations was assessed by real time-PCR using the following markers: NSCs *Pax6*, *Msi1* and *Nestin* (A–C); NPCs *Mash1 and Ngn1* (D–E); early neurons *Tubb3* (F) and mature neurons, *Scn2a* and *L1cam* (G–H). Data are represented as mean±SEM. *$P<0.05$ and **$P<0.01$, significantly different from REST-100 and REST/KD-50.
doi:10.1371/journal.pone.0003656.g002

Table 1. The summary of FACS analysis of neural populations derived from control and Rest mutant ES cells with or without laminin treatment.

REST mutant	Cell type					
	NSC		*NPC*			*Neuron*
	$Sox1^+/Nestin^-$	$Sox1^+/Nestin^+$	$Mash1^+/Tau^-$	$Mash1^+/Tau^+$	$Mash1^-/Tau^+$	$Map2^+$
No laminin treatment						
REST-100	20.7±0.8	77.4±1.3	47.2±2.7	41.7±3.6	1.2±0.2	83.1±2.7
REST/KD-50	20.9±1.2	76.2±1.6	44.5±2.6	36.4±1.8	1.6±0.5	81.3±1.0
REST-null	45.1±1.1**	52.9±2.1**	25.9±3.3*	24.4±1.3*	1.3±0.1	64.4±1.0**
REST-null+MTV	41.1±0.5**	54.5±1.9**	29.8±2.1*	22.7±1.4*	1.4±0.2	59.2±6.0**
REST-null+REST	33.9±1.1**¥	62.9±1.4*#	39.1±1.6#	31.5±2.1#	1.1±0.1	77.6±0.3¥
Laminin treatment						
REST-100	14.6±1.3	78.8±3.1	38.3±2.1	31.8±2.4	0.5±0.1	74.8±0.3
REST/KD-50	13.8±1.6	77.1±2.1	40.8±2.3	28.5±2.6	0.4±0.1	74.1±0.4
REST-null	18.7±1.4	74.9±2.5	37.8±1.9	31.9±2.2	0.4±0.1	76.2±2.8
REST-null+MTV	19.1±1.5	75.2±2.3	37.1±2.2	29.5±2.1	0.5±0.1	75.3±1.8
REST-null+REST	17.9±1.1	78.4±1.8	35.9±2.4	31.4±1.8	0.6±0.2	75.9±2.1

Data are represented as mean±SEM.
*$P<0.05$ and **$P<0.01$, significantly different from REST-100 and REST/KD-50.
# $P<0.05$ and ¥$P<0.01$, significantly different from REST-null and REST-null+MTV.
doi:10.1371/journal.pone.0003656.t001

NSCs and NPCs, we noticed no significant difference in either the levels of gene expression, or in the number of cells expressing these neuronal markers in cells derived from REST/KD-50 ES cells compared with the control ES cells (Fig. 2F–2H; Table 1; Figs. S4B–S4C and S5B–S5C). However, REST-null ES cells showed a significant impairment in neuronal differentiation, as evidenced by a reduction in *Tubb3* expressing early neurons ($P<0.01$) (Fig. 2F), and a reduced population of Tau^+ neurons (25%) compared to the control cells (42%) ($P<0.05$) (Table 1; Fig. S4B and S4D). Furthermore, we did not detect $TujI^+$ (Tubb3) immunoreactive cells in differentiated REST-null cells at any earlier stage (data not shown), suggesting that Rest abrogation did not result in premature neuronal differentiation. As differentiation proceeded, the number of $Map2^+$ mature neurons was significantly ($P<0.01$) reduced in REST-null cells (64%) compared with control cells (83%) (Table 1; Fig. S5B and S5D). Expression of *Scn2a* and *L1cam* (Fig. 2G–2H) both showed parallel changes. Intriguingly, even though *Tubb3*, *Scn2a* and *L1cam* are all Rest target genes, their expression were not de-repressed in REST-null ES cells during early ES cell differentiation (Fig. 2F–2H), a view consistent with the absence of any effect of acute Rest abrogation on expression of these genes in ES cells (unpublished observations). In conclusion, reduction of Rest levels by 50% has no effect on neurogenesis in terms of the time course, sequence or production of neurons. In contrast, the absence of Rest impedes neurogenesis.

Constitutive expression of Rest rescues REST-null phenotypes

The REST-null ES cells were generated by a combination of gene targeting and RNAi knockdown. To confirm that their phenotype was not due to an off-target event, we constitutively expressed Rest using pMT-NRSF to create REST-null+REST, which raised *Rest* levels to 8% of wild-type levels. Transfection of empty pMT vector was used to generate REST-null+MTV that served as a control (Fig. S1C–S1D). We then assessed the capacity of REST-null+REST ES cells to differentiate into NSCs, NPCs and neurons. REST-null+REST ES cells generated NSCs expressing *Pax6* and *Msi1* at a similar level to that of REST-100 ES cells while *Nestin* was rescued to 80% of REST-100 levels. As predicted, REST-null+MTV cells showed a similar phenotype to the REST-null mutant (Fig. S6A–S6C). In support of these findings, the number of $Nestin^+$ NS cells derived from REST-null+REST ES cells significantly increased to 63% (Table 1 and Fig. S3E–S3F). Moreover, constitutively expressing Rest rescued the capacity of REST-null mutant ES cells to produce NPCs, and neurons (Table 1, Figs. S4E–S4F and S5E–S5F). Our findings suggested that the phenotypic effects of REST-null ES cells are not due to off-target effects. Furthermore, our results indicate that very low levels of Rest are both sufficient and necessary for normal generation and maturation of NSCs.

Rest ablation results in defects in adhesion, cell proliferation and survival

During investigation of the effects of Rest ablation on NSC and neuronal development, we observed that REST-null ES cells exhibited more severe phenotypes when plated on a glass surface than when plated on a plastic surface, whereas REST-100 and REST/KD-50 showed no discernible difference on either surface. On glass, REST-null cells showed defective adhesion and produced very few or no $Nestin^+$ NSCs but did produce normal levels of $Sox1^+$ NSCs as compared to those derived from REST-100 and REST/KD-50 ES cells (Fig. 3A–3C). This phenotype was much less pronounced when REST-null ES cells were plated on a plastic surface where a greater number of $Nestin^+$ NSCs were seen (50%; Table 1). Intriguingly, $NeuN^+$ and/or $Map2^+$ neurons showed marked phenotypic defects on the glass surface, characterised by an absence of migration, and poor elaboration of processes and fasciculation among neuronal colonies as compared to REST-100 and REST/KD-50 ES cells (Fig. 3F–3H and 3K–3M). All phenotypes on the glass surface were rescued, at least in part, by raising *Rest* levels to 8% in REST-null+REST ES cells (Fig. 3D–3E; 3I–3J and 3N–3O). Interestingly, the phenotypic

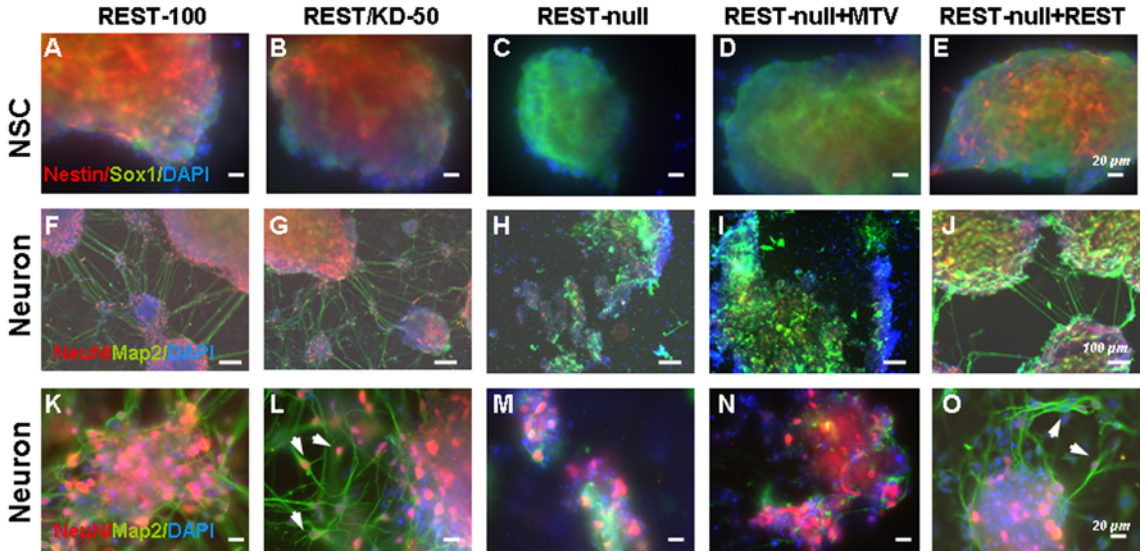

Figure 3. Phenotypic effects of Rest ablation on neural differentiation of ES cells. (A–E) NSCs were derived from the control (REST-100) and 4 Rest mutant ES cells, and identified by Sox1 (green) and Nestin (red) after 4 days of differentiation. Nuclei were stained with DAPI (blue). Few, if any, NSCs generated from REST-null ES cells (C and D) expressed Nestin, but showed positive immunostaining with Sox1. NSCs generated from control (REST-100) and REST/KD-50 ES cells showed much higher levels of Nestin immunostaining in $Sox1^+$ cells (A–B). Constitutive expression of Rest (REST-null+REST) rescues, at least partially, this phenotype with many $Sox1^+$ cells now expressing Nestin (E). (F–O) Neurons derived from the control and 4 Rest mutant ES cells were identified using NeuN (red) and Map2 (green) after 14 days of differentiation. Neurons generated from REST-100 and REST/KD-50 ES cells showed elaborate neurite outgrowth, fasciculation between aggregates/colonies (F, G and in higher power K, L) and migration of NeuN+ cells (see arrows in L). Conversely, neurons derived from REST-null and REST-null+MTV exhibited fragmented neuronal colonies that lacked elaborate processes and migration (H, I and in higher power M, N). Constitutively expressing Rest (REST-null+REST) attenuated the phenotypic effects of Rest ablation: neurite outgrowth, neurite fasciculation (J, O) and neuronal migration was observed (arrows in O). Scale bars: 20 μm (A to E and K to O) and 100 μm (F to J).
doi:10.1371/journal.pone.0003656.g003

defects on the glass surface were also been seen in NSCs and neurons derived from *Rest*−/− ES cells [6] (Fig. S7C–S7K), although in the latter case the Rest mutant retains alternatively spliced isoforms that may not be functional (Fig. S7A–S7B).

Either on plastic or glass surfaces, we found that REST-null ES cells generated fewer cells during neural differentiation than those from REST-100 and REST/KD-50 ES cells. Accordingly, we examined proliferation and cell death during the course of neurogenesis. Using BrdU incorporation, no differences were observed in the proliferation of either $Sox1^+/Nestin^-$ early NSCs derived from control and all Rest mutants or in $Sox1^+/Nestin^+$ late NSCs derived from the control, REST/KD-50 and REST-null+REST ES cells. However, it was difficult to evaluate the $Sox1^+/Nestin^+$ NSCs from REST-null and REST-null+MTV ES mutants, because of their low number and the ease with which they were lost from coverslips during the staining process. We then used TUNEL staining to assess the degree of apoptosis at 4 and 14-days of differentiation, i.e. at the peaks of NSC and neuron generation respectively. The ES monolayer culture system used in this study does not employ mitogens to induce neural differentiation [19], and accordingly, significant cell death occurs during NSC formation, especially during days 3 through 6 of differentiation, but thereafter this becomes much less marked as neuronal differentiation proceeds. At the NSC stage, cell death was equally prevalent in all samples derived from either control cells or Rest mutants (Fig. 4A–4E). However, at the neuronal stage, there was markedly more cell death in REST-null cells than those in the control and REST/KD-50 cells (Fig. 4F–4H), which is correlated with the ailing look of neurons derived from REST-null ES cells (Fig. 3H and 3I). Our results indicate that Rest ablation did not impair the proliferation of $Sox1^+/Nestin^-$ NSCs; however it is difficult to assess the proliferation of $Sox1^+/Nestin^+$ NSCs, due to the paucity of $Nestin^+$ NSCs derived from REST-null ES cells. Moreover, *Rest* levels had to be reduced by more than 92% before an increase in cell death at the neuronal stage was observed.

Laminins rescue the phenotype of the REST-null mutant

REST-null defects in cell adhesion may be the cause of its phenotypic effects on $Nestin^+$ NSC production and neuronal differentiation, because cell adhesion defects caused aberrant NSC and neuron development [20–21]. Thus, we further examined the causes of defective adhesion seen in the REST-null mutant. We and others have previously reported that several Rest target genes encode cell adhesion molecules or components of the extracellular matrix (ECM), particularly laminin subunits [7,11]. Accordingly, we considered the notion that dysregulation of the ECM by Rest ablation might be responsible for this aspect of the phenotype. To test this hypothesis, we examined whether we could rescue the adhesion defect and any other phenotypic effects caused by Rest ablation by pre-treatment with ECM components. We plated ES cells from all groups on to either plastic or glass pre-treated with EHS laminins (which contain predominantly Laminin 1 ($\alpha1\beta1\gamma1$)) [22] and subsequently subjected them to neural differentiation. On the glass surface pre-treated with laminins, but not those pre-treated with gelatin, the Rest mutant ES cells behaved like control ES cells, both of which adhered firmly and proliferated well. After 4-days of differentiation (NSC stage), cells from all groups plated onto glass surfaces pre-treated with laminins showed greater survival and significantly less apoptosis than those on untreated surfaces (Fig. 4K–4O). There was no significant difference in cell growth among the treated groups (the control and mutants). The surviving cells were highly proliferative as adjudged by BrdU incorporation (data not shown). Laminin pre-treatment had an even more profound effect after 14-days of differentiation

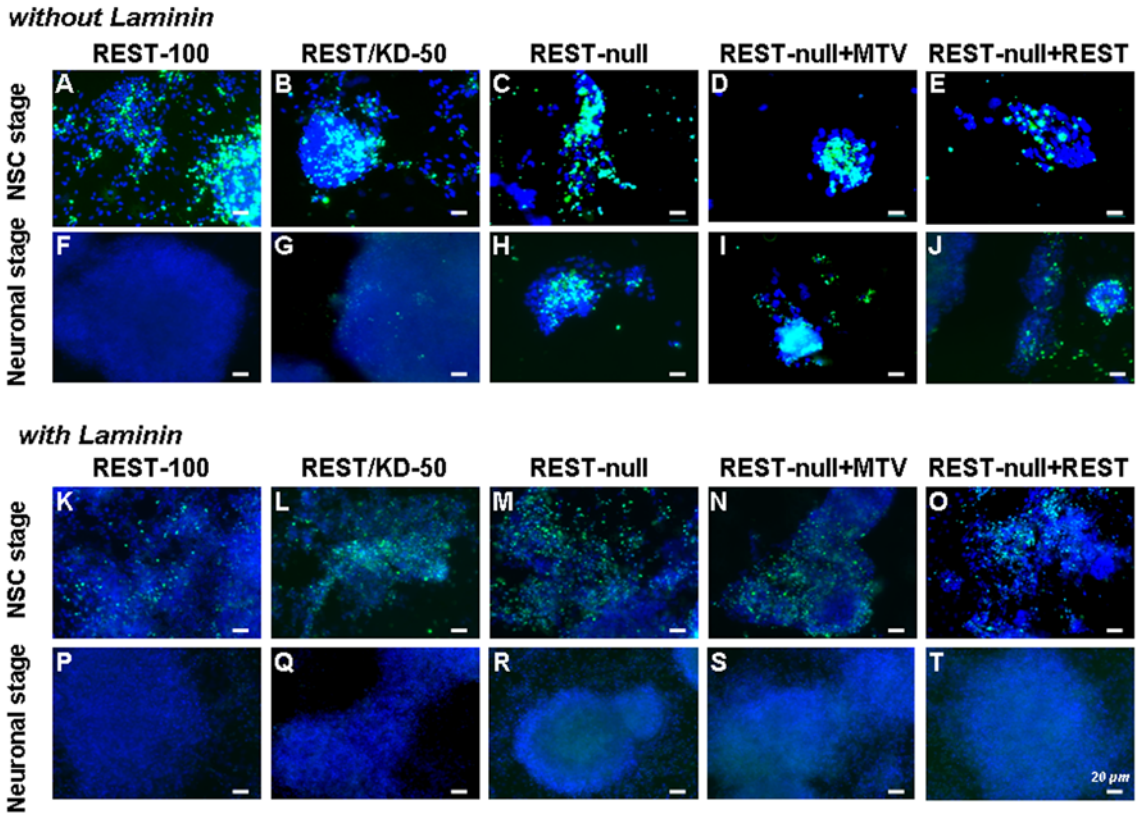

Figure 4. Laminins attenuate cell apoptosis caused by Rest ablation during neural differentiation of ES cells. The control REST-100 and 4 Rest mutant ES cells were either plated on gelatinised glass coverslips (A–J) or on glass coverslips coated with laminins (K–T) and subjected to standard neural differentiation. Cultures were fixed after 4 days of differentiation (A–E and K–O), the peak of NSC generation or fixed after 14 days of differentiation (F–J and P–T), when neurons were prevalent, and cell death in the cultures was assessed using TUNEL staining (green). In all cases cell nuclei were identified by DAPI staining (blue). As expected, cell death was observed when NSCs were generated in all groups (A–E). However, a marked reduction in cell death was observed in all cases when ES cells were plated and differentiated on laminin substrates (compare A–E with K–O). After 14 days of differentiation on gelatinised glass coverslips, markedly more cell death was observed in REST-null than in REST-100 and REST/KD-50 (compare H with F and G). A similar level of death was observed in REST-null+MTV (I). REST-null+REST exhibited less cell apoptosis (J). Laminin-treatment reduced apoptosis in all Rest mutants (compare H–J with R–T). Scale bar: 20 μm.
doi:10.1371/journal.pone.0003656.g004

(neuronal stage). No, or very few, apoptotic cells were detected in either the laminin-treated or control cells without laminin-treatment (Figs. 4F and 4P–4T), whereas significant cell death was found in the Rest mutants in the absence of laminin (Fig. 4H–4J). These data suggested that laminins prevented cell death in the REST-null cells. Intriguingly, the laminin rescue also extended to the specification of NSCs. We reported above that the REST-null ES cells were able to generate early $Sox1^+/Nestin^-$ NSCs but were unable to produce normal numbers of late $Sox1^+/Nestin^+$ NSCs when they were differentiated on a gelatinised glass surface in the absence of laminins (Fig. 3C–3D). This deficiency was rescued by laminin-treatment. Under these conditions, REST-null mutants, like control ES cells, generated equivalent numbers of both early NSCs ($Sox^+/Nestin^-$) and late NSCs ($Sox^+/Nestin^+$) (Fig. 5A–5E; Table 1). Furthermore, laminins rescued the production of NPCs and neurons from the REST-null mutant (Table 1). Neurons derived from REST-null ES cells showed widespread aggregation with extensive fasciculation (Fig. 5H–5I and 5M–5N) compared with those produced on glass in the absence of laminins (Fig. 3H–3I and 3M–3N).

To ensure that the rescue described above was not simply due to the enhanced adhesive properties of laminin, we investigated the ability of fibronectin (a different ECM component with similar adhesive properties to laminin) or poly–D-lysine (a commonly used non-biological substrate for neural cells) to mimic this response. Fibronectin was far less effective in rescuing the generation of $Sox^+/Nestin^+$ cells (late NSCs) from REST-null ES cells than laminin. Some $Sox^+/Nestin^+$ NSCs did develop when grown on fibronectin, however, the number observed was dramatically fewer when compared to that observed when REST-null cells were differentiated on laminins or when REST-100 cells were differentiated (Compare Fig. S8A with Fig. 5A and 5C). Some neurons were observed when REST-null cells were differentiated on fibronectin but again in far fewer numbers than seen after rescue with laminin or after differentiation of control cells (Fig. S8B). Phenotypically, neurons that developed on fibronectin had elongated process, suggesting that fibronectin was able to rescue the neuronal morphology of REST-null derived neurons, at least in part (Fig. S8B). The phenotype observed when REST-null ES cells were differentiated on poly-D-lysine was similar to that observed with gelatine; few $Sox^+/Nestin^+$ NSCs developed and all neurons observed looked ailing, being rounded and devoid of processes (compare Fig. S8A with Fig. 3C and Fig. S8B with Fig. 3H and 3M). Collectively, our results indicate that laminins rescued the adhesion defects seen during differentiation of REST-null ES cells and concomitantly rescued their ability to differentiate into $Nestin^+$ NSCs, NPCs and neurons. This rescue cannot solely be attributed to the adhesive properties of laminin

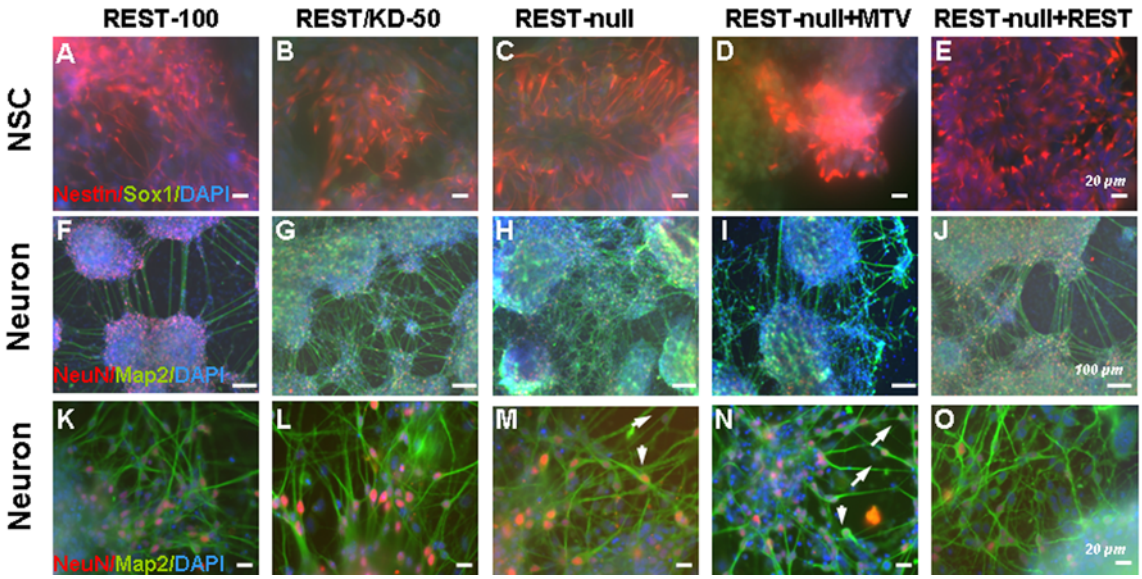

Figure 5. Laminins rescue the phenotypic effects of Rest ablation on the neural differentiation of ES cells. Control (REST-100) and 4 Rest mutants ES cells were grown under neural-differentiating conditions on laminin coated glass coverslips. After 4 days of differentiation some cultures were fixed and labelled with the NSC markers Nestin (red) and Sox1 (green) (A–E). The results show that laminins restored the ability to generate Nestin$^+$ cells in Rest mutants (C–E, compared with Fig. 3C–3E). Sister cultures were allowed to differentiate for 14 days to analyse neuronal differentiation using NeuN (red) and Map2 (green) (F–J and in higher power K–O). Laminins rescued the neuronal phenotypes derived from REST-null ES cells, which included elaboration processes, neurite outgrowth and migration (see arrows in M and N) similar to that seen in neurons derived from control ES cells. Nuclei were stained with DAPI (blue) in all. Scale bars: 20 μm (A to E and K to O) and 100 μm (F to J).
doi:10.1371/journal.pone.0003656.g005

but must involve laminin-directed signalling since fibronectin has similar adhesive properties yet was dramatically less effective at rescuing both the NSC and neuronal differentiation.

Impairment in laminins is caused by Rest ablation

The laminin rescue of the REST-null phenotype indicated that laminins are downstream effectors of Rest. To test this idea, we determined whether the expression of laminins during neurogenesis was impaired by Rest ablation. Laminins have over 15 isoforms, each consisting of a combination of α, β, and γ subunits. In this experiment, we only focused on the effect of Rest deficiency on the expression of the genes encoding α_1 (*Lama1*), β_1 (*Lamb1*), γ_1 (*Lamc1*) and α_2 (*Lama2*) subunits since the EHS laminins used in the rescue experiments are composed mainly of laminin 1 ($\alpha_1\beta_1\gamma_1$). Furthermore α_2 is a known Rest target gene [11] and a major component of the basement membrane in the embryonic CNS that is known to be involved in NSC development [23]. Each of these 4 laminin subunits exhibited distinct expression patterns during neural differentiation of ES cells (Fig. 6). In REST-100 and REST/KD-50 cells, the expression pattern of *Lama1* closely followed the time course of NSC and neuron development. Expression of *Lamb1* and *Lamc1* both showed a very similar pattern with high expression levels in ES cells followed by an initial decline during NSC differentiation and a subsequent gradual increase as neuronal differentiation proceeded. These expression patterns of *Lama1*, *b1* and *c1* are similar to those reported in an earlier *in vitro* study [24]. Intriguingly, the expression pattern of *Lama2* correlated closely with the time course of NSC formation, peaking at 4-days of differentiation, at a similar developmental stage as expression of α_2 *in vivo* [23]. In contrast, REST-null cells exhibited significantly ($P<0.01$) decreased expression levels of *Lama1* throughout neurogenesis (Fig. 6A). Remarkably, raising the *Rest* level to 8% (REST-null+REST) restored *Lama1* levels to 40–50% of those of the control, although the levels remained significantly ($P<0.01$) lower than those seen in control cells. A similar change was also seen in the expression patterns of *Lamb1*, *c1* and *a2*. Rest ablation reduced the levels of *Lamb1*, *c1* and *a2* to below 40% of the level seen in control cells throughout neurogenesis, while raising the *Rest* level to 8% restored, at least partially, the expression levels of *Lamb1* and *a2* (Fig. 6B–6D). Taken together, our results suggest that Rest ablation impairs expression of laminins 1 and 2 ($\alpha_2\beta_1\gamma_1$) during neurogenesis, which leads to defects in cell adhesion, expansion and fasciculation.

Discussion

Development of the vertebrate nervous system is orchestrated by transcriptional programs executed by both transcriptional activators and repressors. Studies suggested that the transcription factor Rest acts as a master regulator to suppress premature differentiation of neuronal progenitors and secure orderly neuronal maturation. Despite a wealth of information on the mechanism of Rest action and on identification of over 2000 target genes, we know very little about the biological function of Rest in the developing and mature nervous system. In our efforts to delineate the function of Rest during neural development, we generated several Rest deficient ES cell mutants to elucidate the role of Rest in the transition from pluripotent ES cells to multipotent NSCs and subsequently to mature neurons. Here, we show that deletion of a single *Rest* allele has no discernible effect on either NSC formation or neurogenesis but severe depletion of *Rest* to levels less than 8% impedes NSC and neuron development, and further that these impairments are mediated by attenuation of laminin levels.

Rest is dispensable for ES cell pluripotency

Recently, a study showed that knocking down Rest by 50% altered ES cell pluripotency and promoted ES cell differentiation into endoderm, mesoderm and ectoderm in ES medium [9].

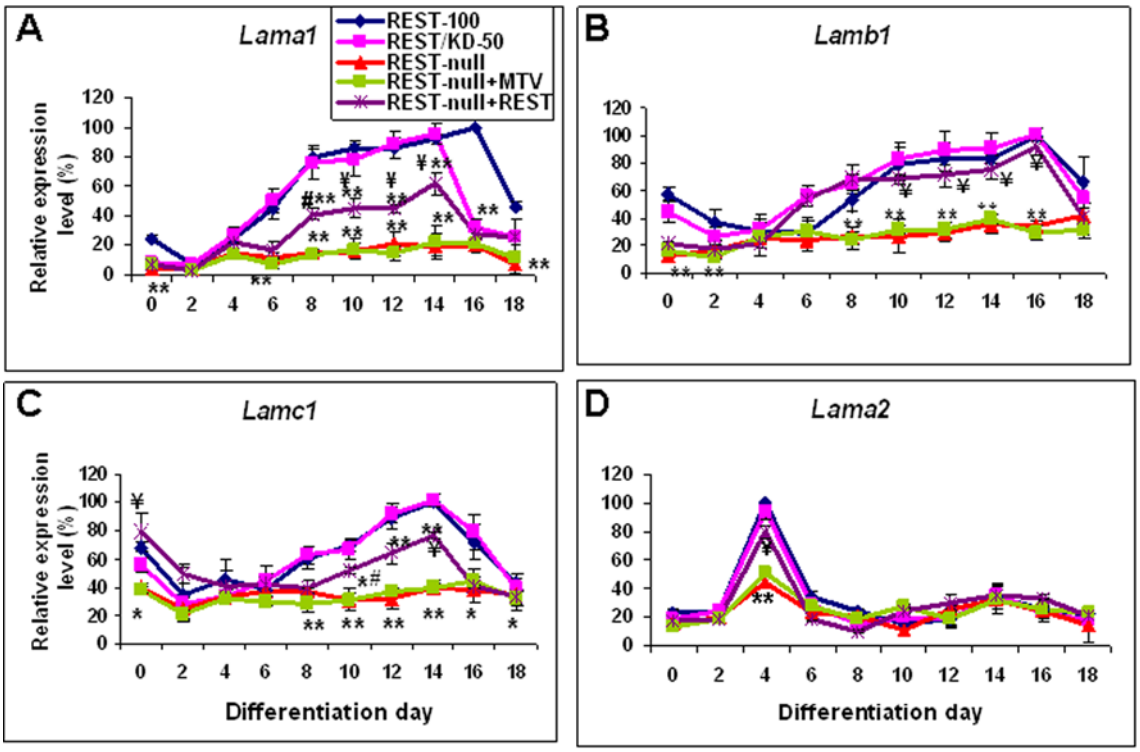

Figure 6. The effects of Rest ablation on the gene expression of laminin subunits during neural differentiation. The expression patterns of *Lama1* (A), *Lamb1* (B), *Lamc1* (C) and *Lama2* (D) were analysed throughout ES cell-derived neural differentiation by real time-PCR. Data are represented as mean±SEM. *P<0.05 and **P<0.01, significantly different from REST-100 and REST/KD-50. #P<0.05 and ¥P<0.01, significantly different from REST-null and REST-null+MTV.
doi:10.1371/journal.pone.0003656.g006

However, our findings show that depletion of Rest levels by 50% to 100% does not change ES cell pluripotency as assessed by expression of pluripotent markers and by lineage competence. In this study, we have generated Rest mutant ES cells, which expressed Rest at 50%, 8% and 0% of the wild-type level. We found that these mutant ES cells did not significantly decrease the expression of *Oct4* and *Nanog*, a finding that is congruent with observations of *Rest*+/− and *Rest*−/− ES cells derived from Rest knockout mice in which gastrulation proceeds normally [6]. Moreover, we also found that two independently derived ES lines with only one allele of *Rest*, REST/KD-50 and *Rest*+/−, both behave like their wild-type counterparts, and are fully capable of normal *in vitro* neural differentiation. These findings are consistent with the findings that, *in vivo*, *Rest*+/− ES cells are pluripotent and are able to generate germ-line mice. Additionally, the mice derived on a *Rest*+/− background showed no discernable phenotypic changes as compared to their wild-type litter-mates [6]. These findings suggest that Rest haplodeficiency does not alter ES cell pluripotency.

Rest ablation impedes NSC and neuron development

There are over 2000 RE1 sites in the human and murine genomes [12] and many RE1-bearing genes encode ion channels, neurotransmitters, growth factors and hormones, and factors involved in axonal guidance and vesicle trafficking, and molecules involved in maintenance of the cytoskeleton [5,25]. The observation that many of these Rest target genes are expressed by postmitotic neurons, helped to foster the initial belief that the role of Rest was to prevent premature expression of neuron-specific genes in NPCs [26–27,6]. Further, it has been proposed that down-regulation of Rest in NPCs is required for their subsequent differentiation [8]. However, we found that Rest ablation in ES cells and NSCs results neither in increased NSC production nor in precocious neuronal differentiation. Rather, Rest ablation significantly decreases the production of Nestin$^+$, *Pax6*- or *Msi1*-expressing NSCs without affecting that of Sox1$^+$ NSCs, suggesting that Nestin$^+$ NSCs are derived from Sox1$^+$ NSCs. This view is confirmed by previous studies showing that the expression of *Nestin* is regulated by co-operative action between Sox1-3 and class III POU transcription factors [28]. Our results indicate that the function of Rest is not restricted to regulating neuronal differentiation as previously conceived, but that Rest also takes part in upstream events regulating the generation of Nestin$^+$ NSCs from Sox1$^+$ NSCs. This regulation of early NSC development is echoed in a previous study that showed that disruption of Rest function in Xenopus disturbs ectoderm patterning and expands the neural plate [18].

Additionally, Rest ablation also reduces the production of Mash1$^+$ (and *Mash1*$^+$) or *Ngn1*$^+$ NPCs. This may be secondary to the diminished NSC population since there are no detectable differences in proliferation or cell death during derivation of NSCs from either the control or REST-null ES cells. Our data show that the role of Rest in NSCs and NPCs is not simply to repress expression of neuronal target genes and to prevent precocious neuronal differentiation, but rather that Rest plays manifold roles at the level of both NSC and NPC generation.

We also find that the absence of Rest in ES cells and NSCs does not cause precocious neuronal differentiation. In fact, even direct Rest target genes, such as the neuronal markers *Tubb3*, *L1cam* and *Scn2A*, are not precociously expressed. This finding resonates strongly with the initial experiments on *Rest*−/− mice, which displayed embryonic lethality around E11, but importantly, showed no widespread precocious expression of Rest target genes.

Only *Tubb3* was seen to be de-repressed in non-neuronal tissues but not in the developing CNS. Furthermore, constitutive expression of Rest in chick spinal cord causes axon pathfinding errors, but only two Rest target genes encoding *Tubb3* and *L1cam* were repressed [17]. Taken together, our findings suggest that the role of Rest in neuronal differentiation is not to simply regulate its neuronal target genes by a simple "on-off" switch. The regulation of Rest in these target genes may be compounded by other transcriptional repressors or co-repressors, such as has been reported for SMCX, a transcriptional repressor that co-regulates Rest neuronal target genes in X-linked mental retardation [29] and NFkappaB that synergistically interacts with Rest in the suppression of *TAC1* in non-neuronal cells [30].

Strikingly, there is also no evidence that the absence of Rest promotes or increases neuron number [31–32]. On the contrary, we find that Rest knockout decreases neuron production and causes severe defects in neuronal interaction (judged by malformation of neuronal processes and fascicles and neuronal migration). The decline in neuron production, in part, is attributed to cell death, because we found that Rest ablation increases neuronal death. These phenomena however can be rescued by increasing levels of *Rest* expression, indicating that Rest is a causal effector. Taken together, the role of Rest during neuronal development is not restricted simply to repress neuron-specific genes in NPCs prior to terminal neuronal differentiation.

Laminin deficiency causes impairment in NSC and neuron development in REST-null ES cells

In this study, the most striking phenotype of Rest mutant ES cells is their defective adhesion, especially on a glass surface. The other phenotypes include impairment in the production of $Nestin^+$ NSCs (albeit the mutants can generate a comparable amount of $Sox1^+$ NSCs), and defects in neuronal migration and process formation. Additionally, Rest ablation results in greater cell death and a consequent reduction in the number of neurons. Interestingly, we also observed these phenotypes in ES cells derived from *Rest*−/− mice [6]. Our finding suggests these are *bona fide* phenotypes of Rest-null mutants and not due to the artefact of a single ES cell line used in this study. In previous studies, we and others identified several Rest target genes that are involved in cell-matrix adhesion and cell-cell interaction, such as *Lama1*, *Lama2*, *Arc*, *Cspg3*, *Unc5d*, *Adam23*, *Catnd2*, *Cdh4*, *L1-cam* and *Mmp24* [7,11,12]. This latter observation prompted us to consider the possibility that dysregulation of cell-matrix adhesion molecules may be responsible for Rest-knockout phenotypes.

Cell-matrix adhesion molecules mediate direct interactions of the cell with its extracellular environment by binding of cell surface molecules with components of ECM, and are crucial for cell migration, differentiation, organisation and embryogenesis [33–35]. In the developing central nervous system, the ECM is present in the basement membrane of the ventricular zone and is essential for ordered differentiation of neuronal subtypes in the cerebral cortex [36]. *In vitro*, the ECM has been shown to play an important role in lineage decision and cell type selection [21,37]. The ECM mainly consists of laminins, fibronectin, type IV collagen, nidogen and heparan sulfate proteoglycans [38–39]. Laminins are a family of extracellular glycoproteins expressed throughout developing neural tissues and each laminin is composed of α, β, and γ polypeptide chains [40]. In this study, EHS laminins rescue the phenotypes of Rest mutant, by restoring their adhesion ability and their differentiation into $Nestin^+$ NSCs, NPCs and mature neurons. Not only do laminins promote neuron migration, neurite outgrowth and elaboration, but they also prevent neuronal cell death caused by Rest ablation. These findings resonate with the known functions of laminins in the NS cell niche where they are required for proliferation, neuronal differentiation and survival, and neurite outgrowth [20,23,41]. Additionally, we found that although fibronectin exhibited similar adhesiveness to that of laminins, it nevertheless was markedly less effective than laminins in restoring the REST-null phenotype, indicating that specific ECM signalling rather than adhesion alone is the key player in REST-null phenotypes.

How does Rest impair the expression of laminins, which subsequently generate phenotypic effects in Rest mutants? We know that the genes encoding laminin subunits α1 and α2 are direct Rest target genes [11] and γ1 is an indirect target since it is regulated by miR-124, which is a direct Rest target gene [42]. During neural differentiation of ES cells, the expression pattern of *Lama1* showed an inverse relationship with that of *Rest*, suggesting Rest may act as a repressor in *Lama1* expression. However, Rest ablation in ES cells caused impairment in stage-dependent *Lama1* expression, indicating that a minimal amount of Rest is required to maintain *Lama1* expression. That this is the case can be seen from the rescue of *Lama1* expression by raising *Rest* levels to 8%. This phenomenon also applies to the *Lama2* expression. In fact, the expression of *laminin* subunits correlates with severity of phenotypic effects of Rest deficiency. In conclusion, our studies show that one of the roles of Rest in neural development is to regulate ECM components, which in turn are required for the transition from ES cell to neural lineage. Furthermore, we show that Rest is required at multiple stages during neural development from production of NSCs through to terminal neuronal differentiation. This contrasts with the contemporary idea that limits Rest to regulation of neuronal development by simply repressing neuron-specific target genes prior to loss of Rest expression during the final stages of terminal neuronal differentiation.

Materials and Methods

Generation of Rest mutant ES cells

To generate Rest mutant ES cells, firstly, we have constructed a conditional knockout targeting vector, REST/ck vector (Fig. S1A) to replace one allele of the *Rest* gene in HM1 ES cells (a gift from Dr. J. Mcwhir, the Roslin Institute) using homologous recombination. In general, HM1 ES cells were transfected with the REST/ck vector digested with Afl II/Bgl II using electroporation (800 V, Time constant 0.2 msec) and in G418 selection from the second day after transfection. Colonies were screened for targeted clones using RT-PCR with two primer pairs, primers 1/2 and primers 3/4 (Fig. S1A). Of 500 colonies, one clone was identified as a REST/ck-targeted clone, which was used to create the control ES cells (called REST-100) and Rest+/− ES cells (called REST/KD-50). REST-100 ES cells were generated by stably transfecting with the empty pSuper vector, whereas REST/KD-50 ES cells were created by transiently expressing *Cre* recombinase (a gift from Dr. Jeremy Brown) to delete one allele of *Rest*. The REST/KD-50 ES cells were then used to create REST-null ES cells by stably expressing a Rest shRNA (5′-GTGTAATCTACAATACCAT-3′) in the presence of puromycin (2 μg/ml) using a pSuper-Rest-shRNA vector [43].

The *Rest* levels expressed from REST-100, REST/KD-50 and REST-null ES cells were 100%, 50% and 1%, respectively as adjudged by quantitative Real-time PCR (Fig. S1B), and confirmed by Western blot analysis (Fig. S1D). In our Western blot analysis, the level of Rest in REST-100 (lane 1) is approximately double that seen in REST/KD-50 (lane 2) when normalised to levels of the house-keeping gene, Gapdh (lower panel) (Fig. S1D). Although REST-null ES cells produced 1% of

wild type *Rest* mRNA levels, as detected by PCR analysis, Rest protein level was undetectable by Western blot analysis using a Rest antibody (Upstate; 07-579) at a 1:1000 dilution. Therefore, we consider this to be a Rest-null mutant. For a rescue experiment, we constitutively expressed *Rest* in the REST-null ES cells with the pMT-NRSF vector (a gift from David Anderson, Caltech [27]) to produce REST-null+REST, which expresses 8% of the control *Rest* levels. Control cells were produced by transfection of REST-null ES cells with empty pMT vector (REST-null+MTV) (Fig. S1C–S1D). Although Rest in REST-null+REST ES cells was not detectable by Western blot analysis, it was detected by immunocytochemical analysis (data not shown). We also showed that *Rest* is effectively silenced throughout the neuronal differentiation process (Fig. S1B–S1C). Furthermore, in contrast to recent observations [9], we also found that Rest deficiency (50% to 100%) did not affect the pluripotency of ES cells as adjudged by the expression levels of *Oct4* and *Nanog* (Fig. S1E).

Quantitative Real Time-PCR

Primer design and experimental details were carried out as described previously [7] and in Methods S1. Primers used in this study are shown in Table S1. All expression levels were normalised to cyclophillin levels and then as a percentage of the highest level of expression of the REST-100 clone. All data were performed in duplicate and repeated three times.

Statistical Analysis

Statistical significance was determined using a two-tailed Student test. P values of <0.05 and <0.01 were considered statistically significant. All results are presented as mean$\pm$standard error of the mean (SEM) from experiments that have been repeated three times.

Neuronal differentiation

Rest mutant and control ES cells were differentiated into NSCs, NPCs and then neurons using a monolayer culture in N2B27 medium [19]. For studying gene expression patterns and for cell type analysis, control and Rest mutant ES cells (600,000 cells/plate) were plated onto 10-cm Petri dishes coated with 0.1% gelatine in ES medium. The next day, the ES cell medium was replaced with N2B27 medium. Medium was changed every 2 days and differentiation continued for 18 days. For studying gene expression patterns, samples were collected at day 0 (ES cell stage, before differentiation) and 2, 4, 6, 8, 10, 12, 14, 16 and 18 days after differentiation. For cell type analysis using FACS, samples were collected separately from 4, 10 and 14 days of differentiation, which cells were plated out either on gelatine or laiminin-treated surface. In immunocytochemical analysis, ES clones were seeded onto gelatinised, polyornithine/fibronectin (10 μg/ml, Sigma), polyornithine/laminin (10 μg/ml, Sigma) or poly-D-lysine (60 μg/ml, Sigma) coated glass coverslips (VWR, 631-0150) in 24-well plates at a density of $1\times10^4/cm^2$ in ES cell medium. The next day, cells were subjected to the differentiation process in N2B27 medium. All experiments were repeated three times.

Immunocytochemistry

ES cells, NSCs and neurons were fixed in 3% paraformaldehyde for 20 min at RT. Antibodies, Nestin (1:500, MAB353, Chemicon) and Sox1 (1:500, AB5934, Chemicon) were used to identify neural stem cells, whereas NeuN (1:500, MAB377, Chemicon) and MAP2 (1:400, ab10588-50, Abcam) were used for staining neurons. All primary antibody staining was carried out at 4°C, overnight. Samples were then stained with appropriate fluorescence-conjugated secondary antibodies at RT for 1 hr and examined under an Axiovision fluorescent microscope (Zeiss).

Flow cytometry

Cells were collected 4, 10 and 14 days after differentiation for FACS analysis of NSCs, NPCs/early neurons and mature neurons, respectively. Cells were trypsinised to dissociate into single cells, fixed in 3% paraformaldehyde for 15 min, permeabilsed with 0.1% saponin (Invitrogen) for 30 min and then stained with Nestin/Sox1 (both 1:250) or Mash1(Chemicon)/Tau (Chemicon) (both 1:200) or Map2 (1:300) in the presence of 0.1% saponin for 1 hr. All procedures were carried out at room temperature. Cells were subsequently stained with their corresponding secondary antibodies: Cy3-anti-mouse/FITC-anti-chicken (both 1:300) for Nestin/Sox1, Cy3-anti-goat/FITC-anti-rabbit (both 1:300) for Mash1/Tau and FITC-anti-chicken (1:300) for Map2. The corresponding controls were stained only with secondary antibodies. Cells were acquired with a FACS LSR with CellQuest software (BD biosciences). Flow cytometry data were analysed using Summit v4.3 (Dako Colorado, Inc). All FACS analysis experiments were repeated three times.

Cell proliferation and apoptosis

5-bromo-2-deoxyuridine (BrdU; 10 μM; Sigma) was added to ES cells grown on polyornithine/laminin (10 μg/ml) coated 13 mm glass coverslips. 16 hrs later, cultures were fixed with 2% paraformaldehyde for 15 min, followed by 95% methanol for 30 min at room temperature. After rinsing with PBS, coverslips were incubated with a biotin conjugated sheep anti-BrdU antibody (1:250; Abcam) overnight at 4°C in PBS containing 0.1% Triton X-100 and 10% normal goat serum (Sigma). BrdU labelled cells were visualised using streptdavidin conjugated to Alexa Fluor 488 (1:500; Invitrogen). After three washes with PBS, coverslips were mounted on slides using Fluoromount-G (Invitrogen) and analysed using an Axiovision fluorescent microscope (Zeiss). Apoptotic cell death was detected by terminal deoxyribonucleotidy transferase-mediated dUTP-digoxigenin nick end labelling (TUNEL) according to manufacturer's instructions (Promega).

Supporting Information

Figure S1 The generation of Rest mutants. (A) The Rest conditional knockout targeting vector (REST/ck) (bottom) was designed according to *Rest* gene (top). The REST/ck vector was constructed by inserting a FRT-tk-neor-FRT-LoxP cassette at the Aat II site in intron 2 and a LoxP site at the Asc I site in the exon 1 of *Rest* gene. This design is to abrogate Rest production by snapping off exons 1 and 2, which encode the transcriptional start sites, the N terminal repression domain and 4 zinc fingers of Rest protein, in the presence of Cre recombinase. Primers shown were used to identify targeted clones. (B–C) *Rest* expression levels during ES cell-derived neural development from the control (REST-100), REST/KD-50, REST-null, REST-null+MTV and REST-null+REST. (Data are represented as mean$\pm$SEM.) (D) Western blot analysis in the control and Rest mutants. Lane 1: REST-100; 2: REST/KD-50; 3: REST-null; 4: REST-null+MTV and 5: REST-null+REST. Gapdh as an internal control. (E) The pluripotency of embryonic stem (ES) cells was not altered in Rest mutants judged by the expression of ES cell markers, *Oct4* and *Nanog*. (Data are represented as mean$\pm$SEM.)
Found at: doi:10.1371/journal.pone.0003656.s001 (0.15 MB TIF)

Figure S2 Gene expression patterns of stage-specific markers during 46C ES-derived neural differentiation. ES cell differentiation into neurons recapitulates neurogenesis in vivo down-regulation of ES cell pluripotent marker *Oct4* and *Rest* (A) to the

sequential development, firstly neural stem cells (*Nestin* and *Pax6*) (B), then neural progenitor cells (*Mash1* and *Ngn1*) (C) and to neurons (*Syn1*, *L1cam* and *Tubb3*) (D). This experiment corroborated the findings in HM1 ES cells.
Found at: doi:10.1371/journal.pone.0003656.s002 (0.07 MB TIF)

Figure S3 FACS analysis of $Sox1^+$ and/or $Nestin^+$ NSCs derived from control and Rest mutant ES cells. (A) Background control showing control (REST-100) cells co-stained with the secondary antibodies (Cyc3-anti-mouse/FITC-anti-chicken) used to visualise the anti-Nestin and anti-Sox1 antibodies respectively. (B–F) Nestin and Sox1 expression on NSCs generated from control and Rest mutant ES cells. Cells in the R5, R2 and R3 areas are classified as $Sox1^+$, $Nestin^+$ and $Sox1^+/Nestin^+$ respectively. These NSC populations are summarised in Table 1.
Found at: doi:10.1371/journal.pone.0003656.s003 (0.25 MB TIF)

Figure S4 FACS analysis of $Mash1^+$ and/or Tau^+ NPCs/early neurons from control and Rest mutants. (A) Background control showing control (REST-100) cells co-stained with the secondary antibodies (Cyc3-anti-goat/FITC-anti-rabbit) used to visualise to the anti-Mash1 and anti-Tau antibodies respectively. (B–F) Mash1 and Tau expression on NPCs/early neurons generated from control and Rest mutant ES cells. Cell in the R5, R2 and R3 areas are classified as Tau^+, $Mash1^+$ and $Tau^+/Mash1^+$ respectively. These populations of NPCs/early neurons are summarised in Table 1.
Found at: doi:10.1371/journal.pone.0003656.s004 (0.22 MB TIF)

Figure S5 FACS analysis of $Map2^+$ neurons from control and Rest mutant ES cells. (A) Background control showing control (REST-100) cells stained with the secondary antibody (FITC-anti-chicken) used to visualise to the anti-Mash1 antibody. (B–F) Map2 expression on neurons generated from control and Rest mutant ES cells. Cells in the R5 area are classified as $Map2^+$ mature neurons. This population of mature neurons is summarised in Table I.
Found at: doi:10.1371/journal.pone.0003656.s005 (0.21 MB TIF)

Figure S6 Constitutively expressing *Rest* in REST-null ES cells rescues their differentiation defects. By constitutively expressing *Rest* in REST-null cells (REST-null+REST) using pMT-NRSF, we raised *Rest* levels to 8% of wild-type levels. We compared the ability of REST-null+REST ES cells to generate NSCs, NPCs and neurons with that of the REST-null ES cells transfected with empty vector (REST-null+MTV) by real time-PCR analysing the expression of stage-specific differentiation markers: *Pax6*, *Msi1* and *Nestin* to detect neural stem cells (NSCs) (A–C); *Ngn1* and *Mash1* to detect neural progenitor cells (NPCs) (D, E); *Tubb3* to detect young neurons (F) and *Scn2a* and *L1cam* to detect mature neurons (G–H). Raising *Rest* expression level to 8% restored the gene expression levels of stage-specific markers to those observed in the control ES cells. Data are represented as mean±SEM. *$P<0.05$ and **$P<0.01$, significantly different from REST-null+REST.
Found at: doi:10.1371/journal.pone.0003656.s006 (0.09 MB TIF)

Figure S7 Confirmation of REST-null phenotypes in the ES cells derived from Rest knockout mice (Chen et al., 1998). (A) Rest protein expression analysed by Western blot. An alternatively spliced Rest isoform, which has a deletion in the entire exon 2 encoding the N-terminus of Rest, can be seen in ES cells derived from *Rest*+/− and *Rest*−/− mice. Gapdh was used as an internal control. (B) The expression levels of *Rest* in wild-type, *Rest*+/− and *Rest*−/− ES cells quantified by real-time PCR using primer sets designed against the N-ternimus and the C-terminus of *Rest* gene. *Rest* is expressed in *Rest*−/− ES at the wild-type level when primers against the C-terminus of *Rest* were used, indicating the existence of an alternatively spliced isoform which corroborated the result analysed by Western blot analysis (A). (C–E) The neural stem cells (NSCs) derived from wild-type, *Rest*+/− and *Rest*−/− ES cells were identified by Sox1 (green) and Nestin (red) from a 4-day differentiation. Nuclei were stained with DAPI (blue). The NSCs from *Rest*−/− ES cells show less Nestin expression in $Sox1^+$ cells as compared to those from wild-type and *Rest*+/− ES cells, which is resemble to the finding in REST-null mutants (Fig. 3C and 3D). (F–H) Low power and (I–K) high power images of neurons derived from the wild-type, *Rest*+/− and *Rest*−/− ES cells. Neurons were identified by NeuN (red) and Map2 (green) after 14 days of differentiation. Nuclei were counterstained with DAPI (blue). The neurons generated from wild-type and *Rest*+/− ES cells show similar phenotypes to those derived from REST-100 and REST/KD-50 ES cells (Fig. 3F–G and K–L), whereas the neurons from *Rest*−/− to those from REST-null ES cells, which are devoid elaborated processes and migration (Fig. 3H–I and M–N).
Found at: doi:10.1371/journal.pone.0003656.s007 (0.66 MB TIF)

Figure S8 The effect of fibronectin and ploy-D-lysine on REST-null phenotypes. Control (REST-100) and REST-null ES cells were plated onto coverslips coated either with poly-D-lysine or fibronectin. The next day, cells were driven along a neural differentiation pathway in B2N27 medium. After 4 days of differentiation cells were fixed and analysed for the presence of neural stem cells by staining with Sox1 (green) and Nestin (red) (A) and the presence of neurons by staining with Map2 (green) and NeuN (red) after 14 days of differentiation (B). Nuclei were stained with DAPI (blue) (scale bar: 25 μm). All images were captured using a Zeiss fluorescence microscope equipped with an ApoTOME.
Found at: doi:10.1371/journal.pone.0003656.s008 (0.73 MB TIF)

Methods S1 Supplemental data
Found at: doi:10.1371/journal.pone.0003656.s009 (0.03 MB DOC)

Acknowledgments

We would like to thank Dr. Michelle Peckham, Dr. Nikolai D. Belyaev and Dr. Lezanne Ooi (University of Leeds) for their contributions to this paper.

Author Contributions

Conceived and designed the experiments: YMS ZFC BPW. Performed the experiments: YMS MC SF HHL. Analyzed the data: YMS. Contributed reagents/materials/analysis tools: YMS ZFC. Wrote the paper: YMS. Edited the manuscript: BPW NJB. Finacial support: NJB.

References

1. Coucouvanis E, Martin GR (1995) Signals for death and survival: a two-step mechanism for cavitation in the vertebrate embryo. Cell 83: 279–287.
2. Gardner RL, Rossant J (1979) Investigation of the fate of 4–5 day post-coitum mouse inner cell mass cells by blastocyst injection. J Embryol Exp Morphol 52: 141–152.
3. Lawson KA, Pedersen RA (1992) Clonal analysis of cell fate during gastrulation and early neurulation in the mouse. In Post-implantation Development in the Mouse. Chichester: Wiley (Ciba Found. Symp. 165). pp 3–26.
4. Rubenstein JLR, Shimamura K (1998) Regionalisation of the prosencephalic neural plate. Ann Rev Neurosci 21: 445–477.
5. Schoenherr CJ, Paquette AJ, Anderson DJ (1996) Identification of potential target genes for the neuron-restrictive silencer factor. Proc Natl Acad Sci U S A 93: 9881–9886.
6. Chen Z-F, Paquette AJ, Anderson DJ (1998) NRSF/REST is required in vivo for repression of multiple neuronal target genes during embryogenesis. Nat Genet 20: 136–142.

7. Sun Y-M, Greenway DJ, Johnson R, Street M, et al. (2005) Distinct profiles of REST interactions with its target genes at different stages of neuronal development. Mol Biol Cell 16: 5630–5638.
8. Ballas N, Grunseich C, Lu DD, Speh JC, Mandel G (2005) REST and its corepressors mediate plasticity of neuronal gene chromatin throughout neurogenesis. Cell 121: 645–657.
9. Singh SK, Kagalwala MN, Parker-Thornburg J, Adams H, Majumder S (2008) REST maintains self-renewal and pluripotency of embryonic stem cells. Nature. pp 23. [Epub ahead of print].
10. Johnson DS, Mortazavi A, Myers RM, Wold B (2007) Genome-wide mapping of in vivo protein-DNA interactions. Science 316: 1497–1502.
11. Otto SJ, McCorkle SR, Hover J, Conaco C, Han JJ, et al. (2007) A new binding motif for the transcriptional repressor REST uncovers large gene networks devoted to neuronal functions. J Neurosci 27: 6729–6739.
12. Johnson R, Gamblin RJ, Ooi L, Bruce AW, Donaldson IJ, et al. (2006) Identification of the REST regulon reveals extensive transposable element-mediated binding site duplication. Nucleic Acids Res 34: 3862–3877.
13. Ooi L, Wood IC (2007) Chromatin crosstalk in development and disease: lessons from REST. Nat Rev Genet 8: 544–554.
14. Roopra A, Qazi R, Schoenike B, Daley TJ, Morrison JF (2004) Localized domains of G9a-mediated histone methylation are required for silencing of neuronal genes. Mol Cell 14: 727–738.
15. Shi Y, Lan F, Matson C, Mulligan P, Whetstine JR, et al. (2004) Histone demethylation mediated by the nuclear amine oxidase homolog LSD1. Cell 119: 941–953.
16. Battaglioli E, Andrés ME, Rose DW, Chenoweth JG, Rosenfeld MG, et al. (2002) REST repression of neuronal genes requires components of the hSWI.SNF complex. J Biol Chem 277: 41038–41045.
17. Paquette AJ, Perez SE, Anderson DJ (2000) Constitutive expression of the neuron-restrictive silence factor (NRSF)/REST in differentiating neurons disrupte neuronal gene expression and causes axon pathfinding errors in vivo. Proc Natl Acad Sci U S A 97: 12318–12323.
18. Olguín P, Oteíza P, Gamboa E, Gómez-Skármeta JL, Kukuljan M (2006) RE-1 silencer of transcription/neural restrictive silencer factor modulates ectodermal patterning during Xenopus development. J Neurosci 26: 2820–2829.
19. Ying QL, Stavridis M, Griffiths D, Li M, Smith A (2003) Conversion of embryonic stem cells into neuroectodermal precursors in adherent monoculture. Nat Biotechnol 21: 183–186.
20. Andressen C, Adrian S, Fässler R, Arnhold S, Addicks K (2005) The contribution of beta1 integrins to neuronal migration and differentiation depends on extracellular matrix molecules. Eur J Cell Biol 84: 973–982.
21. Chen SS, Fitzgerald W, Zimmerberg J, Kleinman HK, Margolis L (2007) Cell-Cell and Cell-Extracellular Matrix Interactions Regulate Embryonic Stem cell. Differentiation 25: 553–561.
22. Ekblom P, Timpl R (1996) The Laminins. Harwood academic publisher: CRC Press.
23. Lathia JD, Patton B, Eckley DM, Magnus T, Mughal MR, et al. (2007) Patterns of laminins and inegrins in the embryonic ventricular zone of the CNS. J Comp Neuro 505: 630–643.
24. Aumailley M, Pesch M, Tunggal L, Gaill F, Fässler R (2000) Altered synthesis of laminin 1 and absence of basement membrane component deposition in β1 integrin-deficient embryoid bodies. J Cell Sci 113: 259–268.
25. Bruce AW, Donaldson IJ, Wood IC, Yerbury SA, Sadowski MI, et al. (2004) Genome-wide analysis of repressor element 1 silencing transcription factor/neuron-restrictive silencing factor (REST/NRSF) target genes. Proc Natl Acad Sci U S A 101: 10458–10463.
26. Chong JA, Tapia-Ramírez J, Kim S, Toledo-Aral JJ, Zheng Y, et al. (1995) REST: a mammalian silencer protein that restricts sodium channel gene expression to neurons. Cell 80: 949–957.
27. Schoenherr CJ, Anderson DJ (1995) Silencing is golden: negative regulation in the control of neuronal gene transcription. Curr Opin Neurobiol 5: 566–571.
28. Tanaka S, Kamachi Y, Tanouchi A, Hamada H, Jing N, et al. (2004) Interplay of Sox and Pou factors in regulation of the Nestin gene in Neural primordial cells. Mol Cell Biol 24: 8834–8846.
29. Tahiliani M, Mei P, Fang R, Leonor T, Rutenberg M, et al. (2007) The histone H3K4 demethylase SMCX links REST target genes to X-linked mental retardation. Nature 447: 601–605.
30. Greco SJ, Smirnov SV, Murthy RG, Rameshwar P (2007) Synergy between the RE-1 silencer of transcription and NFkappaB in the repression of the neurotransmitter gene TAC1 in human mesenchymal stem cells. J Biol Chem 282: 30039–30050.
31. Su X, Kameoka S, Lentz S, Majumder S (2004) Activation of REST/NRSF target genes in neural stem cells is sufficient to cause neuronal differentiation. Mol Cell Biol 24: 8018–8025.
32. Thiel G, Lietz M, Leichter M (1999) Regulation of neuronal gene expression. Naturwissenschaften 86: 1–7.
33. Berrier AL, Yamada KM (2007) Cell-matrix adhesion. J Cell Physiol 213: 565–573.
34. Larsen M, Artym VV, Green JA, Yamada KM (2006) The matrix reorganized: extracellular matrix remodeling and integrin signaling. Curr Opin Cell Biol 18: 463–471.
35. Geiger B, Bershadsky A, Pankov R, Yamada KM (2001) Transmembrane crosstalk between the extracellular matrix–cytoskeleton crosstalk. Nat Rev Mol Cell Biol 2: 793–805.
36. Haubst N, Georges-Labouesse E, De Arcangelis A, Mayer U, Götz M (2006) Basement membrane attachment is dispensable for radial glial cell fate and for proliferation, but affects positioning of neuronal subtypes. Development 133: 3245–3254.
37. Goetz AK, Scheffler B, Chen H-X, Wang S, Suslov O, et al. (2006) Temporally restricted substrate interactions direct fate and specification of neural precursors derived from embryonic stem cells. Proc Natl Acad Sci U S A 103: 11063–11068.
38. Erickson AC, Couchman JR (2000) Still more complexity in mammalian basement membranes. J Histochem Cytochem 48: 1291–1306.
39. Timpl R (1996) Macromolecular organization of basement membranes. Curr Opin Cell Biol 8: 618–624.
40. Powell SK, Kleinman HK (1997) Neuronal laminins and their cellular receptors. Int J Biochem Cell Biol 29: 401–414.
41. Colognato H, ffrench-Constant C, Feltri ML (2006) Human diseases reveal novel roles for neural laminins. TRENDS in Neurosci 28: 480–486.
42. Conaco C, Otto S, Han J-J, Mandel G (2006) Reciprocal actions of REST and a microRNA promote neuronal identity. Proc Natl Acad Sci U S A 103: 2422–2427.
43. Loh YH, Wu Q, Chew JL, Vega VB, Zhang W, et al. (2006) The Oct4 and Nanog transcription network regulates pluripotency in mouse embryonic stem cells. Nat Genet 38: 431–440.

Appendix 3

Neuronatin Promotes Neural Lineage in ESCs Via $Ca2^{+}$ Signaling

Hsuan-Hwai Lin, Esther Bell, Dafe Uwanogho, Leo W. Perfect, Harun Noristani, Thomas J. D. Bates, Vladimir Snetkov, Jack Price, Yuh-Man Sun

STEM CELLS (2010) 28:1950–1960.

STEM CELLS®

EMBRYONIC STEM CELLS/INDUCED PLURIPOTENT STEM CELLS

Neuronatin Promotes Neural Lineage in ESCs Via Ca^{2+} Signaling

HSUAN-HWAI LIN,[a,b] ESTHER BELL,[c] DAFE UWANOGHO,[a] LEO W. PERFECT,[a] HARUN NORISTANI,[a] THOMAS J. D. BATES,[c] VLADIMIR SNETKOV,[d] JACK PRICE,[a] YUH-MAN SUN[a]

[a]Institute of Psychiatry, King's College London, Centre for the Cellular Basis of Behaviour London, United Kingdom; [b]Department of Internal Medicine, Tri-Service General Hospital, National Defense Medical Center, Taipei, Taiwan, Republic of China; [c]MRC Centre for Developmental Neurobiology, Kings College London, Guy's Campus, London, United Kingdom; [d]Department of Asthma, Allergy and Respiratory Science, Franklin-Wilkins Building, King's College London, London, United Kingdom

Key Words. Neural development • Embryonic stem cells • Calcium signaling • FGF/Erk pathway • Nnat • BMP pathway

ABSTRACT

Neural induction is the first step in the formation of the vertebrate central nervous system. The emerging consensus of the mechanisms underling neural induction is the combined influences from inhibiting bone morphogenetic protein (BMP) signaling and activating fibroblast growth factor (FGF)/Erk signaling, which act extrinsically via either autocrine or paracrine fashions. However, do intrinsic forces (cues) exist and do they play decisive roles in neural induction? These questions remain to be answered. Here, we have identified a novel neural initiator, neuronatin (Nnat), which acts as an intrinsic factor to promote neural fate in mammals and *Xenopus*. ESCs lacking this intrinsic factor fail to undergo neural induction despite the inhibition of the BMP pathway. We show that Nnat initiates neural induction in ESCs through increasing intracellular Ca^{2+} ($[Ca^{2+}]_i$) by antagonizing Ca^{2+}-ATPase isoform 2 (sarco/endoplasmic reticulum Ca^{2+}-ATPase isoform 2) in the endoplasmic reticulum, which in turn increases the phosphorylation of Erk1/2 and inhibits the BMP4 pathway and leads to neural induction in conjunction with FGF/Erk pathway. STEM CELLS *2010;28:1950–1960*

Disclosure of potential conflicts of interest is found at the end of this article.

INTRODUCTION

During mouse embryogenesis, the inner cell mass of the blastocyst differentiates into pluripotent primitive ectoderm and gives rise to a structure known as the epiblast [1]. The epiblast responds to extrinsic signals and generates three primary germ layers: ectoderm, mesoderm, and endoderm [2]. At the stage of neural induction, the ectoderm gives rise to the neuroectoderm (called the neural plate, composed of neuroepithelial cells/neural stem cells [NSCs]) [3]. Knowledge of the mechanism underlying neural induction is primarily derived from studies in *Xenopus*, in which bone morphogenetic proteins (BMPs) act as a decisive inhibitory force during neural induction. This generates the neural default model, which postulates that in the absence of BMP signaling, ectodermal cells will adopt a neural fate [4]. However, the default model remains a debated issue [5, 6]. To date, several signaling pathways, including BMP [7–10], FGF [11–17], Ca^{2+} [18, 19], Wnt [20–23], and Shh [24] have been shown to play critical roles in neural induction in various species. BMP4, FGFs, Wnt, and Shh exert their regulatory roles in neural induction by binding to their receptors in the cell membrane of ectodermal cells, which in turn trigger intracellular signaling cascades. These factors exert extrinsic influences on ectodermal cells to inhibit or induce neural induction. So far, no intrinsic factor (other than Smad7, if it can be considered as one) [25] has been identified and its role in neural induction is basically unknown.

In a wider study to screen for genes involved in neural induction, we have identified a novel intrinsic neural initiator, Neuronatin (Nnat). *Nnat* is a maternal imprinted gene located on mouse chromosome 2 [26], which encodes a membrane protein in the endoplasmic reticulum (ER) [26] and is predominantly expressed in the developing brain [26, 27]. Transcription processing of *Nnat* gene leads to the generation of two alternatively spliced isoforms (α and β mRNA) [28] and their expression patterns suggest that *Nnat* plays a role in brain development [29, 30]. However, its precise functions during central nervous system development remain to be elucidated. In this study, we address the role and mechanistic action of Nnat in neural induction and neuronal differentiation using an in vitro mammalian embryonic stem cell (ESC)-derived neural lineage model [31, 32], which recapitulates

Author contributions: H.-H.L.: collection and/or assembly of data; E.B.: collection and/or assembly of data, financial support, conception and design, and data analysis and interpretation for *Xenopus*' study; T.J.D.B.: collection and/or assembly of data; D.U.: collection and/or assembly of data; L.W.P. and H.N.: collection and/or assembly of data; V.S.: collection and/or assembly of data; J.P.: financial support; Y.-M.S.: conception and design, financial support, collection and/or assembly of data, data analysis and interpretation, manuscript writing, and final approval of manuscript; E.B., D.U., L.W.P., V.S. and J.P.: edited the manuscript.

Correspondence: Yuh-Man Sun, Ph.D., The James Black Centre, Institute of Psychiatry, King's College London, 125 Coldharbour Lane, London SE5 9NU, United Kingdom. Telephone: 44-0-20-7848-5311; Fax: 44-0-20-7848-0986; e-mail: yuh-man.sun@kcl.ac.uk Received June 10, 2010; accepted for publication September 4, 2010; first published online in STEM CELLS *EXPRESS* September 24, 2010. © AlphaMed Press 1066-5099/2009/$30.00/0 doi: 10.1002/stem.530

neural development in vivo, and an in vivo *Xenopus* neural induction system. Our findings reveal that Nnat is an intrinsic neural initiator that functions by triggering Ca^{2+} signaling that leads to ESC differentiation toward the neural lineage and also alters neural patterning in *Xenopus*.

Materials and Methods

Generation of Nnat ES Mutants

46C ESCs (a gift from Prof. A. Smith, Cambridge) were used to create Nnat-knockdown (Nnat-KD) and Nnat-overexpression (Nnat-OE) ESCs. To generate Nnat-KD ESCs, the ESCs were stably transfected with two designed Nnat short hairpin RNA (Nnat-shRNA) pENTR/H1/TO vectors, which were designed to knockdown both *Nnatα* and *β* isoforms. The sequences of the two oligos were 5′-gcatttactgggtaggattcg-3′ and 5′-gcacacatattcctgccttgc-3′. Three clones were selected for further analysis after 14-day Zeocin (50 μg/ml) selection. As three clones exhibited a similar knockdown level of *Nnat* and have shown a similar phenotype, we designated one clone as Nnat-KD ESCs. To generate Nnat-OE ESCs, the cells were stably transfected separately with the pNEBRX1-Hygro vector (BioLabs, Cheltenham, UK, http://www.neb.com/nebecomm/default.asp) containing a full-length cDNA of *Nnatα* or *Nnatβ*, and the cells were under Hygromycin selection (200 μg/ml). The ESC line stably transfected with Nnatα was designated as Nnatα-OE, whereas transfected with Nnat*β* as Nnat*β*-OE ESCs. The control ESCs were stably transfected with empty pENTR/H1/TO and pNEBRX1-Hygro vectors.

ESC Monolayer Differentiation

ESCs were differentiated toward the neural lineage using monolayer culture in N2B27 medium as previously described [31]. In general, ESC-derived neural differentiation spans 14 days, which consisted of four stages: ESC (day 0), NSCs (day 6), radial glia-like progenitors (day 10), and neurons (day 14). Cells were collected from those days for immunocytochemical and fluorescence-activated cell sorting (FACS) analysis. As Sox1-eGFP$^+$/Nes$^+$ NSCs usually appear 2 days after the addition of N2B27 to cells. In the thapsigargin (Tg)- and 2,5-di-*t*-butyl-1,4-benzohydroquinone (BHQ)-rescuing experiments, we administrated the drugs at the same time as N2B27 was first given to cells, whereas in FGF4 and FGF5-rescuing experiments, drugs were administrated 1 day after the cells were changed to N2B27 medium. To determine the effects of the BMP4, FGF, and Erk1/2 signaling pathways on Tg or FGFs rescue of neural induction, ESCs were treated with 25 nM Tg or FGF4 (5 ng/ml; 10 ng/ml for FGF5) in conjunction with either BMP4 (10 ng/ml), PD173074 (100 ng/ml), or 5 μM PD184352. Cells were then collected at 6-day differentiation for analyzing Sox1-eGFP$^+$/Nes$^+$ NSCs. To determine the effects of BMP4 antagonists on neural induction in Nnat-KD ESCs, the cells were treated with Nog (200 ng/ml), Chrd (300 ng/ml), and Fst (300 ng/ml) alone or in combination as N2B27 was applied to the cells. Cells then were collected at 4-day differentiation for analyzing Sox1-eGFP$^+$ NSCs.

Embryonic Body Formation

ESCs were plated out at 1×10^7 cells/10 cm plate in bacterial plates in ES medium without leukemia inhibitory factor (LIF). Embryonic bodies (EBs) were collected 6 days after differentiation for isolation of total RNA.

FACS Analysis

Fluorescently labeled cells were FACS sorted and counted using a BD FACSAria (BD Bioscience, Oxford, UK, http://www.bd.com/) according to manufacturers' instructions and procedure described in our previous study [33].

Intracellular Ca^{2+} Imaging and Recording

For intracellular Ca^{2+} level ($[Ca^{2+}]_i$), recording cells were cultured to confluence on 13-mm-laminin-coated glass coverslips. Coverslips were incubated in the dark for 40 minutes with either 1 μM calcium green-1/AM or 0.5 μM Fura PE-3/AM. Time course of $[Ca^{2+}]_i$ responses was recorded using microspectrofluorimeter (Cairn Research, Faversham, U.K.). Cell chamber was continuously perfused with HEPES-buffed physiological salt solution, and ratio of Fura PE-3 emission intensities at excitation wavelengths 340 and 380 nm ($R_{340/380}$) was taken as a measure of $[Ca^{2+}]_i$.

Quantitative Real-Time Polymerase Chain Reaction

Primer design and experimental procedures were described in our previous study [33]. All expression levels were normalized to cyclophillin levels. All data were performed in duplicate and some were repeated three times.

Statistical Analysis

Statistical significance was determined using a two-tailed Student's *t* test. *p* values of $<.05$ and $<.01$ were considered statistically significant. All results are presented as mean ± SD of the mean from experiments that have been repeated three times.

Immunocytochemistry

ESCs, NSCs, and neurons were fixed in 3% paraformaldehyde for 20 minutes at room temperature (RT). Antibodies included Oct4 (1:500, AB3209, Chemicon, Hampshire, UK, http://www.applegate.co.uk/all-industry/chemicon-europe-1216260.htm), Nes (1:500, MAB353, Chemicon), Pax6 (1:500, Hybridoma bank, Iowa, USA, http://dshb.biology.uiowa.edu/), RC2 (1:500, Hybridoma bank), NeuN (1:500, MAB377, Chemicon), MAP2 (1:400, ab10588-50, Abcam, Cambridge, UK, http://www.abcam.com/), sarco/endoplasmic reticulum Ca^{2+}-ATPase isoform 2 (SERCA2; 1:500, sc-8094, Santa Cruz, Heidelberg, Germany, http://www.scbt.com/), and Nnat (sc-30188, Santa Cruz and ab27266, Abcam). All primary antibody staining was carried out at 4°C overnight. Samples were then stained with appropriate fluorescence-conjugated secondary antibodies at RT for 1 hour and examined under an Axiovision fluorescent microscope aided with an APTOM device (Zeiss).

Xenopus Embryo, Animal Cap Assay, and Microinjection

The RNAs of Nnat isoforms were produced by using the mMessage mMachine SP6 kit (Ambion, Warrington, UK, http://www.ambion.com/). For phenotype analysis, embryos were injected in one cell at the 2-cell-stage with 1 ng of either Nnatα or Nnat*β* and left to late neurula or early tadpole stages. For cap assay, embryos were injected either in the ventral marginal zone or animal pole at the one- to two-stage with 1 ng RNA. All procedures were according to our previous study [34].

Western Blot Analysis

The experiments to investigate the effect of Tg-mediated Ca^{2+} signaling on the phosphorylation of Erk were carried out in Nnat-KD ESCs. For dose-response study, 1 μM, 100 nM, and 25 nM thapsigargin were added to Nnat-KD ESCs in ES medium for 5 minutes and cells were harvested. For time course study, thapsigargin were added to Nnat-KD ESCs in ES medium for different time periods (e.g., 5, 10, 20, and 60 minutes) and cells were harvested. For investigating the involvement of FGF pathway in Tg-mediated p-Erk signaling, the ESCs were pretreated with PD173074 for 2 hours to block FGF pathway, then treated with or without Tg and cells were washed and collected. All collected cells were subjected to Western blot analysis hybridized with p-Erk1/2 antibody (Cell Signaling, Hitchin, UK, http://www.cellsignal.com/). For establishing the effect of Tg on BMP4-mediated p-Smad1, ESCs were pretreated with BMP4 for 1 hour and then treated with Tg for 10, 30, and 60 minutes. Cells were washed and harvested for Western blot analysis hybridized with

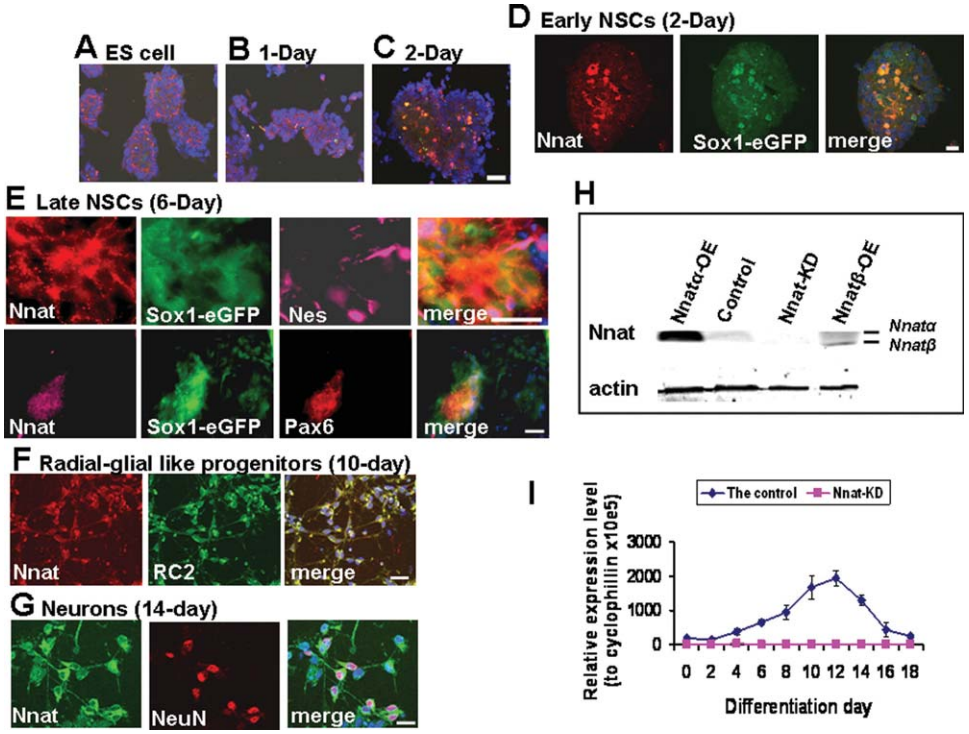

Figure 1. The expression of Nnat during ESC-derived neural differentiation and in the generated Nnat ES mutants. **(A–G):** Immunocytochemical analysis of Nnat expression. Nnat is expressed in a subpopulation of ESCs (before differentiation) **(A)** and 1 day after differentiated is initiated **(B)**. After 2-day differentiation, Nnat is abundantly expressed in Sox1-eGFP$^+$ early NSCs **(C)** and at higher magnification **(D)**. As differentiation proceeded, Nnat-positive cells are also costained with the late NSC markers, Nes, and Pax6 **(E)**, radial-glial-like progenitor marker, RC2 **(F)**, and neuronal marker NeuN **(G)**. **(H):** The levels of Nnatα and β in 12-day differentiated cells derived from control and Nnat ESC mutants were measured using Western blot analysis. Nnat ESC mutants are Nnatα-OE, Nnatβ-OE, and Nnat-KD ESCs. **(I):** Confirmation of Nnat-KD throughout 18 days of differentiation by qRT-PCR. Data shown are the mean $\pm$ SD ($n = 2$). Scale bar = 50 μm, 20 μm ([**D**]; [**E**], top panel; and [**G**]). All nuclei were stained with DAPI (blue). Abbreviations: DAPI: 4′,6′-diamidino-2-phenylindole; eGFP, enhanced green fluorescent protein; Nnat, neuronatin; Nnat-KD, Nnat-knockdown; Nnatα-OE, neuronatin αoverexpression; Nnatβ-OE, neuronatin βoverexpression; NSC, neural stem cell; qRT-PCR, quantitative real time-polymerase chain reaction.

p-Smad1 antibody (Cell Signaling). Nnat antibody for Western blot analysis was purchased from Abcam (ab27266).

Co-immunoprecipitation of SERCA and Nnat

Co-immunoprecipitation procedures were based on the Universal magnetic co-IP kit (Active Motif, Rixensart, Belgium, www.activemotif.com/). Nnat (sc-30188, Santa Cruz) and SERCA2 (1:500, sc-8094, Santa Cruz) antibodies were used in co-immunoprecipitation (co-IP) assay.

Chemicals

BMP4, FGF4, follistatin, chordin, and noggin were from R&D System, PD184352 from Axon Medchem (Groningen, Netherlands, http://www.axonmedchem.com/news.html), BHQ and 1,2-Bis (2-aminophenoxy) ethane-N,N,N′,N′-tetraacetic acid tetrakis (acetoxy methyl ester) (BAPTA-AM) from Calbiochem (Abington, UK, http://www.emdchemicals.com/life-science-research/calbiochem/c_PmSb.s1ON3EAAAEj0uBXhFCU), and Calcium Green-1/AM from Invitrogen. The rest of drugs were from Sigma.

Results

The Expression Pattern of Nnat During Neural Induction/Differentiation and in Nnat ESC Mutants

In this study, we used Sox1-eGFP knock-in 46C ESCs, in which enhanced green fluorescent protein (eGFP) expression is driven by the *Sox1* promoter and so is concomitantly activated with the expression of an early neuroectodermal marker Sox1. This allows for the appearance of Sox1-eGFP$^+$ cells to be used as readout for neural induction [35]. We have found that Nnat was initially expressed in a subpopulation of ESCs and its expression retained in 1-day differentiated cells (Fig. 1A, 1B). As differentiation proceeded, Nnat became abundantly expressed in Sox1-eGFP$^+$ neuroectodermal cells (early NSCs; Fig. 1C, 1D), Sox1-eGFP$^+$/Nes$^+$ or Sox1-eGFP$^+$/Pax6$^+$ late NSCs (Fig. 1E), RC2$^+$ radial-glial like progenitor cells (Fig. 1F), and then neurons (Fig. 1G). However, Nnat expression in progenitor cells and neurons is much weaker than in NSCs. Our data showed that Nnat expression is closely associated with the neural lineage, suggesting that Nnat is involved in aspects of neural development.

Nnat consists of two spliced isoforms, a full-length *Nnatα* and a short form *Nnatβ* [28]. To address the role of Nnat in neural development, we generated Nnat-overexpressing (Nnatα-OE and Nnatβ-OE) ESCs and Nnat-KD ESCs (knocking down both α and β isoforms). The Nnat ESC mutants were confirmed by the expression levels of Nnatα and β using Western blot analysis (Fig. 1H). Nnatα was detected in control, Nnatα-OE, and Nnatβ-OE ESCs but not in Nnat-KD ESCs. Nnatβ was only detected in Nnatβ-OE ESCs, suggesting that Nnatβ isoform is expressed at a lower level than that of Nnatα isoform. *Nnat* knockdown throughout 18 days of neural differentiation was confirmed by quantitative real-time polymerase chain reaction (PCR; Fig. 1I).

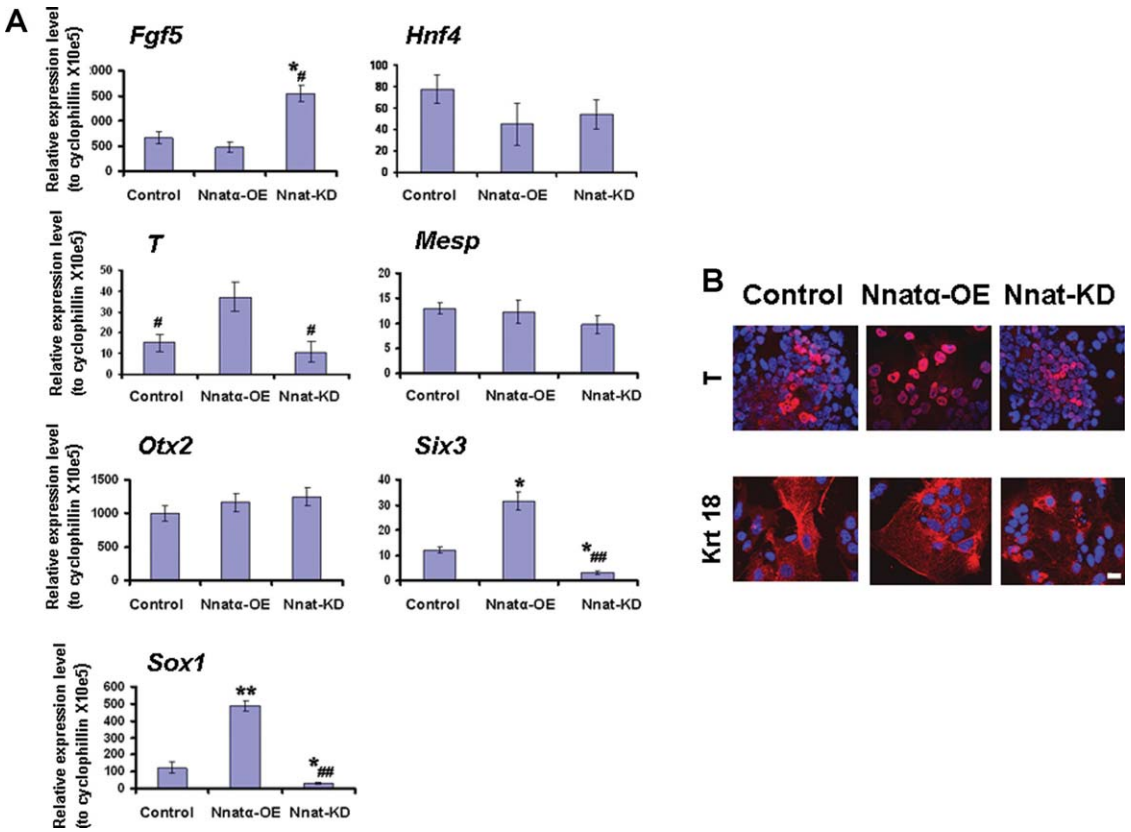

Figure 2. The competence of Nnat overexpressing and knockdown ESCs to give rise to the three primary germ cells. **(A):** Quantitative RT-PCR analysis for markers of the three primary germ cells using RNAs derived from control, Nnatα-OE, and Nnat-KD ESCs using an embryoid body (EB) formation assay. The total RNA from each ESC line was collected from 6-day differentiated EBs and the cDNAs were used to analyze the various cell markers: *Fgf5* (primitive ectodermal cells), *Hnf4* (endodermal cells), *T* and *Mesp* (mesodermal cells), *Otx2* (ectodermal cells), and *Six3* and *Sox1* (neuroectodermal cells). Data shown are the mean ± SD ($n = 3$). *, $p < .05$ and **, $p < .01$, significantly different from the control group; #, $p < .05$ and ##, $p < .01$, significantly different from the Nnatα-OE group, two-tailed Student's *t* test. **(B):** ICC analysis of the mesodermal and epidermal cells derived from control, Nnatα-OE, and Nnat-KD ESCs identified by staining with T and Krt18, respectively. Scale bar = 50 μm. All nuclei were stained with DAPI (blue). Abbreviations: DAPI: 4′,6′-diamidino-2-phenylindole; ICC, immunocytochemical; Nnatα-OE, neuronatin α-overexpression; Nnat-KD, neuronatin-knockdown; RT-PCR: real time-polymerase chain reaction.

The Phenotypic Effects of Nnat Dysregulation on ESC-Derived Neural Lineage

We first determined whether Nnat affects ESC differentiation into the three primary germ cells using an embryoid body formation assay. Using quantitative PCR analysis for markers of the three germ layers, we found that like control ESCs, Nnatα-OE, and Nnat-KD ESCs can be differentiated toward primitive ectoderm (*Fgf5*) and then to mesoderm (*T* and *Mesp*), endoderm (*Hnf4*), and ectoderm (*Otx2*) fates (Fig. 2A). Nnat-KD ESCs generated significantly higher *Fgf5*-expressing cells, whereas Nnatα-OE ESCs produced more *T*-expressing mesodermal cells. Using immunocytochemical (ICC) analysis, both Nnat ES mutants were shown to produce T^+ mesodermal cells and $Krt18^+$ epidermal cells (Fig. 2B), further suggesting that Nnat dysregulation did not prevent ESCs from differentiating into three primary germ cells. However, the ectodermal cells derived from Nnat-KD ESCs failed to differentiate into neuroectodermal cells (*Sox1* and *Six3*), whereas Nnatα-OE ESCs produced significantly more neuroectodermal cells compared with the control, suggesting that Nnat promotes neural lineage in ESCs.

To further corroborate these results, we delineated the phenotypic effects of Nnat dysregulation in neural specification using a monolayer culture. We found that Nnat-KD ESCs exhibited protracted Oct4 expression even after 14 days under neural differentiation conditions (Fig. 3D–3F), whereas the expression of Oct4 in the control cells was significantly reduced by 6-day neural differentiation (at NSC stage; Fig. 3A–3C). In contrast, Nnatα-OE ESCs exhibited less Oct4 staining, concomitant with the precocious expression of Sox1-eGFP (Fig. 3G–3I). As differentiation proceeded, Nnat-KD ESCs generated only a few small rounded $Sox1\text{-}eGFP^+$ cells (Fig. 3M), which never become Nes^+. These cells were distinct from those derived from control ESCs (Fig. 3K), which were flatter, larger in size, and Nes^+ (Supporting Information Fig. S1). Interestingly, the $Sox1\text{-}eGFP^+$ cells generated from Nnat-KD ESCs failed to differentiate into microtubule-associated protein 2 ($Map2^+$) neurons (Fig. 3T, 3U), whereas control ESCs generated numerous $Map2^+$ neurons (Fig. 3Q, 3R). Conversely, even in ESC medium, Nnatα-OE ESCs prematurely produced $Sox1\text{-}eGFP^+/Nes^+$ NSCs (Fig. 3N) and Map2 stained neuron-like cells (Fig. 3V). The aforementioned data were confirmed by FACS analysis, which showed that Nnatα-OE ESCs generated three times more $Sox1\text{-}eGFP^+/Nes^+$ NSCs (Fig. 3Y) and $NeuN^+$ neurons (Fig. 3Z) than control, whereas Nnat-KD ESCs displayed few, if any, NSCs and neurons. We also found Nnat*β*-OE ESCs exhibited a similar phenotype to that of Nnatα-OE ESCs (data not shown). We demonstrated that the phenotype of Nnat-KD ESCs is not due to an off-target effect. We showed that the restoration of Nnat expression in Nnat-KD ESCs (called Nnat-KD+Nnat ESCs; Supporting Information Fig. S2A) rescued the phenotypic defects in the

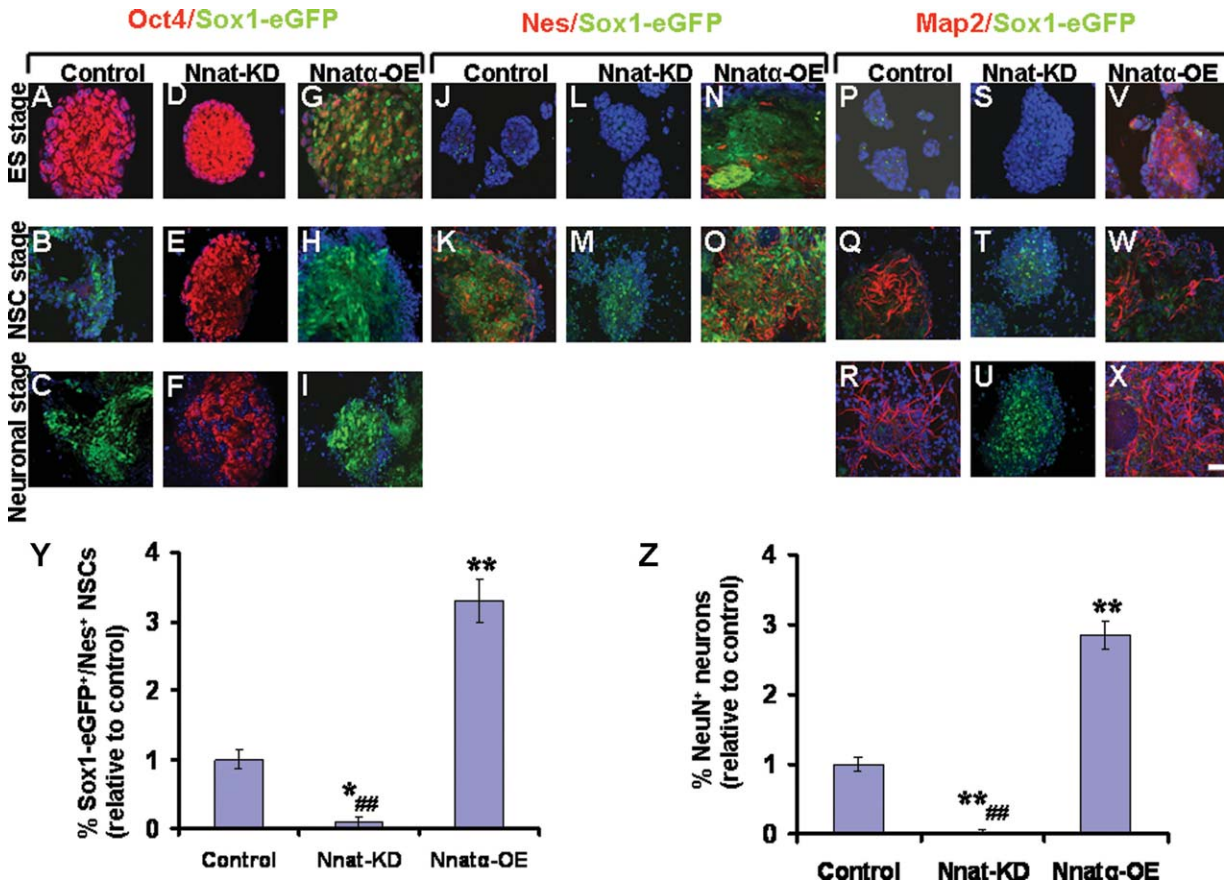

Figure 3. Nnat promotes the neural lineage. The role of Nnat in neural development was examined using an embryonic stem cell (ESC)-derived neural differentiation system over a 14-day time period. **(A–X):** Control, Nnat-KD, and Nnatα-OE ESCs were driven along neural differentiation using monolayer culture in N2B27 medium. Samples were collected for immunocytochemical analysis at ESC stage (before differentiation), NSC stage (6-day differentiation), and neuronal stage (14-day differentiation). The samples were stained with cell-specific markers, Oct4 (red), Nes (red), and Map2 (red), which represent ESCs, NSCs, and neurons, respectively. Scale bar = 50 μm. All nuclei were stained with DAPI (blue). **(Y):** Quantification of Sox1-eGFP$^+$/Nes$^+$ neural stem cells derived from control, Nnat-KD, and Nnatα-OE ESC using fluorescence-activated cell sorting (FACS) analysis. **(Z):** Quantification of NeuN$^+$ neurons derived from control, Nnat-KD, and Nnatα-OE ESC using FACS analysis. Data shown are the mean ± SD ($n = 3$). *, $p < .05$ and **, $p < .01$, significantly different from the control group; $^{\#}$, $p < .05$ and $^{\#\#}$, $p < .01$, significantly different from the Nnatα-OE group, two-tailed Student's t test. Abbreviations: DAPI: 4′,6′-diamidino-2-phenylindole; eGFP, enhanced green fluorescent protein; ES, embryonic stem; Nnat-KD, neuronatin-knockdown; Nnatα-OE, neuronatin α-overexpression; NSC, neural stem cell.

production of NSCs and neurons in Nnat-KD ESCs to the phenotypes observed in control ESCs (Supporting Information Fig. S2B–S2D). In summary, our results suggest that Nnat predisposes ESCs to differentiation and then initiates neural induction and promotes downstream neuronal differentiation.

Nnat Affects the Neural Patterning of *Xenopus laevis*

We employed a *Xenopus* neural induction model to examine whether Nnatα and Nnatβ exhibit the same effect in vivo. Our results showed that Nnatα (78% of 104 injections) and Nnatβ (95% of 88 injections) changed the patterning of *Xenopus* embryos, including cement gland formation (Fig. 4A–4F). In particular, Nnatβ injection resulted in distorted and truncated embryos (Fig. 4C, 4F). With regard to neural patterning, Nnatβ exhibited a more potent effect than Nnatα; as seen by the expanded Ncam staining (Fig. 4G–4I). To confirm these results, we also performed animal caps experiments. We found that *nrp1*, a pan-neural marker, and *otx*, a forebrain/midbrain expressed gene, were upregulated in the embryos injected with Nnatα or β (Fig. 4J). Our data suggest that Nnat promotes the neural fate in *Xenopus*. Nnat also increased mesoderm production judging by *nxk2.5* expression (a heart/mesoderm marker; Fig. 4J), which is consistent with our findings in mammalian system that Nnatα-OE ESCs generate significantly more *T*-expressing mesodermal cells (Fig. 2A). Our findings suggest that the role of Nnat in neural induction is conserved from mammals to *Xenopus*.

Nnat-Mediated Neural Induction Is Via Ca^{2+} Signaling

To elucidate the molecular mechanism of Nnat action, we showed that Nnat physically interacts with SERCA2 using co-IP assay (Fig. 5A) and in situ Proximity Ligation assay using Duolink system (data not shown). SERCA2 is the most dominant SERCA isoform expressed during neural differentiation, suggesting that Nnat exerts its effects by interacting with SERCA2. SERCA is a major component of cellular homeostasis and it maintains physiologically low cytosolic Ca^{2+} levels by pumping $[Ca^{2+}]_i$ into the ER. To examine whether Nnat acts positively or negatively on SERCA, we monitored $[Ca^{2+}]_i$ in control, Nnatα-OE, and Nnat-KD ESCs. We found that Nnatα-OE ESCs exhibited uniformly higher $[Ca^{2+}]_i$ than that of Nnat-KD ESCs (Fig. 5B), whereas the control ESCs showed both high and low levels, corresponding to the "salt and pepper" expression pattern of Nnat in ESCs described earlier (data not

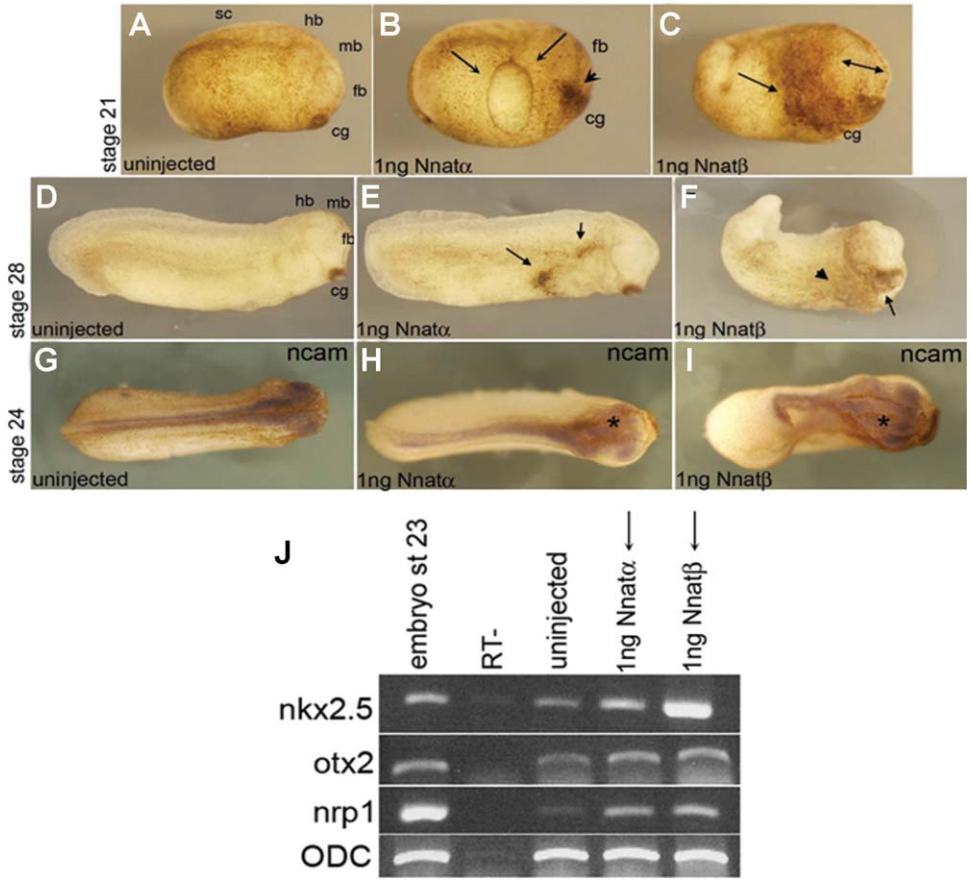

Figure 4. The effects of mouse Nnatα and *β* on neural patterning in *Xenopus laevis*. **(A–I):** The representative images of *Xenopus* embryos, which were injected in one cell at the two-cell stage with 1 ng of either Nnatα or Nnat*β* and the morphology was evaluated at late neurula or early tadpole stages. At neurula stage, **(A)** uninjected control embryo, **(B)** Nnatα injection results in an edema-like structure (see black arrows), and an enlarged cement gland (arrowhead), whereas **(C)** Nnat*β* injection not only causes an enlarged cement gland (see arrow) but also an expanded forebrain (double-headed arrow). At early tadpole stages, **(D)** uninjected control embryo, **(E)** Nnatα-injected embryos exhibit an abnormal phenotype with ectopic pigmentations (see arrows) and **(F)** Nnat*β*-injected embryos show a distorted and truncated phenotype with an enlarged cement gland (arrow) and a clear expansion of the neural plate. The abnormal neural phenotypes were confirmed by Ncam staining (a pan-neural marker): **(G)** control uninjected embryo, **(H)** Nnatα-injected embryo with noticeable neural plate expansion in the injected side (*), and **(I)** Nnat*β*-injected embryo with a profound neural plate expansion in the injected side (*). **(J):** In animal caps assay, injecting either Nnatα or *β* at one- to two-cell stage leads to increase in the expression of neural markers, nrp1 and otx, and a mesodermal marker nkx2.5, as assayed by RT-PCR. ODC was used as a loading control. Abbreviations: cg, cement gland; fb, forebrain; hb, hindbrain; mb, midbrain; sc, spinal cord; Ncam, neural cell adhesion molecule; Nnatα, neuronatin α; Nnat*β*, neuronatin *β*; ODC, ornithine decarboxylase; RT, no reverse transcriptase; RT-PCR, real time-polymerase chain reaction.

shown). Our results show that Nnat increases $[Ca^{2+}]_i$ by antagonizing SERCA. If this hypothesis is correct, we would expect that the specific SERCA blockers, thapsigargin (Tg) and BHQ, would mimic Nnat actions and be able to rescue the neural defective phenotype of Nnat-KD ESCs. Significantly, we found that Tg and BHQ increased $[Ca^{2+}]_i$ (Fig. 5F), which in turn rescued the ability of Nnat-KD ESCs to produce NSCs and neurons (Fig. 5C). These data were corroborated by quantitative FACS analysis (Fig. 5D, 5E). Tg rescued the NSC production of Nnat-KD ESCs to the level of control ESCs (Fig. 5D). However, neuronal production was significantly less robust than that of control ESCs (Fig. 5E). This incomplete rescue was possibly due to the fact that only a single dose of Tg was given before neural induction, thus only the immediate functions of endogenous Nnat would be restored. Nnat is also expressed in subsequent stages of neural development (Fig. 1), implying later roles in neurogenesis in addition to the early role in neural induction. We have observed that the increase in the duration or frequency of 25 nM Tg treatment results in cell death.

To further establish that the Tg-mediated rescue of Nnat-KD defects in neural induction was via Ca^{2+} signaling, we assessed whether the blockade of Ca^{2+} signaling, using membrane permeable Ca^{2+} chelator BAPTA-AM, would abolish the rescue by Tg in Nnat-KD ESCs. We found that BAPTA-AM not only prevented the rescue effect of Tg on neural induction (Fig. 5G) but also mitigated neural induction in control and Nnat-OE ESCs (Supporting Information Fig. S3), indicating that Ca^{2+} signaling is a prerequisite for neural specification. Taken together, our results suggest that Nnat acts in a cell autonomous fashion to initiate neural induction via Ca^{2+} signaling by antagonizing SERCA2 in the ER.

Tg-Mediated Ca^{2+} Signaling Increases the Phosphorylation of Erk1/2 and Cross Talks with FGF/Erk Pathway to Initiate Neural Induction

According to the recent emerging consensus on the regulation of neural induction, the FGF/Erk pathway is one of main regulatory routes in vertebrates [16, 17, 36–38]. We wished to determine the functional relationship between Ca^{2+} signaling and FGF/Erk pathway in Nnat-mediated neural induction. First, we examined whether the FGF/Erk pathway is involved

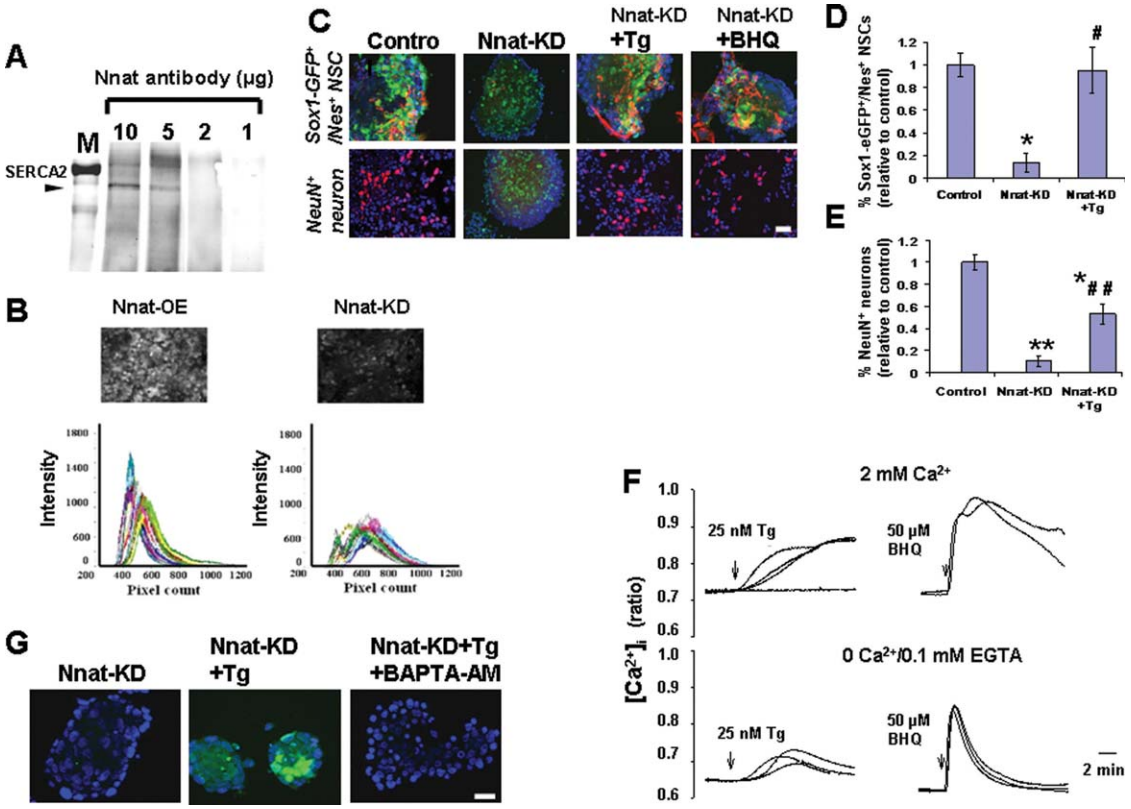

Figure 5. Nnat action is via Ca^{2+} signaling through negatively regulating SERCA2. **(A):** Dose-dependent pull down SERCA2 (100 kDa) by Nnat antibody using co-immunoprecipitation assay, suggesting that Nnat physically interacts with SERCA2. **(B):** Ca^{2+} imaging (top panel) and histograms (bottom panel) generated from Nnat-OE and Nnat-KD ESCs, in which the former exhibits higher $[Ca^{2+}]_i$ than that of the latter using Ca^{2+} green-1AM dye. **(C):** SERCA blockers, Tg and BHQ, rescue Nnat-KD phenotypes in the production of Sox1-GFP^+/Nes^+ (red) NSCs, and $NeuN^+$ (red) neurons. Scale bar = 50 μm. **(D):** Quantification of Sox1-$eGFP^+$/Nes^+ NSC derived from control, Nnat-KD ESCs, and Nnat-KD ESCs treated with Tg (Nnat-KD+Tg) using fluorescence-activated cell sorting (FACS) analysis. Data shown are the mean ± SD ($n = 3$). **(E):** Quantification of $NeuN^+$ neurons derived from control, Nnat-KD, and Nnat-KD+Tg ESCs using FACS analysis. Data shown are the mean ± SD ($n = 3$). *, $p < .05$ and **, $p < .01$, significantly different from the control group; $^{\#}$, $p < .05$ and $^{\#\#}$, $p < .01$, significantly different from the Nnat-KD group, two-tailed Student's t test. **(F):** Changes in intracellular $[Ca^{2+}]_i$ levels in Nnat-KD ESCs following Tg or BHQ treatment were measured using the $R_{340/380}$ emission intensities ratio of Fura PE-3. **(G):** Inhibition of Tg-rescued neural induction in Nnat-KD ESCs by chelating Tg-increased $[Ca^{2+}]_i$ using an intracellular calcium chelator BAPTA-AM. Scale bar = 50 μm and all nuclei were stained with DAPI (blue). Abbreviations: BAPTA-AM, 1,2-Bis (2-aminophenoxy) ethane-N,N,N′,N′-tetraacetic acid tetrakis (acetoxy methyl ester); BHQ, 2,5-di-*t*-butyl-1,4-benzohydroquinone; DAPI: 4′,6′-diamidino-2-phenylindole; GFP, green fluorescent protein; eGFP, enhanced green fluorescent protein; Nnat-KD, neuronatin-knockdown; Nnatα-OE, neuronatin α-overexpression; NSC, neural stem cell; SERCA2, sarco/endoplasmic reticulum Ca^{2+}-ATPase isoform 2; Tg, thapsigargin.

in Tg rescue of neural induction in Nnat-KD ESCs using a biochemical approach. We found that the Tg rescue was abrogated by both PD173074 and PD184352 (Fig. 6A), which are specific blockers for FGF-R and p-Erk1/2, respectively. These blockers also abolished neural induction in control ESCs, whereas PD173074 partially and PD184352 completely blocked neural induction in Nnatα-OE ESCs (Fig. 6A). This suggests that both the FGF and p-Erk pathways are involved in Nnat-directed neural induction but that the p-Erk signaling is the most crucial pathway. We then assessed whether exogenous FGFs could rescue the neural defective phenotypes in Nnat-KD ESCs. We found that treating Nnat-KD ESCs with either FGF4 or FGF5 restored the ability of these cells to produce NSC and neurons to the levels seen with Tg-treatment (Fig. 6B, 6C) and these effects were also eliminated by PD173074 and PD184352 treatment (Fig. 6D). Intriguingly, we also discovered that the Tg-mediated Ca^{2+} signaling cross talks with the FGF/Erk pathway at the p-Erk level. Treating Nnat-KD ESCs with 25 nM Tg, the dose at which Tg rescued the neural phenotypes of Nnat-KD ESCs (Fig. 5C), directly increased the phosphorylation of Erk1/2 within 10 minutes (Fig. 6E) without affecting the mRNA levels of FGF4, FGF5, Raf, Erk1, and Erk2. This Tg-mediated increase in p-Erk1/2 was not abolished by PD173074 treatment (Fig. 6E), indicating that the increase in p-Erk1/2 was independent of FGF signaling. Collectively, our results suggest that during neural induction the FGF/Erk pathway co-operate, either by acting downstream from or in parallel to, Nnat-mediated Ca^{2+} signaling. The Erk1/2 signaling may be a key player in neural induction by acting as a convergent point between FGF- and Nnat-mediated signaling.

Nnat-Mediated Ca^{2+} Signaling Suppresses the Expression of BMP4 and Its Direct Target Genes

We further investigated whether Nnat-mediated signaling also cross talks with the BMP pathway, which is considered to be the principal signaling pathway in the default model of neural induction [6]. We found that the Tg rescue of neural induction in Nnat-KD ESCs was inhibited by BMP4 (Fig. 7A). However, while BMP4 abolished neural induction in control ESCs, BMP4 only partially inhibited neural induction in Nnatα-OE ESCs (Fig. 7A), suggesting that Nnat can counteract or override the BMP4-directed inhibition of neural induction. We then sought

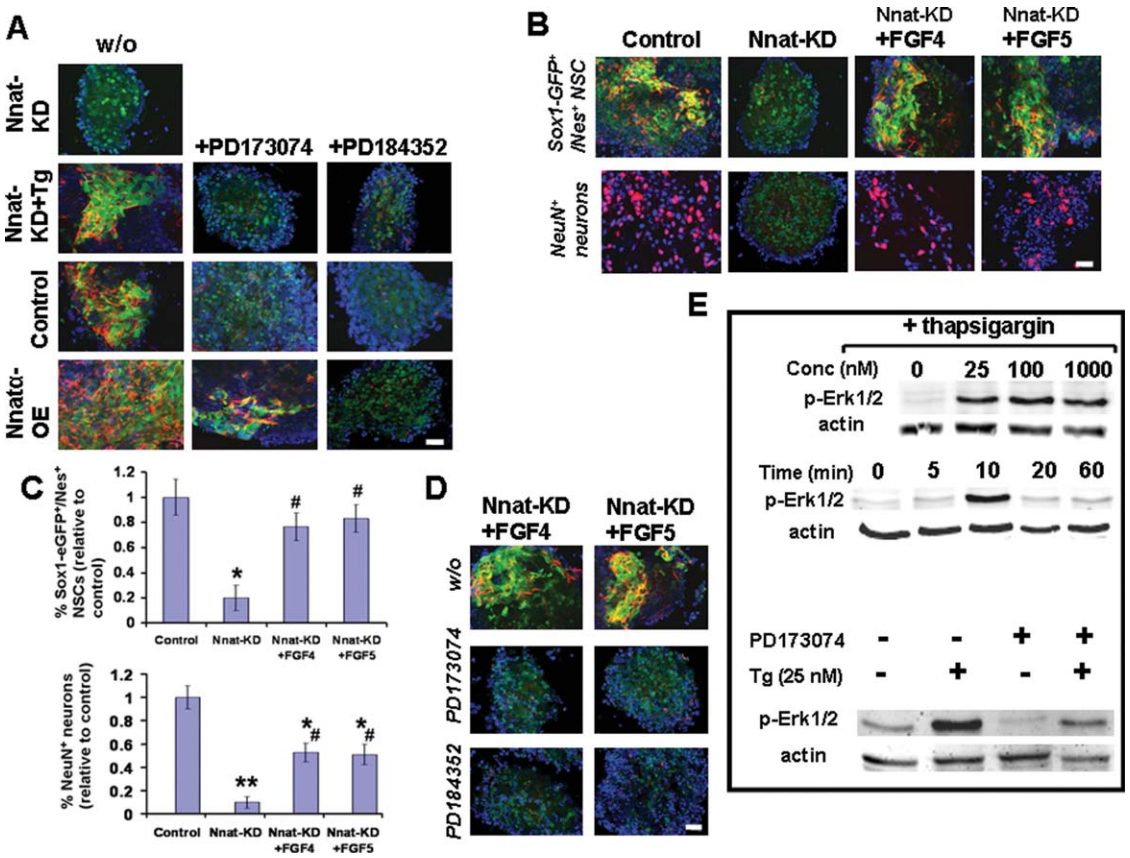

Figure 6. Nnat-mediated Ca^{2+} signaling increases p-Erk1/2 and cross talks with FGF/Erk pathway in neural induction. **(A):** The inhibitory effect of PD173074 (a FGF-R blocker) and PD184352 (a p-Erk1/2 blocker) on neural induction. Without the presence of blockers, Nnat-KD ESCs failed to initiate neural induction (fail to generate Sox1-eGFP$^+$/Nes$^+$ [red] NSCs), which was rescued by Tg treatment (Nnat-KD+Tg). In the presence of the blockers (+PD173074 or +PD184352), neural induction in control and Nnat-KD+Tg ESCs was abolished, whereas PD173074 partially and PD184352 completely inhibited neural induction in Nnatα-OE ESCs. **(B):** The rescue effects of FGF4 or FGF5 on Nnat-KD phenotype in the production of Sox1-eGFP$^+$/Nes$^+$ (red) NSCs and NeuN$^+$ (red) neurons. **(C):** Quantification of NSC and neuron population generated from control, Nnat-KD, and Nnat-KD ESCs treated with FGF4 (Nnat-KD+FGF4) or FGF5 (Nnat-KD+FGF5) using fluorescence-activated cell sorting analysis. Data shown are the mean ± SD ($n = 3$). *, $p < .05$ and **, $p < .01$, significantly different from the control group; #, $p < .05$, significantly different from the Nnat-KD group, two-tailed Student's t test. **(D):** The FGF4 and FGF5 rescue of neural induction in Nnat-KD ESCs were abrogated by the presence of PD173074 or PD184352. **(E):** Increase in the phosphorylation of Erk1/2 after 5 minutes treated with various concentrations of Tg (top panel), the time points of the increment with 25 nM Tg treatment (middle panel), and the effect of PD173074 on Tg-induced p-Erk1/2 (bottom panel). Scale bar = 50 μm and all nuclei were stained with DAPI (blue). Abbreviations: DAPI, 4′,6′-diamidino-2-phenylindole; eGFP, enhanced green fluorescent protein; FGF4, fibroblast growth factor 4; FGF5, Fibroblast growth factor 5; GFP, green fluorescent protein; Nnatα-OE, neuronatin α-overexpression; Nnat-KD, neuronatin-knockdown; NSC, neural stem cell; Tg, thapsigargin; w/o, without.

to determine where the cross talk occurs between Nnat-mediated Ca^{2+} signaling and the BMP4 pathway. We found that Nnat-mediated Ca^{2+} signaling significantly suppressed the expression of BMP4 and its direct target genes, *Msx1* and *Msx2* (Fig. 7B). However, we did not find that Tg-mediated Ca^{2+} signaling affected BMP4-mediated phosphorylation of Smad1 at the C-terminus (Fig. 7C). Whether the Tg-mediated Ca^{2+} signaling regulates the phosphorylation of the linker region of Smad1, which has been shown to antagonize the BMP4/Smad1 signaling, remains to be determined. Our results suggest that Nnat-mediated Ca^{2+} signaling inhibits the BMP4 pathway in neural induction at least by suppressing *BMP4* expression. As the BMP pathway is the decisive influence in neural induction in the default model, we wished to test whether, in the absence of the Nnat-directed intrinsic cue, inhibition of BMP is sufficient to induce neural induction in Nnat-KD ESCs. Our findings showed that Nog, Chrd, and Fst, which are antagonists of BMP pathway, either alone or in combination, could not induce neural induction in Nnat-KD ESCs (Fig. 7D), whereas the combination of antagonists prevented the inhibitory effect of BMP4 on neural induction in control ESCs (data not shown). This indicates that the Nnat-led intrinsic cue is crucial in neural induction; without this intrinsic cue, ESCs fail to initiate neural induction despite the inhibition of BMP pathway.

Discussion

We show that Nnat is initially expressed in a subpopulation of ESCs and then in the neural lineage as differentiation proceeds, which correlates with the expression profile of Nnat in vivo [29–30, 39]. We further demonstrate that in loss-of-function studies, Nnat-KD ESCs fail to produce neuroectodermal cells and neurons using both monolayer culture and embryoid body formation approaches, despite the fact that they are differentiated into primary germ cells in embryoid body assay. Conversely, in gain-of-function studies, Nnat-OE ESCs precociously produce neuroectodermal cells and neuron-like cells even in pluripotent medium (containing LIF and serum) and

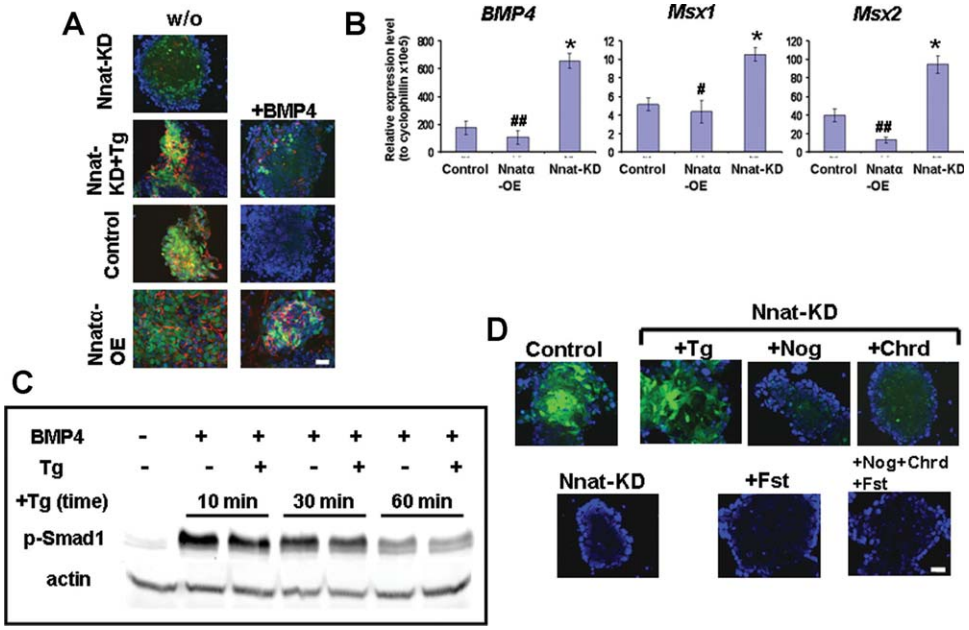

Figure 7. Nnat-mediated Ca^{2+} signaling interacts with BMP4 pathway in neural induction by suppressing the transcription of BMP4 and its target genes. **(A):** The inhibitory effect of BMP4 on neural induction. Without the presence of BMP4, Nnat-KD ESCs failed to generate Sox1-eGFP$^+$/Nes$^+$ (red) neural stem cells, which was rescued by Tg treatment (Nnat-KD+Tg). In the presence of BMP4 (+BMP4), neural induction in control and Nnat-KD+Tg ESCs was abolished, whereas BMP4 only partially inhibited neural induction in Nnatα-OE ESCs. **(B):** Gene expression profiles of *BMP4* and its target genes, *Msx1* and *Msx2* in ESCs show that the expression of those genes is suppressed in Nnat-mediated Ca^{2+} signaling. Data shown are the mean ± SD ($n = 3$). *, $p < .05$, significantly different from the control group; $^{\#}$, $p < .05$ and $^{\#\#}$, $p < .01$, significantly different from the Nnat-KD group. **(C):** The effect of Tg on BMP4-mediated C-terminal phosphorylation of Smad1 at indicated duration of Tg treatment. **(D):** Inhibition of BMP pathway by antagonists, Nog, Chrd and Fst, does not induce neural induction in Nnat-KD ESCs. Control and Nnat-KD ESCs were driven along neural differentiation. At 4-day differentiation, control ESCs generate many Sox1-eGFP$^+$ neuroectodermal cells, whereas Nnat-KD ESCs fail to produce neuroectodermal cells. The failure of neural induction in Nnat-KD ESCs is rescued by Tg treatment, but not by BMP antagonists. Scale bar = 50 μm and all nuclei were stained with DAPI (blue). Abbreviations: DAPI, 4′,6′-diamidino-2-phenylindole; BMP4, bone morphogenetic protein 4; Nnatα-OE, neuronatin α-overexpression; Nnat-KD, neuronatin-knockdown; Tg, thapsigargin; w/o, without.

generate three times more neuroectodermal cells and neurons than those derived from control ESCs in differentiation medium. Our findings suggest that Nnat possesses the ability to push ESCs out of the "ground state" and initiate differentiation and then drive the ESCs toward a neural fate. This is supported by our observations that Nnat-OE ESCs express low levels of the pluripotent marker Oct4 and are predisposed to differentiation. In contrast, Nnat-KD ESCs protract the expression of Oct4 even in differentiation media. Moreover, our unpublished data show that Nnat-KD ESCs are refractory to BMP4-induced non-neural differentiation but respond to BMP4-driven differentiation after treatment with Tg, which mimics the action of Nnat. Intriguingly, we find that Tg-mediated Ca^{2+}signaling in Nnat-KD ESCs results in an increase in the phosphorylation of Erk1/2. As the Erk1/2 MAP kinase pathway has been shown to promote ESCs differentiation [14, 15, 40, 41], we propose that Ca^{2+}-mediated Erk1/2 signaling can, at least in part, contribute to the differentiation-prone phenotype observed in Nnat-OE ESCs. Our findings suggest that Nnat not only triggers ESC differentiation but also sequentially promotes neural fate.

We establish that the Nnat-initiated neural induction results from Nnat-mediated increase in $[Ca^{2+}]_i$ from internal stores by potentially antagonizing SERCA2 in the ER. Furthermore, we also show that both mouse Nnat isoforms exhibit a similar role in in vivo neural patterning in *Xenopus*. Our results are concomitant with previous findings in frogs, which showed that Ca^{2+} is a potent neural initiator in animal caps and embryos [18, 19, 42–45]. In *Xenopus*, an increase in $[Ca^{2+}]_i$ due to an efflux of Ca^{2+} from internal stores triggers neural fate in the dissociation of animal caps [45]. The importance of internal store-mediated Ca^{2+} signaling in early brain development is also shown by Tg-induced Holoprosencephaly in Zebrafish [46]. Our study is the first to show that Ca^{2+} signaling plays a crucial role in neural induction in mammals and also the first to demonstrate that Nnat promotes neural lineage in mammals and *Xenopus*. Interestingly, Nnat also promotes mesodermal cells in the mouse and *Xenopus* models. It has been shown that the Spemann's organizer induces neural tissue from dorsal ectoderm and dorsalizes lateral and ventral mesoderm in *Xenopus*, suggesting that mesoderm plays a role in neural induction [7]. However, we do not think that the Nnat-mediated neural induction in *Xenopus* is through mesodermal interactions. This is supported by our observations that Nnat initiates neural induction in control and Nnat-OE ESCs without the presence of mesodermal cells as judged by the absence of T^+ cells. Moreover, Nnat-KD ESCs do produce mesodermal cells but fail to generate neuroectodermal cells in an embryoid body formation assay.

We further show that Ca^{2+}-mediated Erk1/2 signaling may be responsible for Nnat-initiated neural induction in ESCs. We explore the mechanism of Nnat action in neural induction by employing Tg to mimic the action of Nnat. Our findings reveal that Tg-mediated Ca^{2+} signaling directly increases the phosphorylation of Erk1/2. The p-Erk1/2 signaling pathway has been shown to be the critical pathway in FGF-, RA-, and Syndecan 4-regulated neural induction [13–17, 47]. Our findings suggest that Nnat-initiated neural induction may occur in part via p-Erk1/2 signaling. This is substantiated by our findings that the blockage of p-Erk1/2 by mitogen-activated protein kinase/extracellular signal-regulated kinase inhibitor PD184352 eliminates the Tg- and Nnat-

initiated neural induction in Nnat-KD and Nnatα-OE ESCs, respectively. Although PD184352-treated ESCs have been reported to be retained in the "pluripotent state" [14], we have observed that around 30% of PD184352-treated cells have differentiated phenotypes (big, flat, and low Oct4 expression) but are not Sox^+ neuroectodermal cells, suggesting that blocking p-Erk1/2 signaling by PD184352 inhibits neural induction. Taken together, Nnat-mediated Ca^{2+} signaling may increase p-Erk1/2, which in turn leads to neural specification in ESCs. However, we cannot rule out that Nnat-mediated Ca^{2+} signaling may also trigger other pathways to regulate neural induction.

To date, a body of evidence suggests that in addition to BMP inhibition, other signals are required for neural induction, especially the FGF pathway. FGF signaling has been shown to play a pivotal role in the acquisition of neural fate in *Xenopus*, chick, Ciona, and mammals [11, 12, 14, 15, 48–50]. Further studies showed that the FGF/Erk pathway is the principal signaling in regulating the neural fate in mouse ESCs [15–17] and *Xenopus* [13]. We show that Nnat-mediated Ca^{2+} signaling interacts with FGF/Erk signaling to regulate neural induction. Our findings reveal that Tg-mediated neural induction in Nnat-KD ESCs and neural induction in control ESCs are abrogated by the FGF-R inhibitor PD173074, whereas this inhibitor only partially blocks Nnat-initiated neural induction in Nnatα-OE ESCs. Moreover, FGF4 or FGF5 treatment rescues the failure of neural induction in Nnat-KD ESCs, despite the cells expressing normal levels of FGF4 and significantly higher levels of FGF5. We also show that Tg-mediated Ca^{2+} signaling directly increases p-Erk1/2 independently of the FGF pathway. Collectively, our findings suggest that the FGF/Erk signaling pathway is involved in neural induction by acting in co-operation with Ca^{2+}-mediated p-Erk signaling and the overall levels of p-Erk1/2 produced by these pathways are critical for neural induction. This explains why normal ESCs, which possess intact FGF/Erk and putative Nnat-mediated Erk signaling, are able to initiate neural induction. Whereas, Nnat-KD ESCs containing presumably just FGF/Erk signaling, but without Nnat-mediated Erk signaling, need exogenous FGFs to boost the p-Erk levels to that required for neural induction to occur. This intertwined relationship between Ca^{2+} and FGF signaling in neural induction is also demonstrated in *Xenopus*, in which FGF4 directs Ca^{2+} signaling to control early neural genes by activating the dihydropyridine-sensitive Ca^{2+} channels [50].

Neural induction is controlled by extrinsic influences containing positive and negative cues. We show that BMP4 abolishes Tg-initiated neural induction in Nnat-KD ESCs and neural induction in control ESCs. However, BMP4 only partially inhibits neural induction in Nnatα-OE ESCs, suggesting that Nnat promotes neural lineage in ESCs not only by providing a positive influence on neural induction (discussed earlier) but also counteracting BMP4 inhibition. We show that Nnat-mediated Ca^{2+} signaling antagonizes the BMP4 inhibition of neural induction by repressing BMP4 transcription. Intriguingly, we were unable to restore neural induction in Nnat-KD ESCs, despite antagonizing the BMP pathway by the combined treatment with Nog, Chrd, and Fst. This is not due to the treated cells remaining in a pluripotent state, because we observed that the treated cells show an enlarged and flattened phenotype and express low Oct4, which are indications of cell differentiation. Our findings suggest that there are other inhibitory influences in addition to BMP signaling in neural induction.

Conclusion

As the seminal experiment carried out by Spemann and Mangold in 1924 [51], a generally held view in the regulation of neural induction is that it is primarily governed by extrinsic influences (cues) via either autocrine or paracrine fashions acting on ectodermal cells. What roles, if any, do intrinsic cues have in the neural specification of ectodermal cells? In this study, we demonstrate that a novel intrinsic factor, Nnat, plays a decisive role in neural induction in ESCs and neural patterning in *Xenopus*. We propose that Nnat promotes neural lineage in ESCs by increasing $[Ca^{2+}]_i$ via antagonizing SERCA2, which in turn increase p-Erk1/2 and suppresses *BMP4* transcription, leading to neural induction in co-operation with the FGFs/Erk pathway. In conclusion, our findings provide a new dimension in understanding the mechanisms underlying neural induction through the aspect of an intrinsic control. We propose that neural induction is controlled by both extrinsic and intrinsic factors. Extrinsic factors consist of negative (e.g., BMP4 and others) and positive (e.g., FGFs and others) influences. Nnat is a novel intrinsic factor that initiates neural induction by promoting positive cues and inhibiting negative cues.

Acknowledgments

We thank Prof. A. Lumsden for his comments on this article. This work was supported by grants from a KCL start-up fund and a Taiwanese government (the Ministry of National Defense) fund to Y-M.S., a MRC Career Development Fellowship (G120/782) to E.B., and the Charles Wolfson Charitable Trust to J.P.

Disclosure of Potential Conflicts of Interest

The authors indicate no potential conflicts of interest.

References

1 Coucouvanis E, Martin GR. Signals for death and survival: A two-step mechanism for cavitation in the vertebrate embryo. Cell 1995;83:279–287.
2 Gardner RL, Rossant J. Investigation of the fate of 4–5 day post-coitum mouse inner cell mass cells by blastocyst injection. J Embryol Exp Morphol 1979;52:141–152.
3 Temple S. The development of neural stem cells. Nature 2001;414:112–117.
4 Hermmati-Brivanlou A, Melton DA. Inhibition of activin receptor signaling promotes neuralization in *Xenopus*. Cell 1994;77:273–281.
5 Stern CD. Neural induction: 10 years on since the 'default model'. Curr Opin Cell Biol 2006;18:692–697.
6 Muñoz-Sanju I, Brivanlou AH. Neural induction, the default model and embryonic stem cells. Nat Rev Neurosci 2002;3:271–280.
7 Lamb TM, Knecht AK, Smith WC et al. Neural induction by the secreted polypeptide noggin. Science 1993;262:713–718.
8 Sasai Y, Lu B, Steinbeisser H et al. *Xenopus* chordin: A novel dorsalizing factor activated by organizer-specific homeobox genes. Cell 1994;79:779–790.
9 Liem KF, Jr, Tremml G, Roelink H et al. Dorsal differentiation of neural plate cells induced by BMP-mediated signals from epidermal ectoderm. Cell 1995;82:969–979.
10 Di-Gregorio A, Sancho M, Stuckey DW et al. BMP signaling inhibits premature neural differentiation in the mouse embryo. Development 2007;134:3359–3369.

11 Streit A, Berliner AJ, Papanayotou C et al. Initiation of neural induction by FGF signaling before gastrulation. Nature 2000;406: 74–78.
12 Wilson SI, Graziano E, Harland R et al. An early requirement for FGF signaling in the acquisition of neural cell fate in the chick embryo. Curr Biol 2000;10:421–429.
13 Kuroda H, Fuentealba L, Ikeda A et al. Default neural induction: Neuralization of dissociated *Xenopus* cells is mediated by Ras/MAPK activation. Genes Dev 2005;19:1022–1027.
14 Kunath T, Saba-El-Leil MK, Almousailleakh M et al. FGF stimulation of the Erk1/2 signaling cascade triggers transition of pluripotent embryonic stem cells from self-renewal to lineage commitment. Development 2007;134:2895–2902.
15 Stavridis MP, Lunn JS, Collins BJ et al. Discrete period of FGF-induced Erk1/2 signaling is required for vertebrate neural specification. Development 2007;134:2889–2894.
16 Chen CW, Liu CS, Chiu IM et al. The signals of FGFs on the neurogenesis of embryonic stem cells. J Biomed Sci 2010;29:17–33.
17 Cohen MA, Itsykson P, Reubinoff BE. The role of FGF-signaling in early neural specification of human embryonic stem cells. Dev Biol 2010;340:450–458.
18 Moreau M, Leclerc C, Gualandris-Parisot L et al. Increased internal Ca2+ mediates neural induction in the amphibian embryo. Proc Natl Acad Sci USA 1994;91:12639–12643.
19 Moreau M, Néant I, Webb SE et al. Calcium signaling during neural induction in *Xenopus laevis* embryos. Philos Trans R Soc Lond B Biol Sci 2008;363:1371–1375.
20 Wilson SI, Rydström A, Trimborn T et al. The status of Wnt signaling regulates neural and epidermal fates in the chick embryo. Nature 2001;411:325–330.
21 Aubert J, Dunstan H, Chambers I et al. Functional gene screening in embryonic stem cells implicates Wnt antagonism in neural differentiation. Nat Biotechnol 2002;20:1240–1245.
22 Heeg-Truesdell E, LaBonne C. Neural induction in *Xenopus* requires inhibition of Wnt-beta-catenin signaling. Dev Biol 2006; 298:71–86.
23 Tonge PD, Andrews PW. Retinoic acid directs neuronal differentiation of human pluripotent stem cell lines in a non-cell-autonomous manner. Differentiation 2010;80:20–30.
24 Maye P, Becker S, Siemen H et al. Hedgehog signaling is required for the differentiation of ES cells into neurectoderm. Dev Biol 2004;265: 276–290.
25 de Almeida I, Rolo A, Batut J et al. Unexpected activities of Smad7 in *Xenopus* mesodermal and neural induction. Mech Dev 2008;125: 421–431.
26 Kagitani F, Kuroiwa Y, Wakana S et al. Peg5/Neuronatin is an imprinted gene located on sub-distal chromosome 2 in the mouse. Nucleic Acids Res 1997;25:3428–3432.
27 Joseph R, Dou D, Tsang W. Molecular cloning of a novel mRNA (neuronatin) that is highly expressed in neonatal mammalian brain. Biochem Biophys Res Commun 1994;201:1227–1234.
28 Joseph R, Dou D, Tsang W. Neuronatin mRNA: Alternatively spliced forms of a novel brain-specific mammalian developmental gene. Brain Res 1995;690:92–98.
29 Wijnholds J, Chowdhury K, Wehr R. Segment-specific expression of the neuronatin gene during early hindbrain development. Dev Biol 1995;171:73–84.
30 Dou D, Joseph R. Cloning of human neuronatin gene and its localization to chromosome-20q 11.2–12: The deduced protein is a novel "proteolipid'. Brain Res 1996;723:8–22.
31 Sun Y-M, Cooper M, Finch S et al. Rest-mediated regulation of extracellular matrix is crucial for neural development. Plos One 2008; 3:e3656.
32 Bibel M, Richter J, Schrenk K et al. Differentiation of mouse embryonic stem cells into a defined neuronal lineage. Nat Neurosci 2004;7: 1003–1009.
33 Sun Y-M, Greenway DJ, Johnson R et al. Distinct profiles of REST interactions with its target genes at different stages of neuronal development. Mol Biol Cell 2005;16:5630–5638.
34 Bell E, Muñoz-Sanjuán I, Altmann CR et al. Cell fate specification and competence by Coco, a maternal BMP, TGFbeta and Wnt inhibitor. Development 2003;130:1381–1389.
35 Aubert J, Stavridis MP, Tweedie S et al. Screening for mammalian neural genes via fluorescence-activated cell sorter purification of neural precursors from Sox1-gfp knock-in mice. Proc Natl Acad Sci USA 2003;1:11836–11841.
36 Delaune E, Lemaire P, Kodjabachian L. Neural induction in *Xenopus* requires early FGF signaling in addition to BMP inhibition. Development 2005;132:299–310.
37 LaVaute TM, Yoo YD, Pankratz MT et al. Regulation of neural specification from human embryonic stem cells by BMP and FGF. Stem Cells 2009;27:1741–1749.
38 Marchal L, Luxardi G, Thomé V. BMP inbihition initiates neural induction via FGF signaling and Zic genes. Proc Natl Acad Sci USA 2009;106:17437–17442.
39 Ruddock NT, Wilson KJ, Cooney MA et al. Analysis of imprinted messenger RNA expression during bovine preimplantation development. Biol Reprod 2004;70:1131–1135.
40 Ying QL, Wray J, Nichols J et al. The ground state of embryonic stem cell self-renewal. Nature 2008;453:519–523.
41 Nichols J, Silva J, Roode M et al. Suppression of Erk signaling promotes ground state pluripotency in the mouse embryo. Development 2009;136:3215–3222.
42 Barth LG, Barth LJ. Sequential induction of the presumptive epidermis of the *Rana pipiens* gastrula. Biol Bull 1964;127:413–427.
43 Grunz H, Tacke L. Neural differentiation of *Xenopus laevis* ectoderm takes place after disaggregation and delayed reaggregation without inducer. Cell Differ Dev 1989;28:211–217.
44 Saint-Jeannet JP, Huang S, Duprat AM. Modulation of neural commitment by changes in target cell contacts in *Pleurodeles waltl*. Dev Biol 1990;141:93–103.
45 Leclerc C, Rizzo C, Daguzan C et al. Neural determination in *Xenopus laevis* embryos: Control of early neural gene expression by calcium. J Soc Biol 2001;195:327–337.
46 Creton R. The calcium pump of the endoplasmic reticulum plays a role in midline signaling during early zebrafish development. Dev Brain Res 2004;151:33–41.
47 Kuriyama S, Mayor R. A role for Syndecan-4 in neural induction involving ERK- and PKC-dependent pathways. Development 2009;136:575–584.
48 Hongo I, Kengaku M, Okamoto H. FGF signaling and the anterior neural induction in *Xenopus*. Dev Biol 1999;216:561–581.
49 Bertrand V, Hudson C, Caillol D et al. Neural tissue in ascidian embryos is induced by FGF9/16/20, acting via a combination of maternal GATA and Ets transcription factors. Cell 2003;115:615–627.
50 Lee KW, Moreau M, Néant I et al. FGF-activated calcium channels control neural gene expression in *Xenopus*. Biochim Biophys Acta 2009;1793:1033–1040.
51 Spemann H, Mangold H. Über Induktion von Embryonanlagen durch Implantation artfremder Organisatoren. Wilhelm Roux Arch Entw Mech Organ 1924;100:599–638.

See www.StemCells.com for supporting information available online.

Appendix 4

PTP1B is an effector of Activin signaling and regulates neural specification of embryonic stem cells

K. Matulka, H-H Lin, H. Hříbková, D. Uwanogho, P. Dvořák and Yuh-Man Sun

Cell Stem Cell (2013) December 5; 13:1–14.

Please cite this article in press as: Matulka et al., PTP1B Is an Effector of Activin Signaling and Regulates Neural Specification of Embryonic Stem Cells, Cell Stem Cell (2013), http://dx.doi.org/10.1016/j.stem.2013.09.016

Cell Stem Cell
Research

PTP1B Is an Effector of Activin Signaling and Regulates Neural Specification of Embryonic Stem Cells

Kamil Matulka,[1,4] Hsuan-Hwai Lin,[2,4] Hana Hříbková,[1] Dafe Uwanogho,[3] Petr Dvořák,[1] and Yuh-Man Sun[1,*]
[1]Department of Biology, Faculty of Medicine, Masaryk University, Brno 62500, Czech Republic
[2]Department of Internal Medicine, Tri-Service General Hospital, National Defense Medical Center, Taipei, Taiwan, Republic of China
[3]Institute of Psychiatry, King's College London, Centre for the Cellular Basis of Behaviour, London SE5 9NU, UK
[4]These authors contributed equally to this work
*Correspondence: wadeley@med.muni.cz
http://dx.doi.org/10.1016/j.stem.2013.09.016

SUMMARY

During embryogenesis, the Activin/Nodal pathway promotes the mesendodermal lineage and inhibits neural fate. The molecular mechanisms underlying this role of the Activin/Nodal pathway are not clear. In this study, we report a role for protein tyrosine phosphatase 1B (PTP1B) in Activin-mediated early fate decisions during ESC differentiation and show that PTP1B acts as an effector of the Activin pathway to specify mesendodermal or neural fate. We found that the Activin/ALK4 pathway directly recruits PTP1B and stimulates its release from the endoplasmic reticulum through ALK4-mediated cleavage. Subsequently, PTP1B suppresses p-ERK1/2 signaling to inhibit neural specification and promote mesendodermal commitment. These findings suggest that a noncanonical Activin signaling pathway functions in lineage specification of mouse and human embryonic stem cells.

INTRODUCTION

Activin/Nodal, members of the transforming growth factor-β (TGF-β) superfamily, exhibit various roles during different stages of embryogenesis. The Activin/Nodal pathway maintains the undifferentiated status of the epiblast in mice (Mesnard et al., 2006), which coincides with the in vitro role of Activin in sustaining the pluripotency of mouse and human embryonic stem cells (ESCs) (Ogawa et al., 2007; Vallier et al., 2005). As development proceeds, the Activin/Nodal pathway plays a crucial role in lineage decisions. In vivo studies showed that different concentrations of Activin elicit distinct responses from *Xenopus* animal caps, ultimately producing a range of mesodermal fates (Green and Smith, 1990). *Nodal*$^{-/-}$ mice fail to form both the mesoderm and the definitive endoderm but show precocious neural differentiation (Camus et al., 2006), suggesting that the Activin/Nodal pathway promotes the mesendodermal lineage and inhibits neural fate. Furthermore, inhibition of Activin signaling has been shown to promote neural fate in human ESCs and induced pluripotent stem cells (iPSCs) (Smith et al., 2008; Chambers et al., 2009). The action in which the Activin/Nodal pathway promotes mesendodermal fate over neural fate has begun to be investigated. Chng et al. (2010) recently suggested that Activin/Nodal signaling acts through Smad-interacting protein 1 (SIP1) to regulate the cell-fate decision between neuroectoderm and mesendoderm fates. However, the precise molecular mechanisms underlying the specification of mesendodermal fate and the inhibition of neural fate by the Activin/Nodal pathway remain to be elucidated.

Activin exerts its effect by initially binding to the type II Activin receptor (ACVRIIB), then recruiting and phosphorylating the type I receptor (ALK4), which in turn phosphorylates and activates SMAD2. SMAD2 then forms a complex with SMAD4 and translocates to the nucleus to regulate gene transcription (Werner and Alzheimer, 2006). In a screening, we have identified PTP1B as an effector in the Activin/Alk(ALK)4 pathway. PTP1B is a widely expressed nonreceptor protein tyrosine phosphatase that is located in the endoplasmic reticulum (ER) (Frangioni et al., 1992). It can directly dephosphorylate and inactivate a diverse range of substrates, including receptor protein tyrosine kinases (RPTKs; e.g., insulin receptor [IR], epidermal growth factor receptor [EGF-R], platelet derived growth factor receptor, and insulin-like growth factor receptor), components of growth factor pathways (e.g., Jak2, p63DOK, and Src), and SH3-containing proteins (e.g., p130Cas, Fak, and Crk), which have critical roles in integrin signaling (Dadke and Chernoff, 2002; Bourdeau et al., 2005). PTP1B has also been shown to decrease levels of p-Erk1/2 in various studies (Ferrari et al., 2011; Haj et al., 2003). PTP1B plays a role in diabetes (Combs 2010), obesity (Bence et al., 2006), cancer (Julien et al., 2007; Bentires-Alj and Neel, 2007), and cell proliferation (Arias-Salgado et al., 2005).

Here, we show that PTP1B is recruited to Alk(ALK)4 and forms part of a noncanonical Activin signaling pathway that controls mesendoderm or neuroectoderm lineage specification.

RESULTS

The Activin/Alk(ALK)4 Pathway Induces Mesendodermal Fate and Suppresses Neural Fate

We sought to determine the role of Activin in cell fate decision at different stages of mouse and human ESC differentiation. To this

Please cite this article in press as: Matulka et al., PTP1B Is an Effector of Activin Signaling and Regulates Neural Specification of Embryonic Stem Cells, Cell Stem Cell (2013), http://dx.doi.org/10.1016/j.stem.2013.09.016

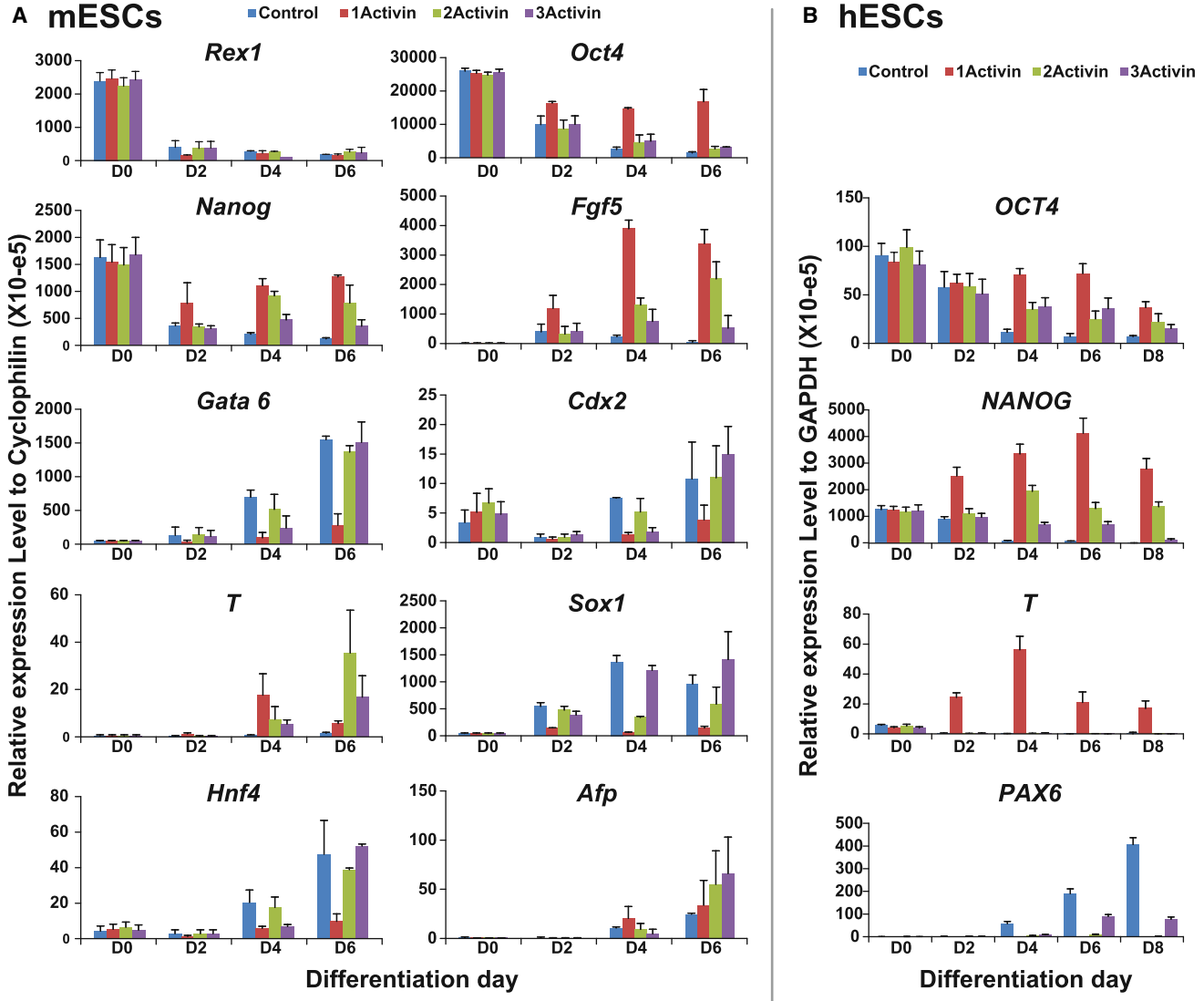

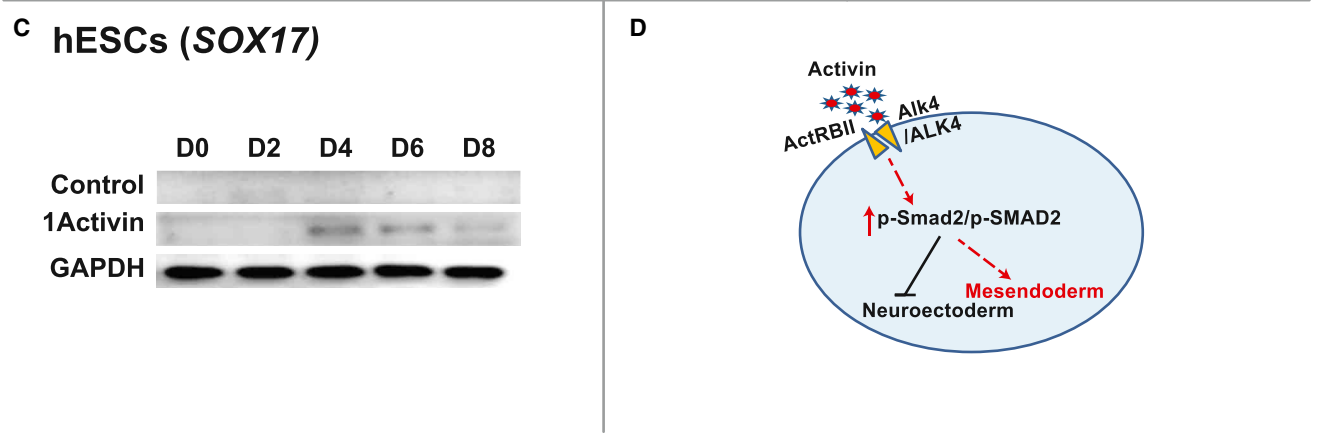

Figure 1. Activin Promotes either Pluripotency or Mesendodermal Fates while Inhibiting Neural Fate

During (A) mESC and (B) hESC differentiation, expression levels of stage-specific genes in the presence of stage-dependent treatments of Activin were measured by quantitative real-time PCR. Activin was administered to cells continuously from 1-day (1Activin), 2-day (2Activin), or 3-day (3Activin) differentiation.

(legend continued on next page)

end, both hESCs and mESCs were transferred to N2B27 differentiation medium, and then Activin (10 ng/ml) was added after 1 day of differentiation (1Activin), 2 days of differentiation (2Activin), or 3 days of differentiation (3Activin). The cells were then allowed to differentiate for either 6 (mESCs) or 8 (hESCs) days in the continued presence of Activin (Figure S1Aavailable online). In mESCs, we found that 1Activin sustained more than 60% of the gene expression levels of *Oct4* and *Nanog* during the 6 days of differentiation, while the expression levels of the two genes dropped below 5% in nontreated cells (Figure 1A). Of note, 1Activin did not maintain the expression of another pluripotent marker, *Rex1* (Figure 1A). However, 1Activin enhanced the expression of *Fgf5*, a marker of epiblast cells (Figure 1A). Our findings suggest that Activin promotes the development of epiblast cells from mESCs. As differentiation proceeded, the Activin treatments (2Activin and 3Activin) exhibited less effect on the expression levels of *Oct4*, *Nanog*, and *Fgf5* in mESCs (Figure 1A), suggesting that the effect of Activin on pluripotency is restricted to a certain time window during ESC differentiation. We also examined the impact of Activin on other lineages during differentiation. We found that Activin treatment promoted mesendodermal fate specification as judged by *T* and T expression (Figures 1A and S1B), while only 1Activin inhibited primitive endoderm (*Gata 6*), trophectoderm (*Cdx2*), endoderm (*Hnf4* and *Afp*), and neuroectoderm (*Sox1*) fates (Figure 1A).

Activin also exhibited a similar pattern of effects in hESCs, with a few exceptions. During the 8 days of hESC differentiation, 1Activin maintained high *OCT4* expression (Figure 1B). Interestingly, 1Activin resulted in more than a 2-fold increase in the expression levels of *NANOG* throughout the 8 day differentiation period, far greater than that seen in mESCs (Figures 1A and 1B). Because *Nanog* is expressed in ESCs and epiblast cells (Mitsui et al., 2003), our results suggest that the high expression levels of *NANOG* in hESCs induced by Activin may represent an epiblast stage. However, *FGF5* expression was hardly detected in all groups of cells (data not shown). As in mESCs, 1Activin also promoted mesendodermal (*T*, T, and *SOX17*) and inhibited neuroectodermal (*PAX6*) fate specification (Figures 1B, 1C, and S1B). The reason we used *PAX6* rather than *SOX1* to identify human neuroectoderm is because *PAX6* is expressed earlier than *SOX1,* which shows a reciprocal expression order in mouse and human (Figure S1C). Furthermore, there were extremely low levels of expression for the phenotypic markers of primitive endoderm, trophectoderm, and endoderm (data not shown). Interestingly, 2Activin and 3Activin not only exhibited less effect on the promotion of the mesendodermal phenotype but also alleviated the inhibition of other cell fates in mESCs and hESCs (Figures 1A and 1B). Our results suggest that Activin-mediated early fate decision in ESCs occurs in the first 2 days of differentiation. In summary, as ESC differentiation proceeds, Activin promotes mesendodermal fate while inhibiting neural specification, which may occur via p-Smad(SMAD)2 signaling (Figure 1D).

Blockade of the Activin/Alk(ALK)4 Pathway with SB431542 Promotes Neural Lineage

We showed that mESCs in which neuronatin was knocked down (Nnat-KD) fail to undergo neural induction and are possibly trapped at the epiblast stage (Lin et al., 2010). This was concluded because Nnat-KD mESCs exhibited very high *Fgf5* expression and resisted differentiation. We used the Nnat-KD mESCs to investigate how the inhibition of the Activin/Alk4 pathway affects neural induction. We treated Nnat-KD mESCs, at different days of differentiation (Figure S1A), with one dose of SB431542, a selective inhibitor of Activin/Nodal signaling that acts at ALK4/5/7 to block the downstream p-Smad2/3 signaling cascade (Inman et al., 2002). Intriguingly, we found that +0SB43 or +1SB43 treatment restored the ability of Nnat-KD mESCs to undergo neural induction to levels seen in wild-type mESCs, as assayed by Sox1-GFP expression (Figure 2A). Interestingly, SB431542 failed to rescue neural induction of Nnat-KD mESCs when administered to cells after 2 days of differentiation (i.e., +2SB43 and +3SB43). We also found that the capacity of Nnat-KD mESCs to produce neurons after +1SB43 treatment was restored to that of wild-type cells (Figure 2B). Our results suggest that blocking the Activin/Alk4 pathway rescues neural induction in Nnat-KD mESCs and that the efficacy of this treatment is restricted to the first 2 days of differentiation, echoing the findings shown in Figure 1A.

We further tested whether inhibition of the Activin/Alk4 pathway also promotes neural fate in wild-type mESCs. It has been reported that cells plated at high densities fail to adopt the neural fate, possibly due to inhibitory signals from cell-to-cell contact (Zhou et al., 2008). We adopted a high-density culture system to investigate the effect of SB431542 on neural induction. Cells were plated at a standard density (3×10^4 cells/cm^2) and at high density (36×10^4 cells/cm^2) and were driven toward neural differentiation in the presence or absence of SB431542. Interestingly, we found that SB431542 had no positive effects on the production of neural stem cells (NSCs) at standard density. However, SB431542 caused a significant increase in the number of NSCs under high-density conditions (Figure 2C), indicating that the Activin/Alk4 pathway exerts an inhibitory effect on neural induction in mESCs, which is also corroborated by our other finding that Activin treatment prevented mESCs from adopting a neural fate (Figure S2A).

We further examined whether the inhibition of the Activin/Alk4 pathway also induces neural specification in hESCs. We observed a distinctive difference in neural specification between hESCs and mESCs in our system. Mouse ESCs are capable of generating over 60% NSCs when undergoing neural differentiation in N2B27 medium. However, fewer than 5% of cells became NSCs when hESCs were driven to the neural lineage. Intriguingly, in the presence of SB431542, NSC formation was significantly enhanced for hESCs, as judged by the number of neural rosettes and expression levels of *PAX6* (Figures 2D and 2E), suggesting that the Activin/Alk(ALK)4 pathway plays an inhibitory effect on neural induction in both hESCs and mESCs and

Stage-specific markers indicate pluripotency (*Rex1*, *Oct4*/*OCT4*, and *Nanog*/*NANOG*), epiblast (*Fgf5*), primitive endoderm (*Gata6*), trophectoderm (*Cdx2*), mesendoderm (*T*), neuroectoderm (*Sox1*/*PAX6*), and definitive endoderm (*Hnf4*/*Afp*). All data are represented as mean ± SD (n = 2) and were normalized to the values of cyclophilin and *GAPDH* for mESCs and hESCs, respectively. (C) The expression of *SOX17*, a marker for mesendoderm, was detected by PCR. (D) A schematic diagram summarizing data. See also Figure S1.

Please cite this article in press as: Matulka et al., PTP1B Is an Effector of Activin Signaling and Regulates Neural Specification of Embryonic Stem Cells, Cell Stem Cell (2013), http://dx.doi.org/10.1016/j.stem.2013.09.016

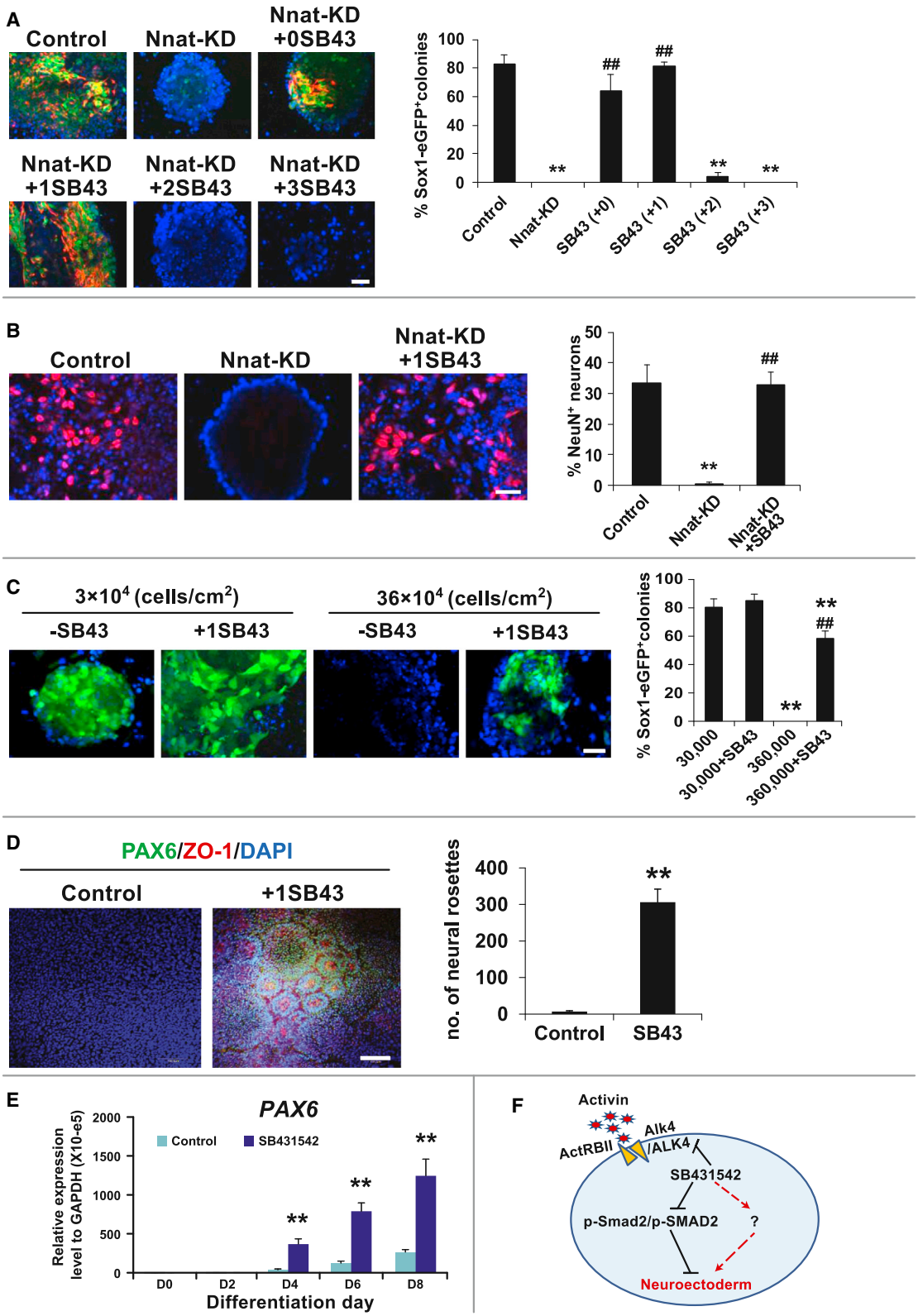

Figure 2. Inhibition of the Activin/Alk(ALK)4 Pathway by SB431542 Promotes the Neural Lineage

(A) Immunocytochemical analysis (ICC; left panel) shows that SB431542 restores neural induction in Nnat-knockdown (Nnat-KD) mESCs, judging by the production of Sox1-eGFP$^+$/Nestin$^+$ (red) neural stem cells. SB431542 was administered to the cells on the same day as differentiation induction (+0SB43) or 1-day (+1SB43), 2-day (+2SB43), or 3-day (+3SB43) differentiation. The right panel shows the quantified data.

(legend continued on next page)

that the effect is functionally specific in neural fate decision (Figure S2B). Collectively, the inhibition of Activin/Alk(ALK)4 signaling by SB431542 leads to neural induction in ESCs, which may be due to either SB431542 inhibiting p-Smad(SMAD)2 signaling or an unknown pro-neural-inducing influence of SB431542, or a combination of both of these mechanisms (Figure 2F).

SB431542 Promotes Neural Fate via p-Erk(ERK)1/2 Signaling

We sought to identify the mechanism underlying SB431542-mediated neural induction. In an accidental discovery, we found that treating mESCs with SB431542 resulted in an increase in p-Erk1/2 levels, which peaked after 10 min of treatment and lasted for 2 hr after treatment (Figures 3A and S3A). We also observed a similar outcome in hESCs; however, the elevated levels of p-ERK1/2 returned to control levels after 1 hr (Figure 3B). These results suggest that SB431542 not only inhibited p-Smad2/3 signaling but also activated p-Erk(ERK)1/2 signaling.

Next, we determined whether SB431542-triggered p-Erk(ERK) 1/2 signaling is involved in SB431542-mediated neural induction. To this end, we examined the effects of p-Erk1/2 signaling inhibitors (PD173074 [a FGFR inhibitor] and PD184352 [a MEK inhibitor]) on SB431542-restored neural induction in Nnat-KD mESCs at different time points during differentiation. We found that, after SB431542 treatment, 89% of the colonies generated by Nnat-KD mESCs were Sox1/eGFP$^+$ NSCs at 6 days of differentiation, and those Sox1/eGFP$^+$ colonies were completely abolished when the cells were cotreated with SB431542 and PD184352 (i.e., +1SB43+1PD18) (Figures 3C and S3B). Interestingly, the later stages of PD184352 treatments (e.g., +2PD18, +3PD18, and +4PD18) sustained the inhibitory effect on neural induction, suggesting that SB431542-mediated neural induction in Nnat-KD ESCs is via p-Erk1/2 signaling. A very similar effect was also observed in control cells treated with PD184352 (Figure 3C), indicating that p-Erk signaling is indeed crucial in SB431542-mediated neural induction. These data were also corroborated using another inhibitor, PD173074, which inhibited neural induction in control and Nnat-KD ESCs less potently (Figure 3D).

The importance of p-Erk1/2 signaling in SB431542-promoted neural induction is also corroborated by our findings in hESCs. We found that, in the absence of SB431542, hESCs underwent neural induction at low efficiency, with less than 5% of the colonies generated containing NSCs (Figure 3E); SB431542 treatment enhanced neural induction in hESCs over seven times that seen in untreated cells. SB431542-mediated neural induction in hESCs was also inhibited by PD184352 and PD173074, similar to our findings in mESCs (Figures 3E and 3F), suggesting that the role of FGF/p-ERK signaling in neural induction is conserved in hESCs. Taken together, our results suggest that SB431542 exerts dual effects by activating p-Erk(ERK)1/2 signaling and inhibiting p-Smad(SMAD)2/3 signaling, with SB431542-mediated p-Erk(ERK)1/2 signaling promoting neural lineages in mESCs and hESCs (Figure 3G).

SB431542 Activates p-Erk1/2 Signaling by Antagonizing a Noncanonical Activin Pathway

We next analyzed whether SB431542 increased p-Erk(ERK)1/2 levels through its inhibitory action on the Activin/Alk(ALK)4) pathway or through its effect on the FGF/p-Erk(ERK)1/2 pathway. First, we tested whether Activin reduces p-Erk(ERK)1/2 levels in ESCs as a premise that the inhibition of Activin pathway leads to an increase in p-Erk(ERK)1/2 level. We found that Activin not only activated p-Smad2 signaling but also inhibited p-Erk1/2 signaling in mESCs (Figure 4A). However, in the presence of SB431542, p-Erk1/2 levels increased despite treatment with Activin (Figure 4A), suggesting that, in part, SB431542 triggers an increase in p-Erk1/2 levels by acting upon components of the Activin/Alk4 signaling pathway. We also observed that Activin attenuated the levels of p-ERK1/2 in hESCs using a phospho-mitogen activated protein kinase (phospho-MAPK) array assay (Figure 4B). Strikingly, among the 18 phospho-MAPKs tested, only the levels of p-ERK1/2 were affected by SB431542 or Activin treatments (Figure S4).

We further established if the increased p-Erk1/2 levels are due to the inhibition of p-Smad2 by SB431542. We found that, in both control and Nnat-KD mESCs, the levels of p-Erk1/2 peaked 10 min after SB431542 treatment, whereas p-Smad2 levels were only reduced after 2 hr of treatment (Figures 4C and 4D). We also observed that SB431542 exhibited no effect on the BMP4/p-Smad1 pathway (Figures 4C and 4D). Our data show that SB431542-triggered p-Erk1/2 signaling precedes the inhibition of p-Smad2 signaling, suggesting that SB431542-mediated p-Erk1/2 signaling is not caused by the inhibition of p-Smad2, p-Smad1, or their downstream components but possibly by upstream elements of the Activin pathway (e.g., Alk4). It is conceivable that SB431542-triggered p-Erk(ERK)1/2 signaling results from crosstalk between SB431542 and the FGF/p-Erk(ERK)1/2 pathway. To test this, we employed a biochemical approach using PD173074 and PD184352. We found that the SB431542-mediated increase in p-Erk(ERK)1/2 levels was abolished in the presence of PD173074 or PD184352 in both mESCs and hESCs (Figure 4E), indicating that the FGF/p-Erk(ERK)1/2 pathway is involved in this process. To determine how the FGF/p-ERK1/2 pathway is involved in the effect of SB431542, we screened a phospho-receptor tyrosine kinase (phospho-RTK) array containing upstream elements of p-ERK1/2 signaling with proteins from SB431542-treated ESCs. We found that none of the 42 tested phospho-RTKs was affected by SB431542

(B) SB431542-restored neuron production in Nnat-KD mESCs by ICC analysis (left panel) and quantified data (right panel) are shown.

(C) In mESCs, SB431542 prevents an inhibitory effect on neural induction mediated by high-density plating shown by ICC analysis (left panel) and quantified data (right panel).

(D and E) In hESCs, SB431542 enhances (D) neural rosette formation identified by PAX6 (green)/ZO-1 (red) staining and (E) *PAX6* expression during neural differentiation, as assessed by quantitative real-time PCR.

(F) A schematic diagram summarizing data.

Scale bars represent 50 μm, except 100 μm in (D). Data shown are the mean ± SD (n = 3). $^{**}p < 0.01$, significantly different from the control group; $^{\#\#}p < 0.01$, significantly different from the SB431542-untreated cells; two-tailed Student's t test. See also Figure S2.

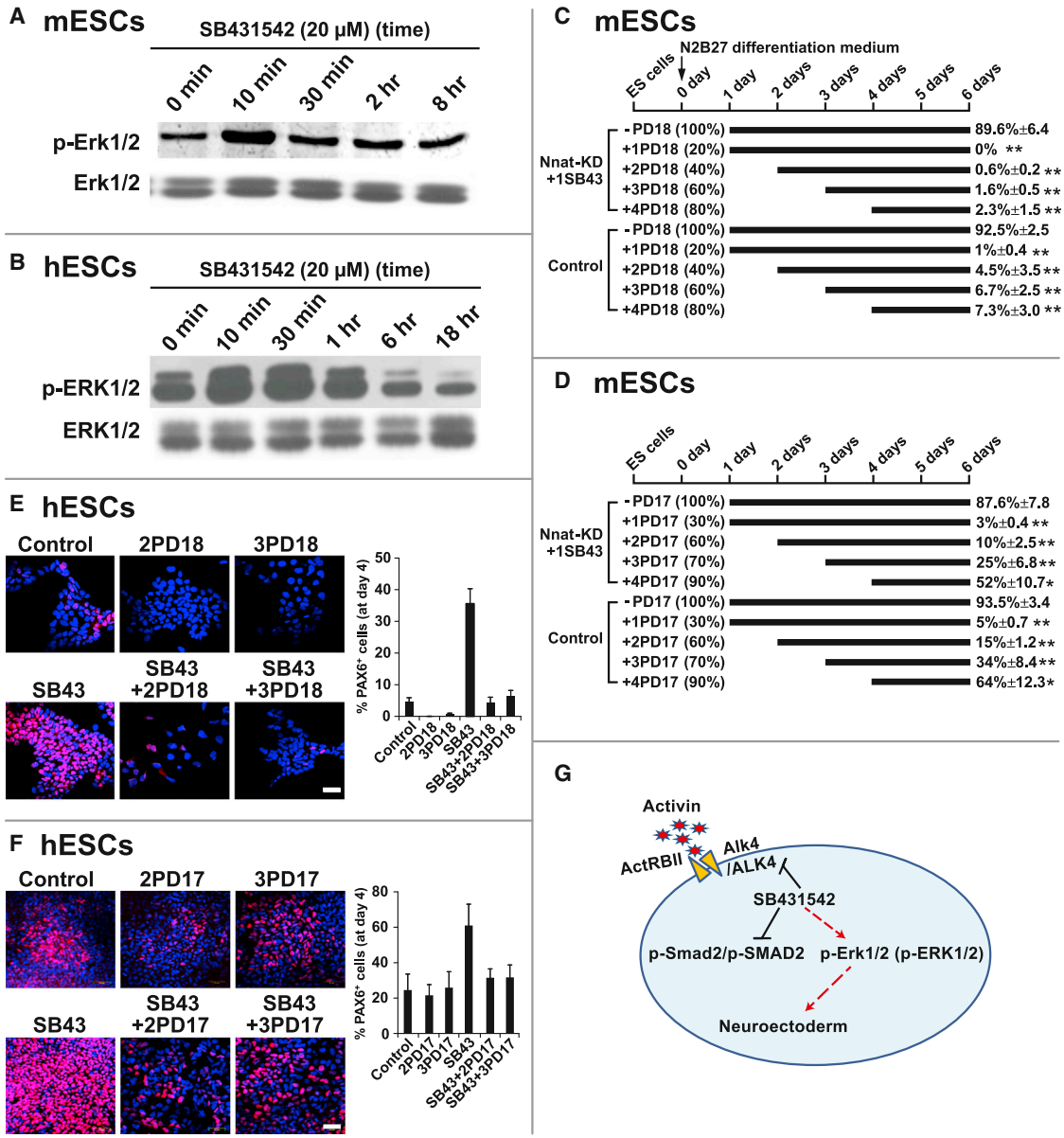

Figure 3. SB431542-Mediated Neural Induction Occurs via p-Erk(ERK)1/2 Signaling

(A and B) The duration of SB431542 treatment results in an increase in p-Erk(ERK)1/2 levels as measured by western blot.

(C and D) The temporal effects of PD184352 (a MEK inhibitor) and PD173074 (a FGFR inhibitor) on SB431542-restored neural induction in mESCs. The top panel depicts the differentiation status of cells. The values are the percentages of Sox1-eGFP$^+$ colonies at 6 days of differentiation and are presented as mean ± SD (n = 3). "+1," "+2," "+3," and "+4" indicate the timing of the treatment: continuously from 1, 2, 3, and 4 days after differentiation, respectively. Cell survival rates after inhibitor treatments are in brackets. *$p < 0.05$ and **$p < 0.01$ are significantly different from the group without drug treatment.

(E and F) PD184352 (E) and PD173074 (F) inhibit SB431542-induced neural induction in hESCs. ICC analysis is shown in the left panel and quantified data, in the right panel. Data are presented as mean ± SD (n = 2). Scale bars represent 50 μm.

(G) A schematic diagram summarizing the data. See also Figure S3.

treatment when compared to the dimethyl sulfoxide (DMSO)-treated control group (Figure 4F), indicating that SB431542-mediated p-ERK1/2 signaling does not act at the level of RTKs. In general, our results suggest that SB431542-triggered p-Erk(ERK)1/2 signaling possibly occurs via antagonizing a noncanonical pathway of Activin that negatively regulates p-Erk(ERK)1/2 levels (Figure 4G).

PTP1B Is a Key Effector in an Activin/ALK4 Noncanonical Pathway to Suppress p-ERK1/2 Signaling

We have shown that Activin inhibits p-Erk(ERK)1/2 signaling and that this inhibition is not due to the downstream action of p-Smad2 signaling. Thus, we sought to determine how Activin mediates inhibition of p-Erk(ERK)1/2 signaling in ESCs. In a broader screening, we discovered that PTP1B is a putative

Please cite this article in press as: Matulka et al., PTP1B Is an Effector of Activin Signaling and Regulates Neural Specification of Embryonic Stem Cells, Cell Stem Cell (2013), http://dx.doi.org/10.1016/j.stem.2013.09.016

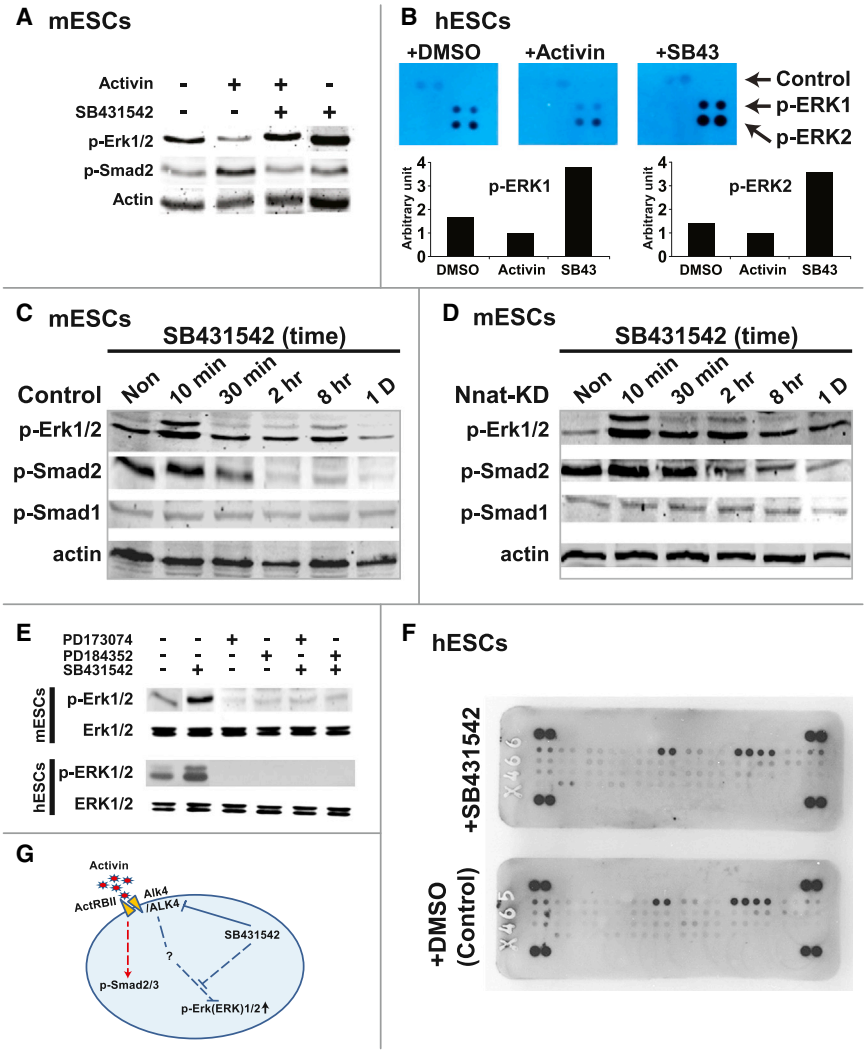

Figure 4. SB431542-Mediated p-Erk1/2 Signaling Precedes the Inhibition of p-Smad2 Signaling

(A) The levels of p-Erk1/2 and p-Smad2 change after 10 min of Activin and/or SB431542 treatment. (B) Activin and SB431542 affect the levels of p-ERK1/2 in hESCs as assayed in a phospho-MAPK array. In (C) control and (D) Nnat-KD mESCs, the duration of SB431542 treatment affects the levels of p-Erk1/2, p-Smad2, and p-Smad1. (E) The effects of PD173074 or PD184352 on the SB431542 elevation of p-Erk(ERK)1/2 levels in ESCs. (F) The effect of SB431542 on 42 phospho-RTKs measured with a phospho-RTK array. (G) A schematic diagram summarizing the data. See also Figure S4.

member of the Activin/Alk(ALK)4 pathway that mediates the inhibition of p-Erk(ERK)1/2 signaling. First, we established that Alk(ALK)4 interacts with PTP1B in mESCs and hESCs using a proximity ligation assay (PLA). Using this assay, numerous fluorescent dots were detected in both types of ESCs, suggesting that Alk(ALK)4 and PTP1B are physically interacting (Figure 5A). This interaction was further confirmed by coimmunoprecipitation (Figure S5A). We serendipitously observed that incubating active recombinant ALK4 and recombinant PTP1B together at 30°C resulted in the apparent cleavage of PTP1B (Figure 5B). To determine whether this cleavage also occurs within a cellular context, we treated hESCs with Activin for various time periods and determined what effects this treatment had on the integrity of endogenous PTP1B. We found that PTP1B was cleaved after 30 min of Activin treatment (Figure 5C), suggesting that Activin causes an interaction between ALK4 and PTP1B that leads to the cleavage of PTP1B by ALK4. We have shown that ALK4 has a protease activity; to our knowledge, PTP1B is the first of its substrates to be identified. Furthermore, treating hESCs with Activin causes PTP1B to translocate from the ER to the cytosol (Figure S5B) and then to cell membrane (Figure S5C), suggesting that PTP1B is cleaved and not degraded. Because ALK4 is a serine/threonine kinase receptor, we examined whether ALK4 affects the phosphorylation status of PTP1B by employing LC/MS/MS protein sequencing. The sequencing data showed that residue Lys292 is the last residue detected in the C-terminal region of PTP1B after incubation with ALK4 (band 3 in Figure 5D). We propose that the possible cleavage site for active ALK4 on PTP1B is located between the residues Glu293 to Arg371. Interestingly, no serine or threonine phosphorylation was identified (Figure 5D).

It is conceivable that PTP1B could physically interact with p-Erk(ERK)1/2 to exert its effect. Intriguingly, we not only found that PTP1B indeed interacted with p-Erk(ERK)1/2, but also discovered that treating ESCs with Activin significantly increased the number of interactions between PTP1B and p-ERK1/2. Conversely, treatment with SB431542 significantly decreased the interaction of these two proteins (Figure 6A). As PTP1B is a phosphatase, it is likely that the interaction between PTP1B and p-ERK1/2 would result in the dephosphorylation of p-ERK1/2. To confirm this, we immunoprecipitated PTP1B from Activin-treated hESCs, incubated it with total protein extracts from hESCs, and then analyzed p-ERK1/2 levels by western blot. We found that the levels of p-ERK1/2 were diminished proportionally to the duration of incubation with PTP1B (Figure 6B), indicating that PTP1B dephosphorylates p-ERK1/2. We also found a similar role for PTP1B in mESCs (Figure S6A). Our results suggest that Activin (via ALK4) decreases p-ERK1/2 levels by releasing PTP1B from the ER, allowing it to interact with and dephosphorylate p-ERK1/2, thus inhibiting neural fate. If our hypothesis that PTP1B dephosphorylates p-ERK1/2 to prevent neural induction is correct, then this interaction should not occur once neural induction has taken place. We found that PTP1B/p-ERK1/2 interactions (indicated in red dots) were abundantly present in undifferentiated hESCs and in cells after 2 days of differentiation; however, the interaction diminished

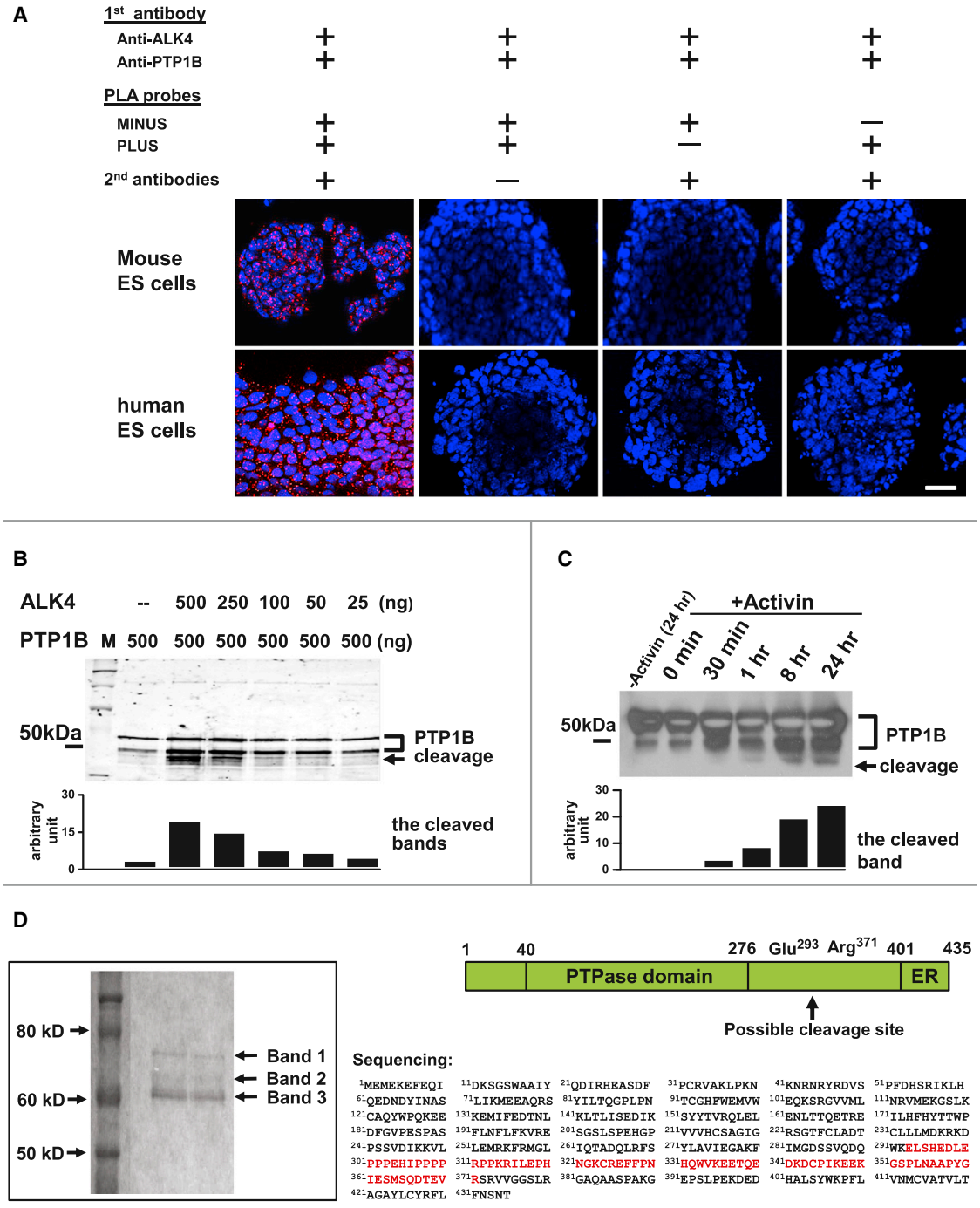

Figure 5. Activin Induces PTP1B Cleavage through Alk(ALK)4

(A) The physical interaction between Alk(ALK)4 and PTP1B (indicated by red dots) in ESCs detected by PLA.

(B) Dose-dependent cleavage of recombinant PTP1B by constitutively active recombinant ALK4 after 15 min incubation at 30°C.

(C) Immunoblot detection of PTP1B cleavage in hESCs treated with Activin for various time periods. ImageJ was employed to quantify the cleaved bands (in B and C).

(D) Sodium dodecyl sulfate polyacrylamide gel electrophoresis of the cleavage products of the ALK4/PTP1B reaction. The schematic diagram depicts the potential cleaved region of PTP1B by ALK4 with the amino acid sequence shown in red to indicate the possible cleavage site as identified by protein sequencing. See also Figure S5.

sharply after 4 days and was absent by 6 days of differentiation (Figure 6C), which coincides with the onset of neural induction. Strikingly, we observed that SOX1^{+} neural rosettes were virtually devoid of PTP1B/p-ERK1/2 interactions, while the interactions were prevalent in non-NSCs (Figure 6C), suggesting that PTP1B/p-ERK1/2 interactions are not present in NSCs,

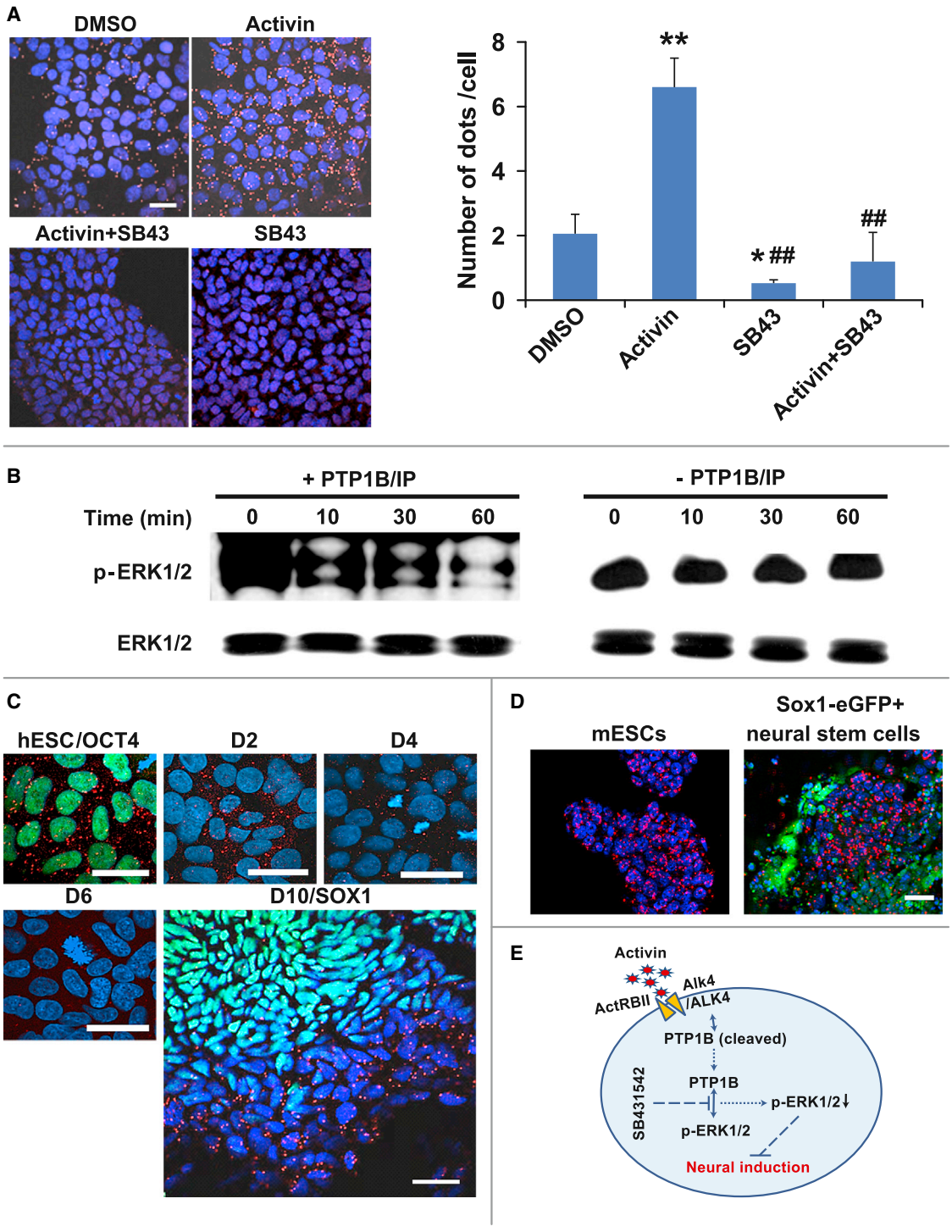

Figure 6. Activin Inhibits Neural Differentiation by Reducing p-ERK1/2 Levels through PTP1B

(A) Activin increases the number of interactions between PTP1B and p-ERK1/2 (indicated by red dots), which was blocked by SB431542 treatment (left panel). Quantified data are shown in the right panel and presented as mean ± SD (n = 3). *$p < 0.05$ and **$p < 0.01$, significantly different from the DMSO-treated control cells; $^{\#\#}p < 0.01$, significantly different from the Activin-treated cells.

(B) PTP1B dephosphorylates p-ERK1/2 in a time-dependent manner, as demonstrated by PTP1B (+PTP1B/IP) pull-down with FGF2-stimulated p-ERK (left panel). Phospho-ERK1/2 was not dephosphorylated when incubated with nonenriched PTP1B (−PTP1B/IP) (right panel).

(C and D) The interaction between PTP1B and p-ERK during neural differentiation in hESCs (C) and mESCs (D) detected by PLA.

(E) A schematic diagram summarizing data.

Scale bars represent 50 μm. See also Figure S6.

Please cite this article in press as: Matulka et al., PTP1B Is an Effector of Activin Signaling and Regulates Neural Specification of Embryonic Stem Cells, Cell Stem Cell (2013), http://dx.doi.org/10.1016/j.stem.2013.09.016

consistent with our theory. Furthermore, a similar pattern was observed during mESC-derived neural differentiation (Figure 6D), indicating that the role of p-Erk(ERK)1/2 in neural induction of ESCs is conserved in human and mouse. We established that the lack of PTP1B/p-ERK1/2 interactions in NSCs is not due to the absence of these two proteins, because PTP1B and p-ERK1/2 proteins were clearly observed in neural rosettes by immunocytochemical analysis (ICC; Figure S6B). We propose that this can be explained by the absence of Activin signaling in neural cells. Indeed, ALK4 was present in ESCs and nonneural cells but was absent in neural rosettes (Figure S6C). In summary, our results show that Alk(ALK)4 recruits and cleaves PTP1B, which then dephosphorylates p-ERK1/2, leading to the inhibition of neural induction. SB431542-mediated neural induction takes place by counteracting the effect of PTP1B (Figure 6E).

PTP1B Bypasses the Activin Pathway to Specify Mesendodermal Fate over Neural Fate

To precisely elucidate the role of PTP1B as a downstream effector of the Activin pathway, we employed gain-of-function and loss-of-function approaches to investigate the effects of PTP1B on the early fate decisions of ESCs. We generated control-KD, PTP1B-knockdown (PTP1B-KD), PTP1B/eGFP-overexpression (PTP1B-OE), and control-OE hESC (eGFP only) lines; expression levels of PTP1B were verified by western blot (Figure 7A). We also showed that the levels of PTP1B exhibited an inverse relationship with the levels of p-ERK1/2 (Figures 7A and S7A) in cells, which corroborates with our findings in Figure 6B. In characterizing PTP1B mutant ESCs, we found there is no discernible difference in the expression of pluripotent markers NANOG or OCT4 in ES medium. However, we found that PTP1B-KD hESCs showed a propensity for the neural fate and a decrease in mesendodermal phenotypes as compared to the control group, judged by the expression of neural markers (*PAX6* and *SOX1*) and mesendodermal markers (*SOX17*, *GSC*, *PDGFR*α, *T*, and *PECAM1*) (Figure 7B). We also found that knocking down PTP1B significantly enhanced PAX6$^+$ NSC production in the absence of SB431542 by 4-fold in three separate PTP1B-KD clones compared to the control (Figure 7C). PTP1B-KD also increased the capacity of hESCs to produce neural rosettes (data not shown). Furthermore, we also found that Nnat-KD mESCs treated with PTP1B inhibitor restored the ability of these cells to undergo neural induction (Figure S7B), suggesting that PTP1B exhibits a negative effect on neural lineages in hESCs and mESCs. On the contrary, PTP1B-OE ESCs were biased toward mesendodermal lineages and exhibited a diminished capacity to adopt neural fates (Figures 7B and 7D). Of note, control and PTP1B-KD ESCs showed an enhancement in their ability to generate mesendodermal fates and an inhibition of neural specification with Activin treatment, while PTP1B-OE hESCs exhibited very similar profiles of mesendodermal markers to those of Activin-treated cells (Figures 7B and 7D), indicating that PTP1B takes part in Activin-promoted mesendodermal decision, possibly in cooperation with p-Smad(SMAD)2 signaling.

We also observed an interesting phenomenon reported by Rodriguez et al. (2007) that high levels of Oct4 expression coincided with upregulated differentiated markers. Our data show that Activin sustained high-level expression of pluripotent markers *OCT4* and *NANOG* during 8-day differentiation and concurrently upregulated mesendodermal markers (Figure 7B), which correlates with our findings shown in Figure 1. Intriguingly, although the sustained high-level expression of *OCT4* and *NANOG* was not seen in PTP1B-OE hECSs (Figure 7B), we did find that several colonies with high OCT4- and NANOG-expressing cells were observed in 8-day differentiation culture and colocalized with the groups of cells that highly expressed PTP1B-eGFP but not those that expressed eGFP alone (Figures S7C and S7D). We also employed a chemically defined culture (CDC) system to establish that the results derived from our study are not specific to the N2B27 culture system we have used. Our results showed that SB431542 also increased the levels of p-ERK1/2 from a 10 min treatment in CDC system (Figures S7Ea), which is consistent with those observed in the N2B27 system. Moreover, PTP1B-KD promotes hESCs undergoing neural induction to a similar rate under SB431542 treatment, whereas only a few of the control-KD cells adopted neural fate (Figures S7Eb), suggesting that the effect of PTP1B on neural induction is not limited to the N2B27 medium, but also exists in CDC system. Like in N2B27 medium, the SB431542-mediated neural induction was blocked by FGF/p-ERK1/2 inhibitors in CDC system (Figure S7Ec). In summary, we found that Activin leads to the cleavage of PTP1B by active Alk(ALK)4 and enhances the interaction between PTP1B and p-Erk(ERK)1/2, which results in a reduction in p-Erk(ERK)1/2 levels, which in turn inhibits neural induction in favor of a mesendodermal fate, possibly in collaboration with p-Smad(SMAD)2 signaling (Figure 7E). Conversely, SB431542 inhibits p-Smad(SMAD)2 signaling, blocks PTP1B/p-Erk(ERK)1/2 interactions, and triggers p-Erk(ERK)1/2 signaling, which promotes neural specification (Figure 7E).

DISCUSSION

Embryonic development is controlled by intricate networks that include cytokines, transcription factors, and other regulatory elements. Cytokines induce myriad intracellular activities, including the activation or inhibition of multiple signal transduction pathways, culminating in phenotypic specification. Activin and Nodal play crucial roles during different stages of embryogenesis (Green and Smith, 1990; Camus et al., 2006; Vallier et al., 2004; Singh et al., 2012). Our study demonstrates that PTP1B takes part in the Activin-directed choice between mesendoderm and neuroectoderm. PTP1B exerts its role in this early fate decision possibly by mediating a noncanonical Activin pathway.

Our study shows that inhibition of Activin signaling using SB431542 leads to neural differentiation in hESCs and mESCs, which is consistent with previous studies in hESCs (Smith et al., 2008; Chambers et al., 2009). To define the molecular mechanisms underlying SB431542-mediated neural induction in ESCs, we uncover that the inhibition of the Activin/ALK4 pathway by SB431542 not only inhibits p-SMAD2/3 signaling but also activates p-Erk(ERK)1/2 signaling. We corroborated this finding by screening human phospho-MAPKs more broadly. We have found that SB431542 treatment only increases the levels of p-ERK1/2 and not those of 17 other tested kinases, demonstrating that SB431542-mediated p-ERK1/2 signaling is

Please cite this article in press as: Matulka et al., PTP1B Is an Effector of Activin Signaling and Regulates Neural Specification of Embryonic Stem Cells, Cell Stem Cell (2013), http://dx.doi.org/10.1016/j.stem.2013.09.016

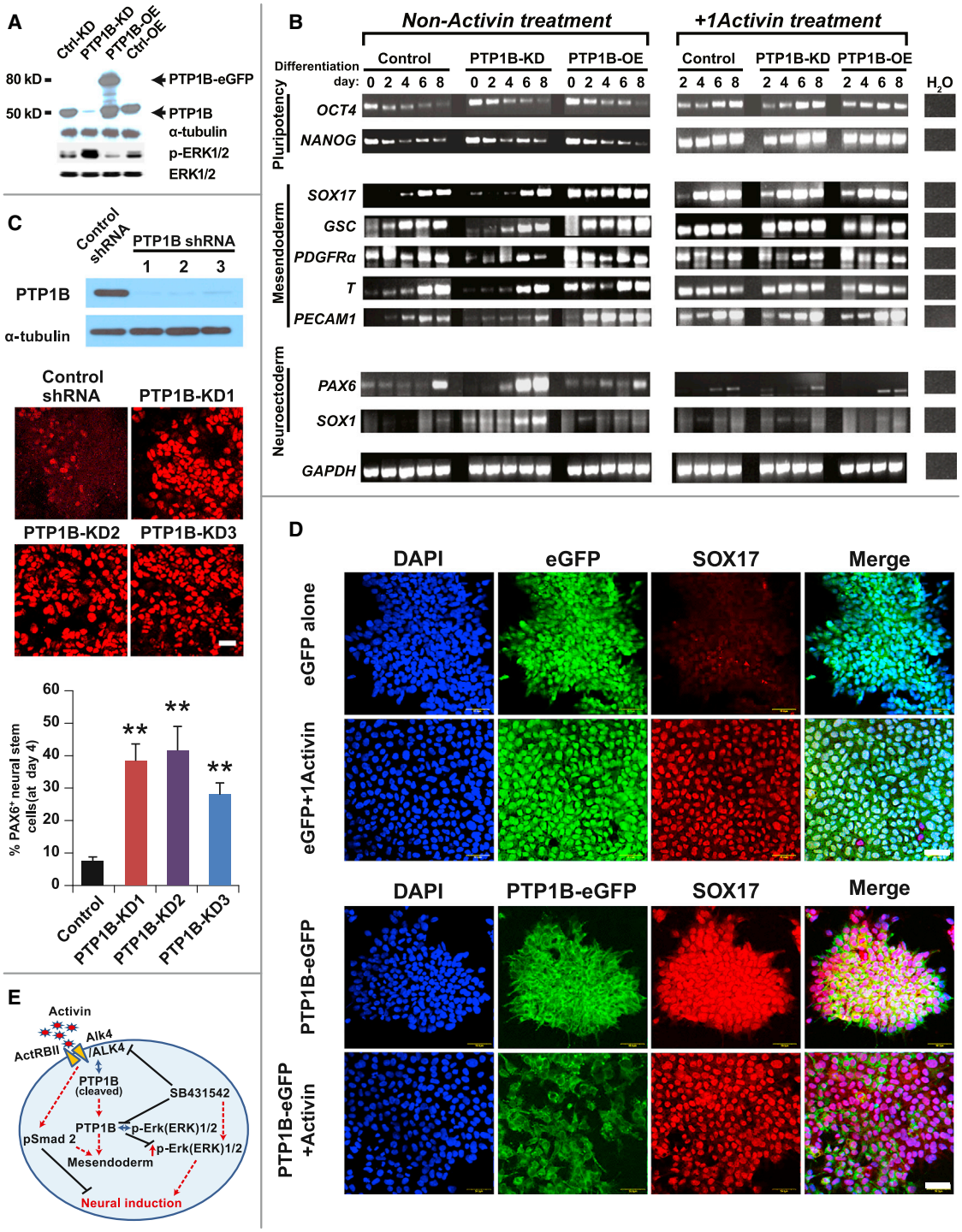

Figure 7. PTP1B Promotes Mesendodermal Fates and Restricts Neural Differentiation

(A) PTP1B hESC mutants were verified by western blot and their effects on the levels of p-ERK1/2.

(B) The expression profiles of fate markers in PTP1B mutant hESCs as assessed by RT-PCR.

(C) Three PTP1B-KD hESC clones were subjected to neural differentiation in the absence of SB431542, and $PAX6^+$ cells (red) were counted. Data are presented as mean ± SD (n = 3). **$p < 0.01$, significantly different from the control group.

(D) PTP1B-eGFP-overexpressing hESCs favor mesendodermal fate, judging by SOX17 expression.

(E) A schematic diagram depicts the conceptual summary derived from this study.

Scale bars represent 50 μm. See also Figure S7.

specific. We also show that SB431542 elevation of p-Erk(ERK) 1/2 levels is dependent on neither SB431542 inhibition of p-SMAD2/3 signaling nor involvement of p-SMAD1 signaling. However, we demonstrate that the p-Erk(ERK)1/2 effect of SB431542 is acting upon the Activin/Alk(ALK)4 pathway, perhaps via a noncanonical pathway of Activin. In the past decade, many studies have highlighted crosstalk between TGF-β1 signaling via Smads and the MAPK pathway (Li et al., 2009; Jiang et al., 2010). To rule out the possibility that crosstalk between SB431542 and the FGF pathway might be involved in SB431542-mediated p-Erk(ERK)1/2 signaling, we analyzed a phospho-RTK array and found that none of the tested phospho-RTKs was affected by SB431542 treatment. However, we did find that FGF/p-Erk(ERK)1/2 signaling inhibitors abolish the SB431542-mediated p-Erk(ERK)1/2 elevation, indicating that p-Erk(ERK)1/2 is the convergence point of the SB431542 actions. We propose that SB431542 counteracts a noncanonical pathway of Activin that directly decreases p-Erk(ERK)1/2 levels.

To identify the key effector that links the noncanonical Activin pathway and p-Erk(ERK)1/2 inhibition, we selected several potential proteins that negatively regulate levels of p-Erk and tested for physical interactions with Alk4. We found that PTP1B was the only one that satisfied both requirements. Our data show that PTP1B is recruited to the Activin pathway by binding to Alk(ALK)4, which mediates the cleavage of PTP1B. Intriguingly, we find that Activin treatment also triggers an increase in the number of physical interaction between PTP1B and p-ERK1/2, which is abolished by SB431542. The interaction of PTP1B/p-ERK1/2 leads the dephosphorylation of p-ERK1/2 and therefore the reduction of p-ERK1/2 levels. Our results are in line with the role of PTP1B in dephosphorylating the insulin receptor EGF-R, MAPK, JNK, SH3-containing proteins (p130Cas, Fak, and Crk) (Dadke and Chernoff, 2002; Jin et al., 2000), and p-ERK1/2 (Ferrari et al., 2011; Haj et al., 2003). Our data suggest that Activin induces the physical interaction between PTP1B and p-ERK1/2 that leads to the inhibition of p-ERK1/2 signaling, which is consistent with our findings that the inhibition of the Activin pathway by SB431542 abolishes PTP1B/p-ERK1/2 interactions and results in an increase in p-ERK1/2 levels. Here we have shown that PTP1B mediates a noncanonical pathway of Activin to regulate p-Erk(ERK)1/2 signaling. We have further demonstrated that SB431542-mediated p-Erk(ERK)1/2 signaling is decisive in neural specification by relieving the inhibitory signal of the Activin/Alk(ALK)4 pathway. Most interestingly, the phenomenon of PTP1B-regulated p-Erk(ERK)1/2 signaling also occurs in ESCs during neural specification, in which period PTP1B/p-Erk(ERK)1/2 interaction is absent in the cells undergoing neural induction, suggesting that p-Erk(ERK)1/2 is critical during neural specification. This finding is concomitant with previous reports that FGF/p-Erk(ERK)1/2 signaling promotes neural specification in ESCs (Vallier et al., 2009a; LaVaute et al., 2009; Na et al., 2010; Lin et al., 2010). Yoo et al. (2011) further showed that the FGF-ERK1/2 signal pathway regulates neuroectoderm specification through regulating PARP-1 activity. Despite most studies supporting the promoting role of FGF signaling in neural specification, some contradictory observations have been reported. We reason that the discrepancy lies in the fashion of FGF signaling manipulations during investigation (see details in the supplemental legend for Figures S4B and S4C).

We generated PTP1B-OE and PTP1B-KD ESCs to evaluate the actions of PTP1B in mediating Activin effects on the specification of mesendoderm and on neural inhibition. Our results showed that overexpressing PTP1B predisposes hESCs to mesendodermal fates, whereas knocking down PTP1B results in a bias toward neural fates. Recent studies suggested that Activin/Nodal signaling acts via NANOG to block ESC differentiation toward neural fate (Vallier et al., 2009b) and through SIP1 (Chng et al., 2010) to regulate the fate decision between neuroectoderm and mesendoderm. Vallier et al. (2009b) reported that NANOG knockdown promotes neural fate, while NANOG overexpression blocks the effect even in the presence of SB431542. Moreover, NANOG overexpression allows mesendoderm specification but not further progression of endoderm differentiation. They also showed that NANOG modulates the activity of the Activin/Nodal pathway by binding to Smad2/3. In our study, PTP1B mediates the action of Activin signaling via ALK4, and PTP1B-OE only attenuates, but not obliterates, neural fate. Furthermore, PTP1B-OE promotes mesendodermal fate, but does not affect further progression of endoderm differentiation. PTP1B-OE does not maintain high levels of *NANOG* expression during differentiation. Our study suggests that PTP1B acts as an alternative pathway within the Activin/Alk(ALK)4 pathway to determine the fate decision between neuroectoderm and mesendoderm in hESCs and mESCs. These findings are in keeping with our hypothesis that PTP1B acts as a downstream effector of the Activin pathway. However, PTP1B did not fully compensate for all functions of Activin/p-Smad(SMAD)2 signaling in ESCs. For instance, unlike Activin, PTP1B-OE hESCs did not maintain the high levels of *OCT4* and *NANOG* expression during differentiation, indicating that PTP1B is not involved in the p-Smad2-mediated expression of *OCT4* and *NANOG* (Chng et al., 2010; Lee et al., 2011). We propose that PTP1B takes part in an Activin signaling pathway that is involved in regulating mesendoderm fate decisions and that this role of PTP1B is conserved in hESCs and mESCs.

In summary, our data suggest that Activin not only activates a canonical p-Smad2 signaling cascade through Alk(ALK)4 but also recruits PTP1B and triggers the interaction between PTP1B and p-Erk(ERK)1/2. This interaction downregulates p-Erk(ERK)1/2 signaling and leads to the inhibition of neural induction. PTP1B also promotes mesendoderm specification, possibly in cooperation with p-Smad2 signaling. Our study demonstrates that PTP1B acts as a member of the Activin/Alk(ALK)4 pathway to regulate p-Erk(ERK)1/2 signaling, which forms noncanonical signaling in Activin networks. Our study confers PTP1B with a role in Activin-mediated functions in hESCs and mESCs.

EXPERIMENTAL PROCEDURES

ESC Maintenance and ESC Monolayer Differentiation

Human ESCs (CCTL14) (passage numbers 25–30) were maintained on feeders as previously described (Eiselleova et al., 2009) and plated onto Matrigel-coated plates in conditioned media supplemented with 4 ng/ml FGF2 for three to five passages before being used for all experiments. Mouse 46C ESCs (a gift from Prof. A. Smith, Cambridge) were maintained as previously described (Sun et al., 2008 and Lin et al., 2010). Human and mouse ESCs were differentiated toward the neural lineage using a monolayer culture (hESCs on Matrigel-coated plates and mESCs on gelatin-coated plates) in N2B27 medium or

chemically defined medium as previously described (Lin et al., 2010 and Vallier et al., 2009a). We adopted the protocol (D'Amour et al., 2005) to drive ESC differentiation toward definitive endododerm. The details of differentiation experiments are described in the Supplemental Experimental Procedures.

Quantitative Real-Time PCR

The cell samples collected from mESCs were analyzed by quantitative real-time PCR using SYBR Green (Bio-Rad). Primer design and experimental procedures were carried out as previously described (Sun et al., 2005). Gene expression levels were normalized to cyclophilin levels. The cell samples collected from hESCs were measured by quantitative real-time PCR using the TaqMan Gene Expression Assay (Applied Biosystems), and gene expression levels were normalized to *GAPDH* levels. All experiments were performed in duplicate with two biological replicates.

PLA

PLA analysis was carried out according to the manufacturer's instructions. Fluorescent red dots were enumerated using MATLAB 7.11.0 software (The MathWorks, Inc.) with the DIPimage toolbox extension and presented as dots per nucleus. Sample preparation is described in the Supplemental Experimental Procedures.

Immunocytochemistry

ESCs, NSCs, and neurons were fixed in 4% PFA for 20 min at room temperature. Antibodies against Oct4 (1:500, AB3209, Chemicon), Nes (1:500, MAB353, Chemicon), Pax6 (1:500, Hybridoma bank), PTP1B (1:500, Santa Cruz Biotechnology), Alk4 (1:500, Santa Cruz Biotechnology), and NeuN (1:500, MAB377, Chemicon) were used.

Generation of PTP1B hESC Mutants

CCTL14 hESCs were used to generate PTP1B-KD and PTP1B-OE ESCs. PTP1B-KD hESCs were generated by stable transfection with PTP1B shRNA (TRCN0000002780) plasmid DNA (Sigma) under puromycin (0.3 μg/ml) selection, while the control cells were transfected with a shRNA backbone vector. PTP1B-KD hESCs were constitutively knocked down. PTP1B-OE hESCs were created by stable transfection with a PTP1B-eGFP fusion vector, which was constructed in the pEF1α-AcGFP1-N1 vector (Clontech, BD Biosciences), and were selected with G418 (100 μg/ml). The eGFP is fused to the C terminus of PTP1B in this vector, and the sequences were verified by sequencing.

Western Blot Analysis

To determine the temporal effects of SB431542 on p-Erk(ERK)1/2 levels, SB431542 was added to mESCs and hESCs in ESC medium for 10 min, 30 min, 1 hr, 2 hr, 6 hr, 8 hr, and 1 day, and cells were harvested at each time point. Other sample preparations are described in the Supplemental Experimental Procedures.

Immunoprecipitation

To determine the biological function of PTP1B/p-ERK1/2 interactions, PTP1B was immunoprecipitated from hESCs that were treated with Activin (10 ng/ml) for 2 hr and incubated for 0, 10, 30, and 60 min with total protein, which was isolated from hESCs treated with FGF2 for 10 min. The samples were subjected to western blot analysis with an anti-p-ERK1/2 antibody.

Protein Sequencing

Protein sequencing was analyzed by LC/MS/MS, and chromatographic separations were performed using an Ultimate LC system (Dionex). The MS/MS analysis was conducted using collision energy profiles that were chosen based on the mass-to-charge ratio (*m/z*) and the charge state of the peptide. Sample preparation is described in the Supplemental Experimental Procedures.

Phospho-RTK and Phospho-MAPK Array Assay

The detailed steps were carried out according to the manufacturer's protocol, and sample preparation is described in the Supplemental Experimental Procedures.

Statistical Analysis

Statistical significance was determined using a two-tailed Student's t test. $p < 0.05$ was considered statistically significant. All results are presented as mean values ± SD from experiments that have been done three times.

SUPPLEMENTAL INFORMATION

Supplemental Information for this article includes Supplemental Experimental Procedures and seven figures and can be found with this article online at http://dx.doi.org/10.1016/j.stem.2013.09.016.

ACKNOWLEDGMENTS

We thank Mr. A. Salykin for help in dot-counting for the PLA. This study was funded by grants from SoMoPro (2SGA2878) and the Ministry of Education, Youth, and Sport of the Czech Republic (MSM0021622430 and CZ.1.07/2.3.00/20.0011).

Received: April 10, 2013
Revised: July 10, 2013
Accepted: September 27, 2013
Published: October 17, 2013

REFERENCES

Arias-Salgado, E.G., Haj, F., Dubois, C., Moran, B., Kasirer-Friede, A., Furie, B.C., Furie, B., Neel, B.G., and Shattil, S.J. (2005). PTP-1B is an essential positive regulator of platelet integrin signaling. J. Cell Biol. *170*, 837–845.

Bence, K.K., Delibegovic, M., Xue, B., Gorgun, C.Z., Hotamisligil, G.S., Neel, B.G., and Kahn, B.B. (2006). Neuronal PTP1B regulates body weight, adiposity and leptin action. Nat. Med. *12*, 917–924.

Bentires-Alj, M., and Neel, B.G. (2007). Protein-tyrosine phosphatase 1B is required for HER2/Neu-induced breast cancer. Cancer Res. *67*, 2420–2424.

Bourdeau, A., Dubé, N., and Tremblay, M.L. (2005). Cytoplasmic protein tyrosine phosphatases, regulation and function: the roles of PTP1B and TC-PTP. Curr. Opin. Cell Biol. *17*, 203–209.

Camus, A., Perea-Gomez, A., Moreau, A., and Collignon, J. (2006). Absence of Nodal signaling promotes precocious neural differentiation in the mouse embryo. Dev. Biol. *295*, 743–755.

Chambers, S.M., Fasano, C.A., Papapetrou, E.P., Tomishima, M., Sadelain, M., and Studer, L. (2009). Highly efficient neural conversion of human ES and iPS cells by dual inhibition of SMAD signaling. Nat. Biotechnol. *27*, 275–280.

Chng, Z., Teo, A., Pedersen, R.A., and Vallier, L. (2010). SIP1 mediates cell-fate decisions between neuroectoderm and mesendoderm in human pluripotent stem cells. Cell Stem Cell *6*, 59–70.

Combs, A.P. (2010). Recent advances in the discovery of competitive protein tyrosine phosphatase 1B inhibitors for the treatment of diabetes, obesity, and cancer. J. Med. Chem. *53*, 2333–2344.

D'Amour, K.A., Agulnick, A.D., Eliazer, S., Kelly, O.G., Kroon, E., and Baetge, E.E. (2005). Efficient differentiation of human embryonic stem cells to definitive endoderm. Nat. Biotechnol. *23*, 1534–1541.

Dadke, S., and Chernoff, J. (2002). Interaction of protein tyrosine phosphatase (PTP) 1B with its substrates is influenced by two distinct binding domains. Biochem. J. *364*, 377–383.

Eiselleova, L., Matulka, K., Kriz, V., Kunova, M., Schmidtova, Z., Neradil, J., Tichy, B., Dvorakova, D., Pospisilova, S., Hampl, A., and Dvorak, P. (2009). A complex role for FGF-2 in self-renewal, survival, and adhesion of human embryonic stem cells. Stem Cells *27*, 1847–1857.

Ferrari, E., Tinti, M., Costa, S., Corallino, S., Nardozza, A.P., Chatraryamontri, A., Ceol, A., Cesareni, G., and Castagnoli, L. (2011). Identification of new substrates of the protein-tyrosine phosphatase PTP1B by Bayesian integration of proteome evidence. J. Biol. Chem. *286*, 4173–4185.

Frangioni, J.V., Beahm, P.H., Shifrin, V., Jost, C.A., and Neel, B.G. (1992). The nontransmembrane tyrosine phosphatase PTP-1B localizes to the endoplasmic reticulum via its 35 amino acid C-terminal sequence. Cell *68*, 545–560.

Green, J.B., and Smith, J.C. (1990). Graded changes in dose of a Xenopus activin A homologue elicit stepwise transitions in embryonic cell fate. Nature *347*, 391–394.

Haj, F.G., Markova, B., Klaman, L.D., Bohmer, F.D., and Neel, B.G. (2003). Regulation of receptor tyrosine kinase signaling by protein tyrosine phosphatase-1B. J. Biol. Chem. *278*, 739–744.

Inman, G.J., Nicolás, F.J., Callahan, J.F., Harling, J.D., Gaster, L.M., Reith, A.D., Laping, N.J., and Hill, C.S. (2002). SB-431542 is a potent and specific inhibitor of transforming growth factor-beta superfamily type I activin receptor-like kinase (ALK) receptors ALK4, ALK5, and ALK7. Mol. Pharmacol. *62*, 65–74.

Jiang, W., Zhang, Y., Wu, H., Zhang, X., Gan, H., Sun, J., Chen, Q., Guo, M., and Zhang, Z. (2010). Role of cross-talk between the Smad2 and MAPK pathways in TGF-beta1-induced collagen IV expression in mesangial cells. Int. J. Mol. Med. *26*, 571–576.

Jin, S., Zhai, B., Qiu, Z., Wu, J., Lane, M.D., and Liao, K. (2000). c-Crk, a substrate of the insulin-like growth factor-1 receptor tyrosine kinase, functions as an early signal mediator in the adipocyte differentiation process. J. Biol. Chem. *275*, 34344–34352.

Julien, S.G., Dubé, N., Read, M., Penney, J., Paquet, M., Han, Y., Kennedy, B.P., Muller, W.J., and Tremblay, M.L. (2007). Protein tyrosine phosphatase 1B deficiency or inhibition delays ErbB2-induced mammary tumorigenesis and protects from lung metastasis. Nat. Genet. *39*, 338–346.

LaVaute, T.M., Yoo, Y.D., Pankratz, M.T., Weick, J.P., Gerstner, J.R., and Zhang, S.C. (2009). Regulation of neural specification from human embryonic stem cells by BMP and FGF. Stem Cells *27*, 1741–1749.

Lee, K.L., Lim, S.K., Orlov, Y.L., Yit, Y., Yang, H., Ang, L.T., Poellinger, L., and Lim, B. (2011). Graded Nodal/Activin signaling titrates conversion of quantitative phospho-Smad2 levels into qualitative embryonic stem cell fate decisions. PLoS Genet. *7*, e1002130.

Li, F., Zeng, B.F., Chai, Y.M., Cai, P., Fan, C., and Cheng, T. (2009). The linker region of Smad2 mediates TGF-β-dependent ERK2-induced collagen synthesis. Biochem. Biophys. Res. Commun. *386*, 289–293.

Lin, H.H., Bell, E., Uwanogho, D., Perfect, L.W., Noristani, H., Bates, T.J., Snetkov, V., Price, J., and Sun, Y.M. (2010). Neuronatin promotes neural lineage in ESCs via Ca(2+) signaling. Stem Cells *28*, 1950–1960.

Mesnard, D., Guzman-Ayala, M., and Constam, D.B. (2006). Nodal specifies embryonic visceral endoderm and sustains pluripotent cells in the epiblast before overt axial patterning. Development *133*, 2497–2505.

Mitsui, K., Tokuzawa, Y., Itoh, H., Segawa, K., Murakami, M., Takahashi, K., Maruyama, M., Maeda, M., and Yamanaka, S. (2003). The homeoprotein Nanog is required for maintenance of pluripotency in mouse epiblast and ES cells. Cell *113*, 631–642.

Na, J., Furue, M.K., and Andrews, P.W. (2010). Inhibition of ERK1/2 prevents neural and mesendodermal differentiation and promotes human embryonic stem cell self-renewal. Stem Cell Res. (Amst.) *5*, 157–169.

Ogawa, K., Saito, A., Matsui, H., Suzuki, H., Ohtsuka, S., Shimosato, D., Morishita, Y., Watabe, T., Niwa, H., and Miyazono, K. (2007). Activin-Nodal signaling is involved in propagation of mouse embryonic stem cells. J. Cell Sci. *120*, 55–65.

Rodriguez, R.T., Velkey, J.M., Lutzko, C., Seerke, R., Kohn, D.B., O'Shea, K.S., and Firpo, M.T. (2007). Manipulation of OCT4 levels in human embryonic stem cells results in induction of differential cell types. Exp. Biol. Med. (Maywood) *232*, 1368–1380.

Singh, A.M., Reynolds, D., Cliff, T., Ohtsuka, S., Mattheyses, A.L., Sun, Y., Menendez, L., Kulik, M., and Dalton, S. (2012). Signaling network crosstalk in human pluripotent cells: a Smad2/3-regulated switch that controls the balance between self-renewal and differentiation. Cell Stem Cell *10*, 312–326.

Smith, J.R., Vallier, L., Lupo, G., Alexander, M., Harris, W.A., and Pedersen, R.A. (2008). Inhibition of Activin/Nodal signaling promotes specification of human embryonic stem cells into neuroectoderm. Dev. Biol. *313*, 107–117.

Sun, Y.M., Greenway, D.J., Johnson, R., Street, M., Belyaev, N.D., Deuchars, J., Bee, T., Wilde, S., and Buckley, N.J. (2005). Distinct profiles of REST interactions with its target genes at different stages of neuronal development. Mol. Biol. Cell *16*, 5630–5638.

Sun, Y.M., Cooper, M., Finch, S., Lin, H.H., Chen, Z.F., Williams, B.P., and Buckley, N.J. (2008). Rest-mediated regulation of extracellular matrix is crucial for neural development. PLoS ONE *3*, e3656.

Vallier, L., Reynolds, D., and Pedersen, R.A. (2004). Nodal inhibits differentiation of human embryonic stem cells along the neuroectodermal default pathway. Dev. Biol. *275*, 403–421.

Vallier, L., Alexander, M., and Pedersen, R.A. (2005). Activin/Nodal and FGF pathways cooperate to maintain pluripotency of human embryonic stem cells. J. Cell Sci. *118*, 4495–4509.

Vallier, L., Touboul, T., Chng, Z., Brimpari, M., Hannan, N., Millan, E., Smithers, L.E., Trotter, M., Rugg-Gunn, P., Weber, A., and Pedersen, R.A. (2009a). Early cell fate decisions of human embryonic stem cells and mouse epiblast stem cells are controlled by the same signalling pathways. PLoS ONE *4*, e6082.

Vallier, L., Mendjan, S., Brown, S., Chng, Z., Teo, A., Smithers, L.E., Trotter, M.W., Cho, C.H., Martinez, A., Rugg-Gunn, P., et al. (2009b). Activin/Nodal signalling maintains pluripotency by controlling Nanog expression. Development *136*, 1339–1349.

Werner, S., and Alzheimer, C. (2006). Roles of activin in tissue repair, fibrosis, and inflammatory disease. Cytokine Growth Factor Rev. *17*, 157e71.

Yoo, Y.D., Huang, C.T., Zhang, X., Lavaute, T.M., and Zhang, S.C. (2011). Fibroblast growth factor regulates human neuroectoderm specification through ERK1/2-PARP-1 pathway. Stem Cells *29*, 1975–1982.

Zhou, J.M., Xing, F.Y., Shi, J.J., Fang, Z.F., Chen, X.J., and Chen, F. (2008). Quality of embryonic bodies and seeding density effects on neural differentiation of mouse embryonic stem cells. Cell Biol. Int. *32*, 1169–1175.

Cell Stem Cell, volume *13*

Supplemental Information

PTP1B Is an Effector of Activin Signaling and Regulates Neural Specification of Embryonic Stem Cells

Kamil Matulka, Hsuan-Hwai Lin, Hana Hříbková, Dafe Uwanogho, Petr Dvořák, and Yuh-Man Sun

Supplemental data

Figure S1.

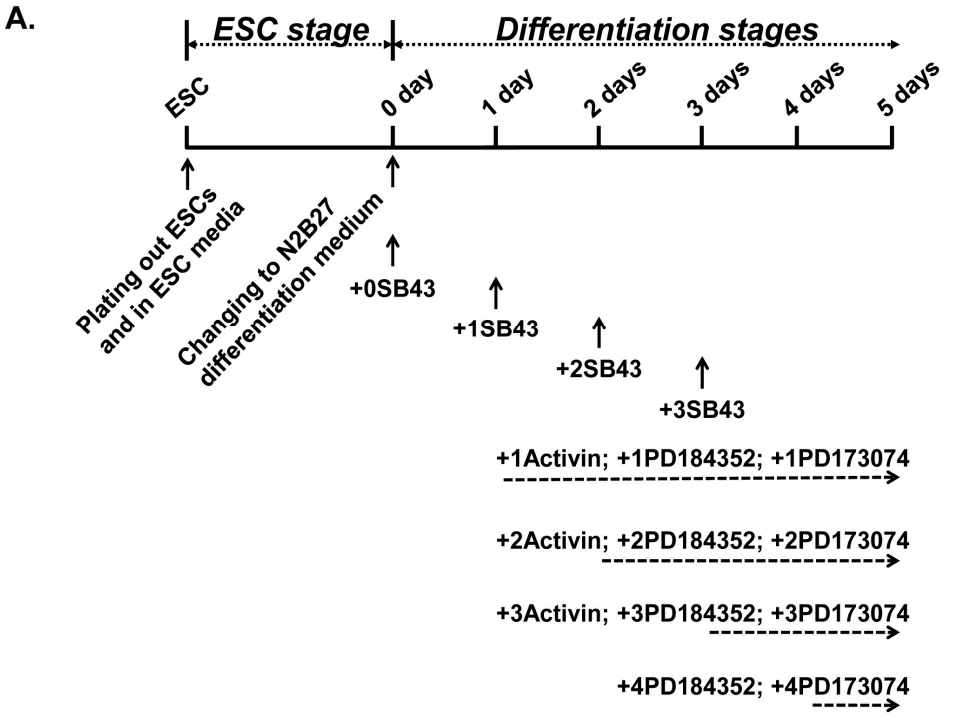

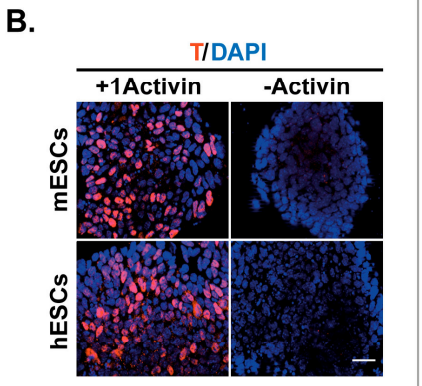

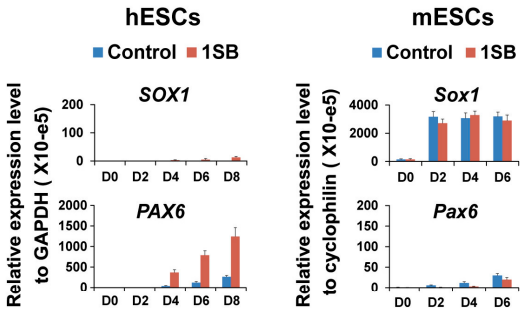

Figure S2.

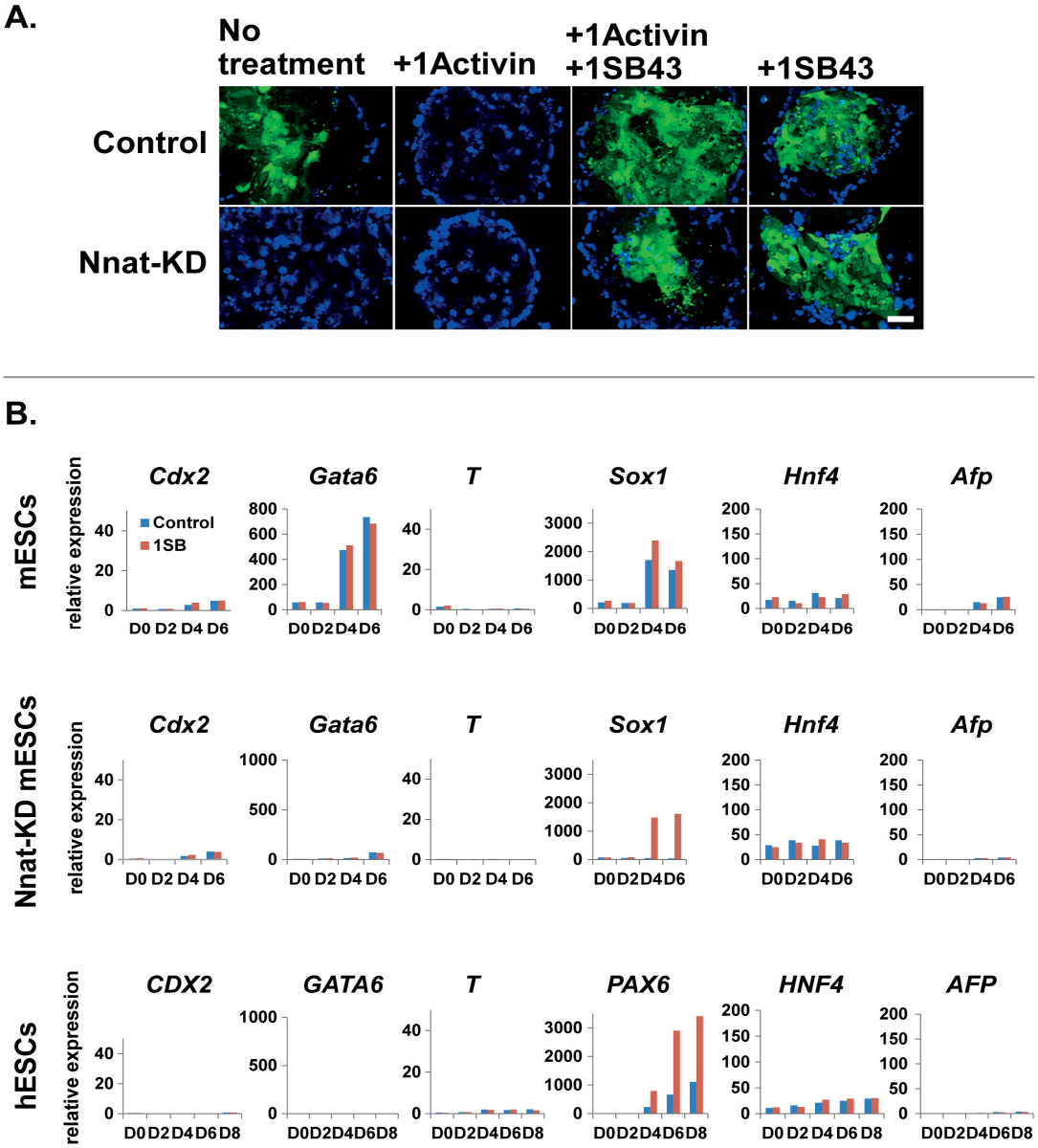
A.
No treatment
+1Activin
+1Activin +1SB43
+1SB43
Control
Nnat-KD
B.
mESCs
Nnat-KD mESCs
hESCs
relative expression
Control
1SB
Cdx2
Gata6
T
Sox1
Hnf4
Afp
CDX2
GATA6
PAX6
HNF4
AFP
D0 D2 D4 D6
D0 D2 D4 D6 D8

Figure S3.

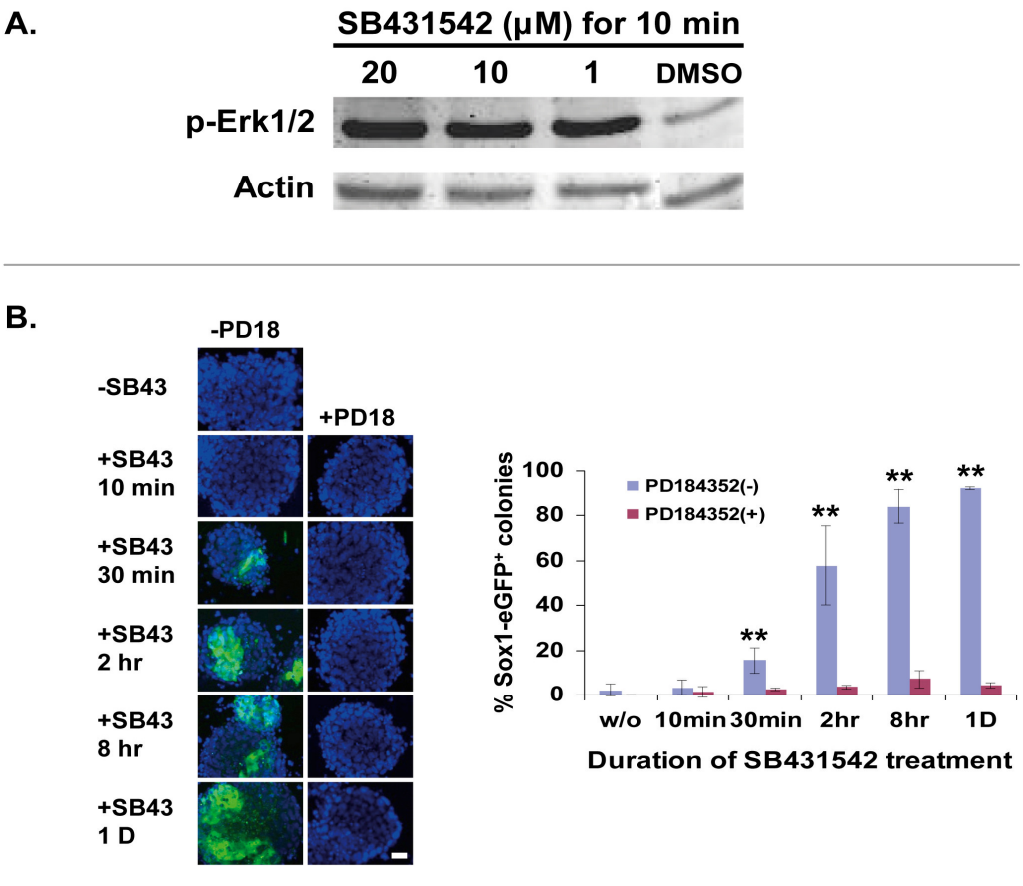
A.
SB431542 (μM) for 10 min
20
10
1
DMSO
p-Erk1/2
Actin
B.
-PD18
+PD18
-SB43
+SB43 10 min
+SB43 30 min
+SB43 2 hr
+SB43 8 hr
+SB43 1 D
% Sox1-eGFP+ colonies
100
80
60
40
20
0
PD184352(-)
PD184352(+)
**
**
**
**
w/o
10min
30min
2hr
8hr
1D
Duration of SB431542 treatment

Figure S4.

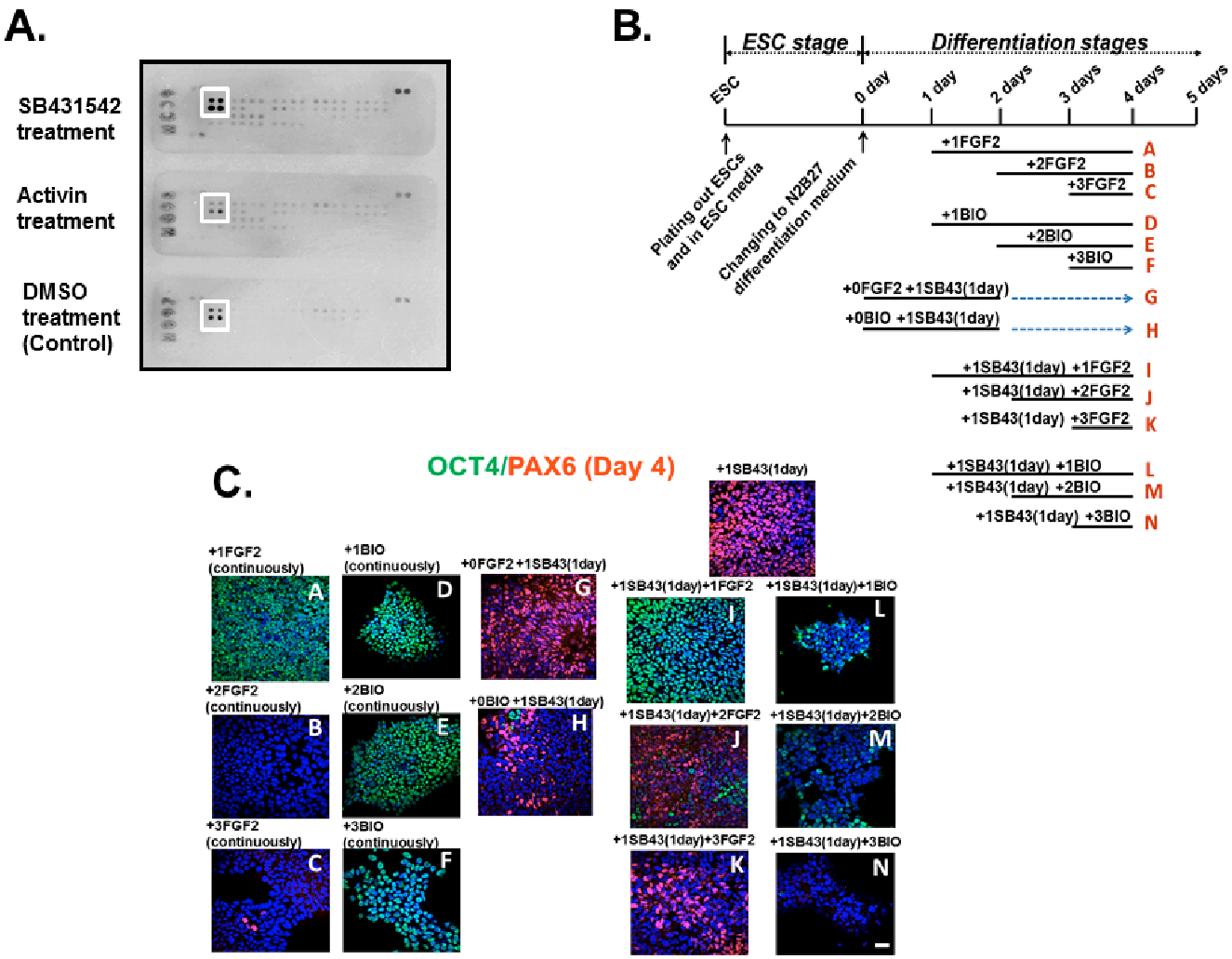
A.
SB431542 treatment
Activin treatment
DMSO treatment (Control)
B.
ESC stage
Differentiation stages
ESC
0 day
1 day
2 days
3 days
4 days
5 days
Plating out ESCs and in ESC media
Changing to N2B27 differentiation medium
+1FGF2
+2FGF2
+3FGF2
+1BIO
+2BIO
+3BIO
+0FGF2 +1SB43(1day)
+0BIO +1SB43(1day)
+1SB43(1day) +1FGF2
+1SB43(1day) +2FGF2
+1SB43(1day) +3FGF2
+1SB43(1day) +1BIO
+1SB43(1day) +2BIO
+1SB43(1day) +3BIO
A
B
C
D
E
F
G
H
I
J
K
L
M
N
C.
OCT4/PAX6 (Day 4)
+1FGF2 (continuously)
+1BIO (continuously)
+0FGF2 +1SB43(1day)
+1SB43(1day)
+1SB43(1day)+1FGF2
+1SB43(1day)+1BIO
+2FGF2 (continuously)
+2BIO (continuously)
+0BIO +1SB43(1day)
+1SB43(1day)+2FGF2
+1SB43(1day)+2BIO
+3FGF2 (continuously)
+3BIO (continuously)
+1SB43(1day)+3FGF2
+1SB43(1day)+3BIO

Figure S5.

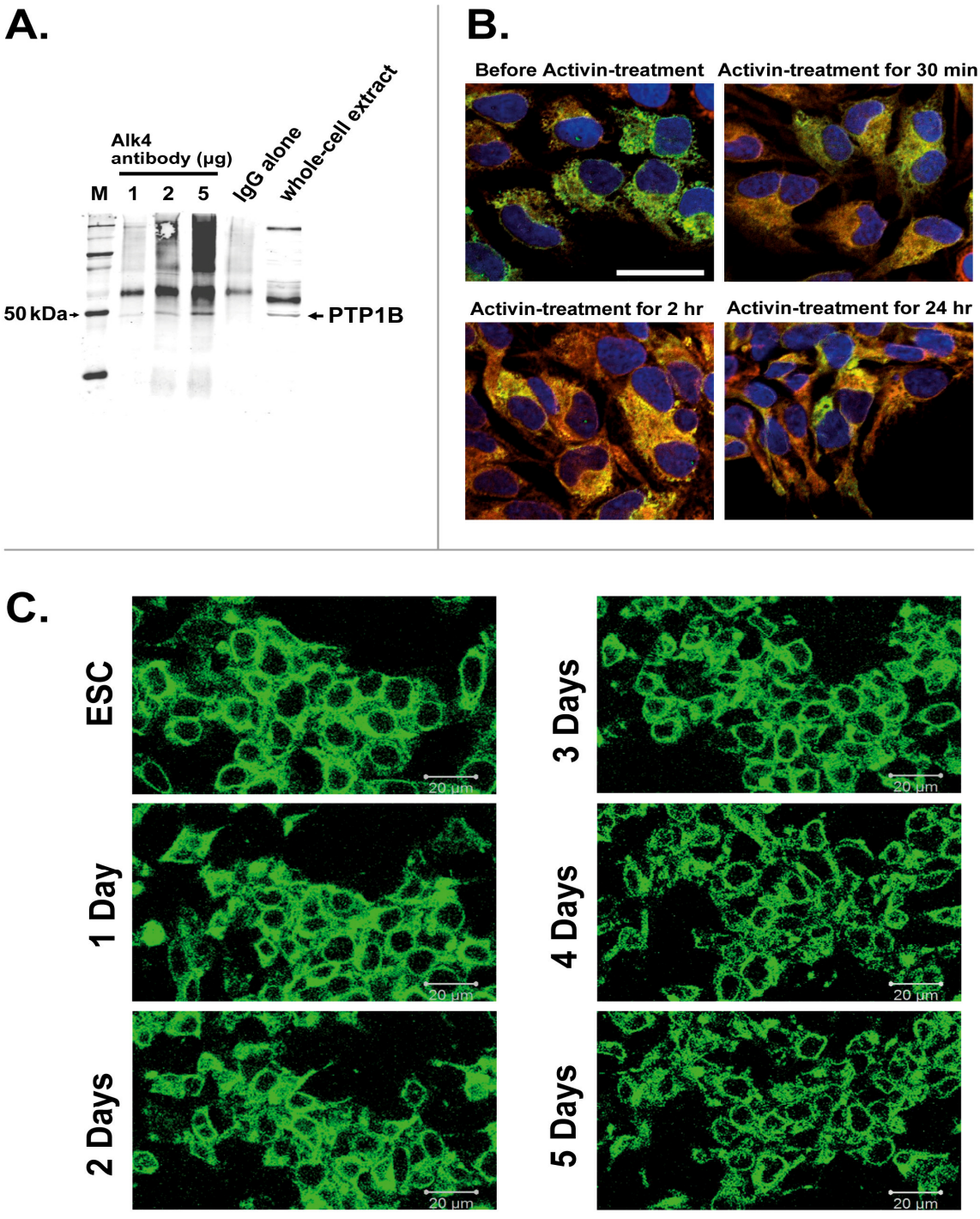
A.
Alk4 antibody (μg)
M
1
2
5
IgG alone
whole-cell extract
50 kDa
PTP1B
B.
Before Activin-treatment
Activin-treatment for 30 min
Activin-treatment for 2 hr
Activin-treatment for 24 hr
C.
ESC
1 Day
2 Days
3 Days
4 Days
5 Days
20 μm

Figure S6.

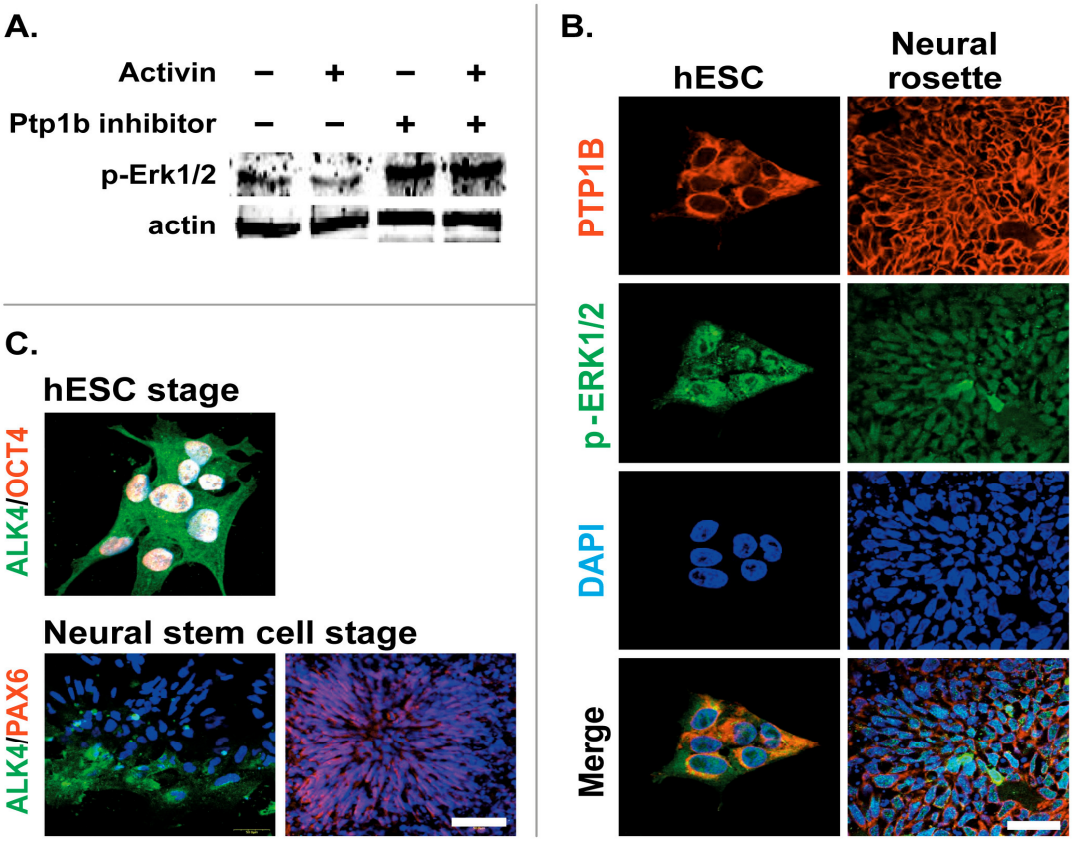
A.
Activin
Ptp1b inhibitor
p-Erk1/2
actin
B.
hESC
Neural rosette
PTP1B
p-ERK1/2
DAPI
Merge
C.
hESC stage
ALK4/OCT4
Neural stem cell stage
ALK4/PAX6

Figure S7.

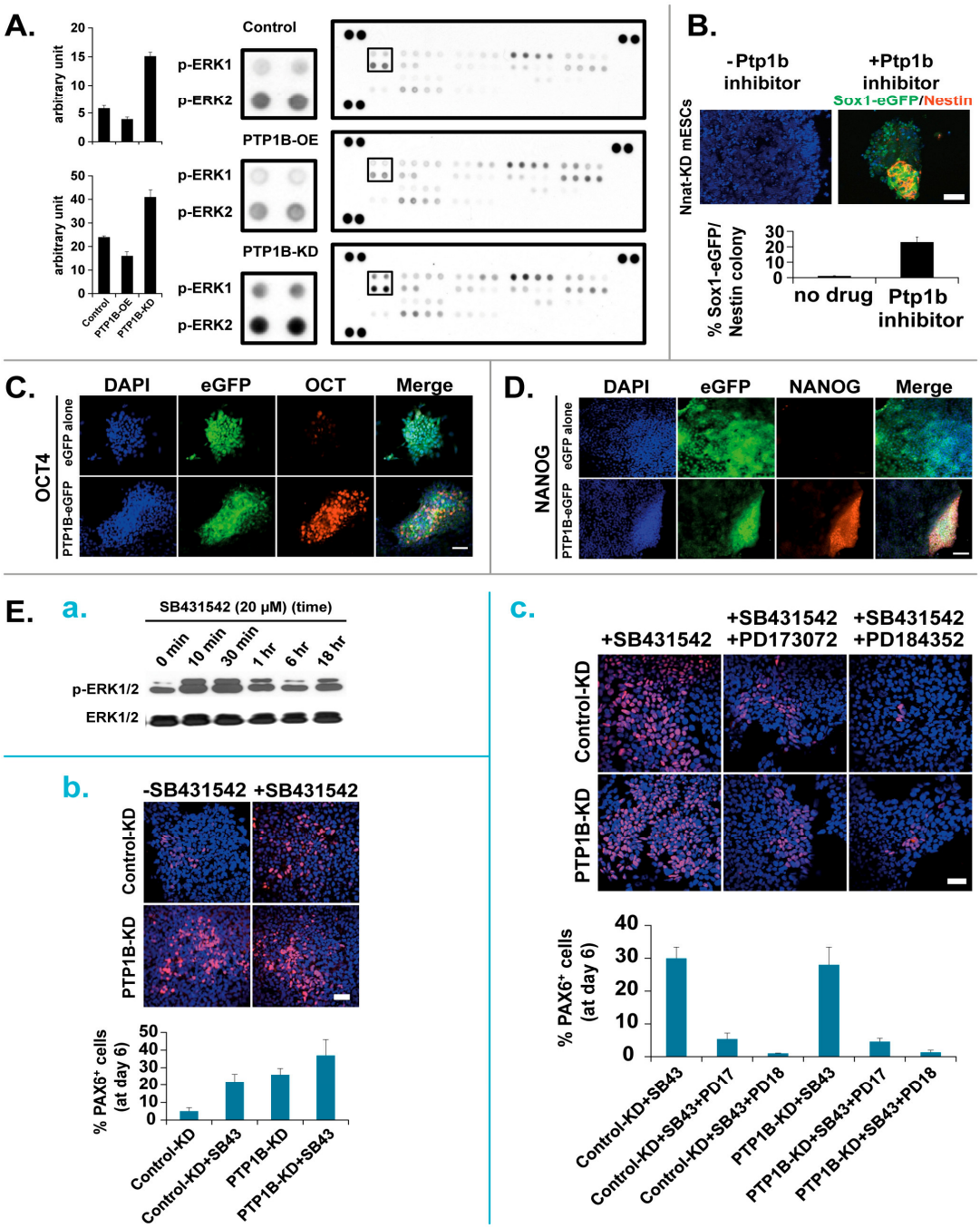
A.
arbitrary unit
Control
p-ERK1
p-ERK2
PTP1B-OE
PTP1B-KD
Control
PTP1B-OE
PTP1B-KD
B.
-Ptp1b inhibitor
+Ptp1b inhibitor
Sox1-eGFP/Nestin
Nnat-KD mESCs
% Sox1-eGFP/ Nestin colony
no drug
Ptp1b inhibitor
C.
DAPI
eGFP
OCT
Merge
OCT4
eGFP alone
PTP1B-eGFP
D.
DAPI
eGFP
NANOG
Merge
NANOG
eGFP alone
PTP1B-eGFP
E.
a.
SB431542 (20 μM) (time)
0 min
10 min
30 min
1 hr
6 hr
18 hr
p-ERK1/2
ERK1/2
b.
-SB431542
+SB431542
Control-KD
PTP1B-KD
% PAX6⁺ cells (at day 6)
Control-KD
Control-KD+SB43
PTP1B-KD
PTP1B-KD+SB43
c.
+SB431542
+SB431542 +PD173072
+SB431542 +PD184352
Control-KD
PTP1B-KD
% PAX6⁺ cells (at day 6)
Control-KD+SB43
Control-KD+SB43+PD17
Control-KD+SB43+PD18
PTP1B-KD+SB43
PTP1B-KD+SB43+PD17
PTP1B-KD+SB43+PD18

Supplemental Figure Legends

Supplemental Fig 1. (related to Figure 1)

(A) Schematic diagram summarizing the time periods of drug administration during ESC differentiation. The diagram depicts the different stages of embryonic stem cell (ESC)-derived differentiation, including before differentiation (ESC stage) and the differentiation stage initiated by culturing ESCs in N2B27 differentiation medium. The first day of changing to N2B27 medium is designated as 0 day and the following days are 1 day, 2 days,…, etc. "+0SB43" refers to the cells treated with one dose of SB431542 as cells were fed with N2B27 medium at the start. "+1SB43" is the cells treated with one dose of SB431542 one day after differentiation. "+2SB43" or "+3SB43" are the cells treated on 2 or 3 days of differentiation, respectively. "+1Activin" refers to the cells treated with Activin continuously from 1 day after differentiation. The same applies to "+1PD184352" and "+1PD173074". The terms starting "+2", "+3", and "+4" indicate the first day of drug administration for Activin, PD184352, and PD173074 treatments. (B) Mouse and human ESCs were treated with 10 ng/ml Activin after 1 day of differentiation (+1Activin) and cells were fixed on 4-day differentiation. Cells were stained with T antibody. Scale bar represents 20 μm. (C) A reciprocal expression order in *PAX6/Pax6* and *SOX1/Sox1* in human and mouse is shown by quantitative RT-PCR. Previous studies also showed that in human ESCs and embryos, PAX6 is one of earliest genes expressed in neuroectodermal cells, earlier than SOX1 expression (Li et al., 2005; Pankratz et al., 2007; Zhang et al., 2007). Data are presented as mean ± s.d. (n = 2). 1SB represents as +1SB431524.

Supplemental Fig 2. Activin specifically suppresses neural fate decision in mESCs and hESCs, related to Figure 2.

(A) Control and Nnat-KD mESCs were driven along neural differentiation, which was indicated by the production of Sox1-GFP$^+$ neural stem cells. Activin treatment at 1-day after differentiation prevents cells from undergoing neural differentiation, to which effect was blocked by a concurrent treatment with Activin inhibitor, SB431542. Scale bar represents 20 μm. (B) The Inhibition of Activin by SB431542 specifically

promotes neural lineage during the early fate decision from ESCs. The gene expression of fate specific markers was analyzed using quantitative real-time PCR. 1SB represents as +1SB431524. Experiment was done once in duplicate.

Supplemental Fig 3. Phospho-Erk1/2 signaling is responsible for SB431542-mediated neural induction, related to Figure 3.

(A) Treatment with various doses of SB431542 augments the levels of p-Erk1/2. (B) The minimal 30-min treatments of SB431542 restore the capacity of Nnat-KD mESCs to undergo neural induction, which is inhibited by a combinational treatment with a MEK inhibitor, PD184352. Cell samples were collected at 6 days of differentiation and examined for Sox1-GFP^{+} neural stem cells. Scale bar represents 50 μm (left panel). The quantified data are shown in the right panel. Data are presented as mean ± s.d. (n = 3). **, $p < 0.01$, significantly different from the PD184352-treated group.

Supplemental Fig 4. (related to Figure 4B).

(A) The effect of the Activin/ALK4 pathway on the levels of phospho-mitogen activated protein kinases (MAPKs) in hESCs The Human Phospho-MAPK Array, including 18 phosphorylated MAPKs, was used according to the manufacturer's instruction. Each array membrane containing duplicated proteins was hybridized with proteins harvested from hESCs treated either with Activin, SB431542, or DMSO (as control). SB431542 treatment noticeably only increases p-ERK1/2 (highlighted in the square) among the 18 MAPKs, while Activin treatment diminishes p-ERK1/2 levels as compared to DMSO treatment. We conducted experiments to explain why contradictory observations exist regarding the regulation of FGF and WNT signaling in neural specification in hESCs (B-C). (B) A summary of treatments. SB43 treatment was given at 1-day differentiation for one dose and only for 1 day. The duration of FGF2 or BIO treatments are indicated by underscore. All cells were fixed at the 4-day differentiation and stained with OCT4/PAX6. The labels A, B, C, …., correspond to the ICC images shown in (C). (C) The effects of manipulations of FGF and

WNT signalling on neural induction in hESCs. Scale bar: 25 µm. Our results reveal that the FGF2 and WNT pathways affect neural induction in hESCs is very much dependent upon the fashion of treatments, including the duration of treatments and the periods of administration of drugs.

The approaches used by investigators can be classified as follows: 1) Using FGF2 alone: is a “gain-of-function” approach, by which no report was found. Our results showed that +1FGF2 continuous treatment keeps hESCs in pluripotency, while +2FGF2 and +3FGF2 treatments resulted in hESC differentiation (no OCT4 staining) but not towards neural fate (no PAX6 staining) (“A”-“C”). Our data suggest that FGF2 constant treatment alone before neural induction either keeps cells in pluripotent state (“A”) or causes neural inhibition (“B” and “C”), which correlates with the findings reported by Greber et al. (2011), in which FGF2 were given 2 days ahead of SB431542 and continuously present. 2) Using SB431542+FGF2: some labs used a combinational approach, SB431542+FGF2, which results in inhibiting Activin signaling and enhancing FGF signaling [Vallier et al. (2009a); (2009b); Lupo et al., 2013]. Vallier et al. found that a combination of SB431542 (10 mM) and FGF2 (12 ng/ml) in CDM generated highly proliferative cells that expressed the neuroectoderm markers Sox1, Sox2, Gbx2, Nestin and NCam, but not the pluripotency markers Oct4, SSEA-3, Tra-1-60 or Nanog, suggesting that under this treatment hESCs undergo differentiation in favour of neural fate. However, according to the fashion of treatments to the cells, they were investigating the effects of FGF2 and Activin signaling on the later stage of neural lineage but not the effect of FGF2 alone on neural induction. Interestingly, Lupo et al. showed that hESCs cultured for 14 days with SB431542+FGF2 reduces the number of PAX6-positive cells and causes formation of CDX2-positive clusters, suggesting that FGF2 treatment promotes Trophectoderm rather than neural fate. Our results showed that hESCs subjected to a combinational treatment SB431542 (1 day)+FGF2, underwent neural induction only in a non-constant FGF2 treatment (“G”, “J” and “K”), in which SB431542 treatment can overwrite the effect of FGF2. A constant FGF2 treatment keeps hESCs in pluripotency even in the presence of SB431542 (“I”), which explains why Greber et al. found that constant FGF2 treatments inhibit neural fate when cells are concurrently treated with SB43+NOG or NOG. 3) Using FGF inhibitors: this is the most common approach. Many labs including our lab have used it and shown that FGF signaling promotes neural lineage (LaVaute et al., 2009; Vallier et al., 2009a and 2009b; Cohen et al., 2010; Na et al., 2010; Yoo et al., 2011). The WNT pathway also plays a role in regulating neural fate in the mouse and chicken *in-vivo*,

while the pathway has been shown to maintain self-renewal of both hESCs and mESCs (Seto et al., 2004; Dravid et al., 2005; Anton et al., 2007; Sineva and Pospelov**,** 2010). We carried out experiments to test the effect of WNT signaling on neural induction in hESCs using BIO treatments ("D"-"F", "H" and "L"-"N") and the results showed some similarities to those of FGF2 treatment with some exceptions. We found that BIO treatment alone kept cells in pluripotency ("D"-"F"), while the combinational treatment with SB43+BIO drove hESCs towards differentiation, but did not promote neural fate (no PAX6 staining) ("L"-"N"). Interestingly, under non-constant treatment of BIO, SB431542 treatment did lead to neural induction with less effect than those found in FGF2 and/or SB43 treatments ["H" compared to "G" and "control" +1SB43(1day)]. Our data suggest that WNT pathway alone promotes pluripotency in hESCs.

Supplemental Fig 5. The interaction between PTP1B and the Activin/Alk(ALK)4 pathway, related to Figure 5.

(A) Dose-dependent pull-down of PTP1B by Alk4 antibody using co-immunoprecipitation assay. Co-immunoprecipitation procedures were based on the Universal magnetic co-IP kit (Active Motif). PTP1B and Alk4 antibodies (Santa Cruz Biotechnology) were used in the co-IP assay. The protein levels of PTP1B were checked by Western blot. (B) The time course of cellular localization of PTP1B before or after Activin treatment in hESCs. Before Activin treatment, overexpressed PTP1B-eGFP (green), and endogenous PTP1B (red) predominately exhibit a punctate staining pattern around the nucleus. A punctate pattern is attenuated after a 30-min treatment with Activin. In the cells treated with Activin for 2 hr, the staining pattern of overexpressed PTP1B-eGFP and endogenous PTP1B (yellow) shows a more cytosolic distribution. After 1-day treatment with Activin, the cytosolic distribution of PTP1B is apparent. Scale bar represents 20 µm. (C) PTP1B-eGFP hESCs were plated out, settled o/n, and fed with hESC medium plus Activin (10 ng/ml) (called the "ESC" stage). The PTP1B-eGFP cells were then maintained in N2B27 in the constant presence of Activin (10 ng/ml) for 5 days. The images were collected at the ESC stage, 1-day, 2-day, 3-day, 4-day and 5-day differentiation. Scale bar represents 20 µm.

Supplemental Fig 6. The interaction between PTP1B and p-Erk(ERK)1/2, related to Figure 6.

(A) Ptp1b decreases the levels of p-Erk1/2. Mouse 46C ESCs were treated with Activin (10ng/ml) and/or Ptp1b inhibitor (sc-222227; 100 μM) for 2 hr after serum starvation for 24 hours. The levels of p-Erk1/2 were evaluated by Western blot. Treatment with Ptp1b inhibitor elevates the levels of p-Erk1/2 even in the presence of Activin, while Activin treatment alone diminishs p-Erk1/2 levels, suggesting that Ptp1b reduces the level of p-Erk1/2 by acting downstream from Activin. (B) PTP1B and p-ERK1/2 are co-expressed in ESCs and neural stem cells (neural rosette). (C) ALK4 is expressed prevalently in hESCs indicated by $OCT4^+$ cells and non-neural cells while it is absent from the $PAX6^+$ neural rosette. Scale bars represent 50 μm.

Supplemental Fig 7. The effects of PTP1B on the levels of p-ERK1/2, neural differentiation and the expression of OCT4 and NANOG, related to Figure 7.

(A) The levels of PTP1B inversely affect the levels of p-ERK1/2 analyzed by phospho-MAPK array. The phosphor-MAPK arrays were hybridized individually with the proteins harvested from control, PTP1B-OE, and PTP1B-KD hESCs. The whole image of arrays is presented in the right panel, enlarged regions of p-ERK1/2 (boxed) in the middle panel, and the quantified data on the dots of the p-ERK1/2 in the left panel using ImageJ. (B) Ptp1b inhibitor restores the capacity for neural differentiation in Nnat-KD mESCs. Nnat-KD mESCs were treated with 50 μM Ptp1b inhibitor (sc-222227) at 1-day differentiation for 48 hours, and the samples were collected at 6-day differentiation. $Sox1\text{-}eGFP^+/Nestin^+$ neural stem cells were observed in Ptp1b inhibitor-treated cells by ICC analysis (top panel). The quantified data is shown in the bottom panel. DAPI: blue. The expression of (C) OCT4 and (D) NANOG is sustained in PTP1B-overexpressing cells after 8-day differentiation in N2B27 differentiation medium. DAPI: blue. Scale bars represent 50 μm. (E) Our proposed regulatory model derived from N2B27 medium is validated in chemically defined medium: a) SB431542-mediated increase in the levels of p-ERK1/2 in cells; b) knocking down PTP1B bypasses the SB431542 treatment to promote neural fate; c) the SB431542-mediated neural induction is blocked by the

inhibitors of FGF/p-ERK1/2 signaling. Data are presented as mean ± s.d. (n = 2). Scale bars represent 20 μm.

Supplemental Experimental Procedures

ESC monolayer differentiation

ESCs were plated at densities of 30,000 cells/cm^2 for mESCs and 7,000 cells/cm^2 for hESCs, respectively. For the high-density experiments, mESCs were plated at 360,000 cells/cm^2. Inhibitors were administered at different stages of differentiation and were summarized in Supplemental Figure 1. To determine the effect of Activin on cell-fate decisions at different stages of differentiation, Activin (10 ng/ml, R&D Systems) was applied to hESCs and mESCs continuously from 1, 2, and 3 days after differentiation, which were designated as 1Activin, 2Activin, and 3Activin, respectively (Supplemental Figure 1). Samples were then collected at days 0 (ESC stage), 2, 4, and 6 for mESCs and an additional sample (day 8) for hESCs. The samples were used to analyze gene expression levels using real-time PCR. The reason for choosing 6 and 8 days of differentiation for mESCs and hESCs, respectively, is that the onset of lineages takes longer to occur in hESCs.

To investigate the effects of SB431542 on the neural differentiation of mESCs and hESCs, one dose of SB431542 (20 μM, Santa Cruz Biotechnology) was administered to ESCs at 0, 1, 2, and 3 days of differentiation, which are designated as +0SB43, +1SB43, +2SB43, and +3SB43, respectively (Supplemental Figure 1). Mouse ESCs were fixed at 4-days of differentiation with 4% paraformaldehyde (PFA) for analyzing the production of neural stem cells (Sox1-GFP$^+$/Nestin$^+$ or Sox1-GFP$^+$ colonies, which contain over 50% GFP$^+$ or Nestin$^+$ cells) and at 12-day differentiation for neuronal production (NeuN$^+$ neurons) using ICC analysis. Human ESC samples were collected at days 0 (ESC stage), 2, 4, 6, and 8 of differentiation and analyzed for PAX6 expression using real-time PCR. Cells were also collected at 12-days of differentiation, and neural rosettes were enumerated. To determine the effects of PD173074 and PD184352 on neural induction or on SB431542-mediated neural induction of mESCs and hESCs, PD173074 (100 ng/ml, Tocris) and PD184352 (5 μM, Santa Cruz Biotechnology) were administered to ESCs continuously from 1, 2, 3, and 4 days of differentiation (Supplemental Figure 1). Mouse ESCs were fixed at 6-days of differentiation, and Sox1-GFP$^+$ colonies were counted. Human ESCs were fixed at 4-days of differentiation, and PAX6$^+$ neural stem cells were counted. The reason why we did not include SOX2 as an early neural stem cell marker is because of the following: 1) SOX2 is expressed in ESCs and in all

stages of differentiation, suggesting that SOX2 cannot distinguish ESCs, differentiated cells, or neural stem cells; 2) SOX2+ cells are prevalent in the 3 days of differentiation, which are predominantly SOX2+/OCT4- cells. These cells are not early neural stem cells, because PAX6 is not expressed at this stage. Therefore the identities of these cells are in question let alone using SOX2+ cells as a readout for neural induction; 3) our unpublished data show that PAX6 is exclusively expressed in neural stem cells without mingling with OCT4 expression, whereas SOX2+/OCT4+ cells are abundantly present in neural induction. Therefore it will be difficult to use SOX2 as an early stem cell marker.

In chemically defined medium (CDM) system, we employed mono-layer culture rather than EB formation. We plated out cells at 7,000 cells/cm^2 onto Matrigel-coated plates in CDM supplemented with Activin (10 ng/ml) and FGF2 (12 ng/ml), changed to CDM next day, and treated cells with or without SB431542 (one dose) 24 hr later. For investigating the effects of inhibitors of FGF/p-ERK1/2, cells were treated with or without the inhibitors from 2-day differentiation. Cells were fixed at 6-day differentiation. For investigating SB431542-mediated p-ERK1/2 signalling, we plated out cells (70,000 cell/well in 6-well plates) and kept in conditional medium o/n, changed to CDM next day, 24 hr later cells treated with SB431542 (20 μM) for 10 min, 30 min, 1hr, 6 hr and 18 hr, and protein were collected at those time points. For investigating the effect of PTP1B on the mesendodermal fate, control (eGFP alone) and PTP1B-OE hESCs were driven toward mesodermal differentiation in the presence or absence of Activin (50 ng/ml). Cells were fixed at 4-day differentiation and analyzed for SOX17 expression.

Sample preparation for proximity ligation assay (PLA)

To determine the effect of Activin and SB431542 on the interaction of Alk(ALK)4/Ptp(PTP)1B and of PTP1B/p-ERK1/2, mESCs and hESCs were fixed with 4% PFA after 10 min treatment with either Activin (10 ng/ml) and/or SB431542 (20 μM) or DMSO (as a control). To investigate the PTP1B/p-ERK1/2 interaction during ESC-derived neural differentiation, mESCs and hESCs were driven towards neural differentiation in N2B27 medium and cell samples were fixed at days 0, 2, 4, 6, and 10 of differentiation.

In a broader screening for the potential factor(s) involved in Activin-mediated inhibition of p-Erk(ERK) signaling in ESCs, we selected several potential proteins that negatively regulate levels of p-Erk and tested

for physical interactions with Alk4 using PLA assay and confirmed with co-IP assay. The selected proteins are Spry1, Spry2, PTP1B, p27 Kip1, SHP-2, Cbl, PKG II, DiRas3, and Gαq protein.

Sample preparation for Western blot analysis

To investigate the effects of SB431542 on the levels of Erk(ERK)1/2 phosphorylation in mESCs and hESCs, a dose-response study was carried out by adding 1, 10, or 20 μM of SB431542 to Nnat-KD ESCs in ES medium for 5 min, cells were harvested, and total protein was isolated. To investigate the effect of PD173074 and PD184352 on SB431542-mediated p-Erk signaling, ESCs were pre-treated with 100 ng/ml PD173074 or 5 μM PD184352 for 1 hr and then treated with or without SB431542. Cells were washed and collected. All collected cells were subjected to Western blot analysis and analyzed using p-Erk1/2, p-Smad2, or p-Smad1 (Cell Signaling) antibodies. Human ESCs were treated with or without Activin (50 ng/ml) for the indicated time points and were harvested for analysis of the cleavage of PTP1B protein.

Sample preparation for protein sequencing

To determine the consequence of ALK4/PTP1B interactions, recombinant PTP1B (500 ng, Cell Sciences) was incubated with various concentrations (25, 50, 100, 250, and 500 ng) of active ALK4 (Sigma) in a kinase dilution buffer (5 mM Tris-HCl [pH 7.5], 2.5 mM glycerol 2-phosphate, 5 mM $MgCl_2$, 1 mM EGTA, 0.4 mM EDTA, 0.05 mM DTT) plus 50 μM ATP, and incubated at 30℃ for 15 minutes. Samples were then separated on a 10% SDS-PAGE gel. All bands stained with colloidal Coomassie Blue were in-gel digested with trypsin and then extracted from the gel by a series of acetonitrile and aqueous washes. The extracts were pooled with the initial supernatant and lyophilized. Each sample was then resuspended in 23 μl of 50 mM ammonium bicarbonate and analyzed by LC/MS/MS.

Sample preparation for phospho-RTK and phospho-MAPK array assays

To investigate the effects of SB431542 inhibition of the Activin/ALK4 pathway on intracellular signaling pathways, we employed the Proteome Profiler™ Human Phospho-RTK and Proteome Profiler™ Human Phospho-MAPK Array assays (R&D Systems). High-density human ESCs (90% confluence) were treated either with 20 μM SB431542 (Santa Cruz Biotechnology), Activin A (R&D Systems), or DMSO

(Sigma Aldrich) as a control for 30 min. Cells were collected in NP-40 lysis buffer (1% NP-40, 20 mM Tris-HCl [pH 8.0], 137 mM NaCl, 10% glycerol, 2 mM EDTA, PhosSTOP, and complete, Mini EDTA-free Protease Inhibitor Cocktail [Roche]). Total protein (300–500 µg, protein concentration assessed by DC Protein Assay [Bio-Rad]) diluted in Array Buffer 1, was applied onto the array membrane. For the dephosphorylation of p-ERK1/2 by PTP1B in vivo, we investigated the levels of p-ERK1/2 in PTP1B-knockdown (PTP1B-KD), control and PTP1B-overexpressing (PTP1B-OE) hESC lines using Phospho-MAPK Array assays. One and half million cells from each group were plated on Matrigel coated 6-cm dishes in CM. 24 hours later, the CM was replaced with N2B27 media. Cells were collected, 24 hours later, into cold lysis buffer provided in the kit, which was supplemented with PhosSTOP and complete protease inhibitors (both Roche). Proteins (300 µg) from each group were used for each array. The quantified data were calculated using ImageJ and normalized to the internal controls.

Supplemental References:

Anton, R., Kestler, H.A., and Kühl, M. (2007). Beta-catenin signaling contributes to stemness and regulates early differentiation in murine embryonic stem cells. FEBS Lett. *581(27)*:5247-5254.

Cohen, M.A., Itsykson, P., Reubinoff, B.E. (2010). The role of FGF-signaling in early neural specification of human embryonic stem cells. Dev Biol. *340(2)*:450-458.

Dravid, G., Ye, Z., Hammond, H., Chen, G., Pyle, A., Donovan, P., Yu, X., and Cheng, L. (2005). Defining the role of Wnt/beta-catenin signaling in the survival, proliferation, and self-renewal of human embryonic stem cells. Stem Cells. *23(10)*:1489-1501.

Greber, B., Coulon, P., Zhang, M., Moritz, S., Frank, S., Müller-Molina, A.J., Araúzo-Bravo, M.J., Han, D.W., Pape, H.C., and Schöler, H.R. (2011). FGF signalling inhibits neural induction in human embryonic stem cells. EMBO J. *30(24)*:4874-4884.

Li, X.J., Du, Z.W., Zarnowska, E.D., Pankratz, M., Hansen, L.O., Pearce, R.A., and Zhang, S.C. (2005).Specification of motoneurons from human embryonic stem cells. Nat Biotechnol. *23(2)*:215-221.

Lupo, G., Novorol, C., Smith, J.R., Vallier, L., Miranda, E., Alexander, M., Biagioni, S., Pedersen, R.A., and Harris, W.A. (2013). Multiple roles of Activin/Nodal, bone morphogenetic protein, fibroblast growth factor and Wnt/β-catenin signalling in the anterior neural patterning of adherent human embryonic stem cell cultures. Open Biol. *3(4)*:120167.

Pankratz, M.T., Li, X.J., Lavaute, T.M., Lyons, E.A., Chen, X., and Zhang, S.C. (2007). Directed neural differentiation of human embryonic stem cells via an obligated primitive anterior stage. Stem Cells. *25(6)*:1511-1520.

Sato, N., Meijer, L., Skaltsounis, L., Greengard, P., and Brivanlou, A.H. (2004). Maintenance of pluripotency in human and mouse embryonic stem cells through activation of Wnt signaling by a pharmacological GSK-3-specific inhibitor. Nat Med. *10(1)*:55-63.

Sineva, G.S., and Pospelov, V.A. (2010). Inhibition of GSK3beta enhances both adhesive and signalling activities of beta-catenin in mouse embryonic stem cells. Biol Cell. *102(10)*:549-560.

Zhang, X., Huang, C.T., Chen, J., Pankratz, M.T., Xi, J., Li, J., Yang, Y., Lavaute, T.M., Li, X.J., Ayala, M., Bondarenko, G.I., Du, Z.W., Jin, Y., Golos, T.G., and Zhang, S.C. (2010). Pax6 is a human neuroectoderm cell fate determinant. Cell Stem Cell. *7(1)*:90-100.